Dissertation

INVESTIGATING THE ROLE OF NR4A1 IN AGGRESSIVE LYMPHOMAS

submitted by
Mag.rer.nat. Karoline FECHTER

for the Academic Degree of
Doctor of Philosophy (PhD)

at the
Medical University of Graz
Division of Hematology

under the Supervision of
Assoz.-Prof. PD Dr.techn. Andreas PROKESCH
PD Mag.rer.nat. Dr.scient.med. Alexander DEUTSCH

2018

Declaration

I hereby declare that this thesis is my own original work and that I have fully acknowledged by name all of those individuals and organisations that have contributed to the research for this thesis. Due acknowledgement has been made in the text to all other material used. Throughout this thesis and in all related publications I followed the "Standards of Good Scientific Practice and Ombuds Committee at the Medical University of Graz".

Part I of this thesis has been published in Karoline Fechter[1], Julia Feichtinger[2,3], Katharina Prochazka[1], Julia Judith Unterluggauer[4], Katrin Pansy[1], Elisabeth Steinbauer[4], Martin Pichler[5], Johannes Haybaeck[4,6,7], Andreas Prokesch[8], Hildegard T. Greinix[1], Christine Beham-Schmid[4], Peter Neumeister[1], Gerhard G. Thallinger[2,3] & Alexander J.A. Deutsch[1]. Cytoplasmic location of NR4A1 in aggressive lymphomas is associated with a favourable cancer specific survival. Sci Rep. 2018 Sep 28;8(1):14528. doi: 10.1038/s41598-018-32972-4. [1]Division of Hematology, Department of Internal Medicine, Medical University Graz, Graz, Austria. [2]Institute of Computational Biotechnology, Graz University of Technology, Graz, Austria. [3]BioTechMed Omics Center Graz, Graz, Austria. [4]Institute of Pathology, Medical University Graz, Graz, Austria. [5]Division of Oncology, Department of Internal Medicine, Medical University Graz, Graz, Austria. [6]Department of Pathology, Otto von Guericke University Magdeburg, Magdeburg, Germany. [7]Institute of Pathology, Medical University Innsbruck, Innsbruck, Austria. [8]Institute of Cell Biology, Histology and Embryology, Medical University Graz, Graz, Austria. Karoline Fechter and Julia Feichtinger contributed equally.

In this sense, all co-authors of this publication have consent to the use of their data in this thesis, and permission to reproduce the published material has been obtained. The respective article is licensed under Creative Common Attribution 4.0 International License (http://creativecommons.org/licenses/by/4.0/), source quotations have been made accordingly and changes to figures or tables have been indicated were applicable. This license allows the use, adaptation, distribution, and reproduction done in this thesis in any medium or format unless otherwise indicated. Responsibility for the information set out in

Part II of this thesis contains unpublished material and is currently under preparation for publication. In order to avoid accusation of double publication, this fact shall be recorded herewith.

PhD student K.F. received funding from the Medical University of Graz through the PhD Program „Molecular Medicine MolMed”.

Acknowledgement

Obwohl zu dieser Dissertation weit mehr Personen und Umstände beigetragen haben als hier aus Platzgründen erwähnt werden können, möchte ich trotzdem einige Personen hervorheben denen ganz besondere Dank gilt. Zu allererst möchte ich mich bei meinen Betreuern, Dr. Alexander Deutsch und Dr. Andreas Prokesch bedanken. Und das nicht ausschließlich für ihr profundes fachliches Wissen und ihre Fähigkeit dies weiterzugeben, sondern auch für ihren Enthusiasmus und den Spaß an der Sache. Weiterer Dank gilt der gesamten Forschungsgruppe der Hämatologie – vor allem Prof. Peter Neumeister und Dr. Katharina Prochazka – für ihre kontinuierliche Unterstützung sowie Dr. Mirjana Efremova, Dr. Julia Feichtinger und Dr Julia Kargl für ihre Beteiligung und Hilfe bei dieser Arbeit. Natürlich nicht zu vergessen ist das gesamte Team des Labors – vielen Dank vor allem an Beata Pursche und Katrin Pansy für die verbrachte Zeit, geteiltes Leid ist bekanntlich halbes Leid.

Ein großes Danke geht an meine Freunde, egal ob sie hier oder in einem anderen Teil der Welt sind, Danke für eure Unterstützung!

Zuletzt kann ich nicht sagen bei wem ich mich mehr bedanken muss. Meinen Eltern, ohne die diese Arbeit niemals möglich geworden wäre, und die mich nicht nur auf diesen Weg gebracht haben, sondern mich auch unermüdlich unabhängig von Anlass und Tageszeit auf diesem unterstützt haben. Besser hätte ich es mir nicht aussuchen können. Ein ganz besonderer Dank gilt meinem Partner und unserer wachsenden Familie für die vergangene und zukünftige Zeit mit und Unterstützung von euch. Kurz gesagt, ich weiß es war nicht immer leicht mit mir und sage einfach einmal DANKE für alles.

Table of Contents

1 Abbreviations

7-AAD	7-Aminoactinomycin D
ABC	Activated B cell-like
ACTb	ß Actin
ADARB	Double-stranded RNA-specific editase B2
AF	Activation function
AICDA	Activation induced cytidine deaminase
AID	Activation induced deaminase
AML	Acute myeloid leukemia
APC	Antigen presenting cell
ARHGEF1	Rho guanine nucleotide exchange factor 1
ASHM	Aberrant somatic hypermutation
β2M	β2 Microglobulin
BCL-xL	BCL-2-like 1
BCL-2	B cell CLL/lymphoma 2
BCL2A1A	BCL-2-related protein A1
BCL2A1D	BCL-2-related protein D1
BCL-6	B cell CLL/lymphoma 6
BCR	B cell receptor
BL	Burkitt lymphoma
BM	Bone marrow
BSA	Bovine serum albumin
BTLA	B- and T lymphocyte attenuator
BUB1	BUB1 mitotic checkpoint serine/threonine kinase
c-FOS	Fos proto-oncogene
c-MYC	Myelocytomatosis oncogene cellular homolog
cAMP/CREB	Cyclic adenosine monophosphate/ cAMP response element-binding protein
CARD11	Caspase recruitment domain-containing protein 11
CAT	Catalase
CCL	C-C motif chemokine ligand
CCNB1	Cyclin B1
CCND1	Cyclin D1
CCND3	Cyclin D3
CCNG2	Cyclin G2
CCR	C-C Motif Chemokine Receptor
CD	Cluster of Differentiation
CD40-L	CD40 Ligand
CDKN1A	Cyclin dependent kinase inhibitor 1A
CDKN1B	Cyclin dependent kinase inhibitor 1B

CFLAR/CFLIP	CASP8 and FADD like apoptosis regulator
CHOP	Cyclophosphamide-Doxorubicin-Vincristine-Prednisone
CI	Confidence interval
cJUN	Jun proto-oncogene
CLL	Chronic lymphocytic leukemia
CLP	Common lymphoid precursors
COL1A	Collagen Type I alpha 1 chain
COO	Cell of origin
CREBBP	CREB binding protein
CSR	Class switch recombination
CTLA4	Cytotoxic T-lymphocyte-associated antigen 4
CXCL	C-X-C motif chemokine ligand
CXCR	C-X-C motif chemokine receptor
DBD	DNA binding domain
DC	Dark zone
DC	Dendritic cell
DH	Double hit
D_H	Diversity segments
DLBCL	Diffuse large B cell lymphoma
DLL1	Delta like canonical Notch ligand 1
DMSO	Dimethyl sulfoxide
DNA	Deoxyribonucleic acid
ds	Double Strand
ds-RNA	Double-stranded RNA
DUSP1	Dual specificity phosphatase 1
EBF	Early B cell factor
EBI3	Epstein Barr virus induced gene 3
eBL	Endemic (African) Burkitt lymphomas
EBV	Epstein-Barr virus
eDLBCL	Extranodal diffuse large B cell lymphoma
EGR3	Early growth response 3
EIF4E	Eukaryotic translation initiation factor 4E
EIF4EBP1	EIF4E binding protein 1
EP300	E1A binding protein p300
ERK1/2	Extracellular signal-regulated kinase 1 and 2
ERK2/5	Extracellular signal-regulated kinase 2 and 5
ETV5	ETS variant 5
EZH2	Enhancer of zeste homologue 2
FasL	Fas ligand
FBS	Fetal bovine serum
FBXO11	F-Box protein 11

FDC	Follicular dendritic cell
FL	Follicular lymphoma
FN1	Fibronectin 1
FO	Follicular B cells
FOXO1	Forkhead box O1
FOXP3	Forkhead box P3
GADD45	Growth arrest and DNA damage inducible alpha
GAL9	Galectin 9
GAPDH	Glyceraldehyde 3-phosphate dehydrogenase
GATA3	GATA binding protein 3
GC	Germinal Center
GC-B	Germinal center B cell
GCB	Germinal center B cell like
GCSAM	Germinal center associated signaling and motility
GM-CSF	Granulocyte−macrophage colony stimulating factor
GNA13	G protein subunit alpha 13
GO	Gene ontology
GSEA	Gene set enrichment analysis
GSK3	Glycogen synthase kinase 3
Gα13	G protein α13
H_2O_2	Hydrogen peroxide
HBSS	Hank's balanced salt solution
HIF1α	Hypoxia-inducible factor 1 α
HIV	Human immunodeficiency virus
HL	Hodgkin lymphomas
HLA	Human leukocyte antigen
HPRT	Hypoxanthine-guanine phosphoribosyltransferase
HR	Hazard ratio
HRS	Hodgkin Reed-Sternberg
HSC	Hematopoietic stem cells
HSV8	Human herpes virus 8
HVEM	Herpesvirus entry mediator
ICB	Immune checkpoint blockade
ICOS	Inducible T cell costimulatory
ICOSL	Inducible T cell costimulatory ligand
ID3	Inhibitor of DNA binding 3, HLH protein
IFNγ	Interferon γ
Ig	Immunoglobulin
IHC	Immunohistochemistry
IL	Interleukin
ILxR	Interleukin x receptor
ILxRα	Interleukin x receptor α chain

IPA	Ingenuity pathway analysis
IPI	International prognostic index
IRAK1/ IRAK4	Interleukin-1 receptor-associated kinase 1/4
IRF4	Interferon regulatory factor 4
JAK/STAT	Janus kinase/ signal transducer and activator of transcription
J_H	Joining segments
JNK	C-Jun terminal kinase
JunB	JunB proto-oncogene
LAG3	Lymphocyte activating gene 3
LBD	Ligand binding domain
LZ	Light zone
MALT	Mucosa-associated lymphoid tissue
MAPK	Mitogen-activated protein kinase
MCL	Mantle cell lymphoma
MCL1	Myeloid cell leukemia sequence 1 (BCL-2-related)
MDM2	Mouse double minute 2
MDS/MPN	Mixed myelodysplastic/ myeloproliferative neoplasm
MDSC	Myeloid-derived suppressor cell
MEF2B	Myocyte – specific enhancer factor 2B
MEF2C	Myocyte–specific enhancer factor 2C
MEP	2-C-methyl-D-erythritol 4 phosphate
MHC	Major histocompatibility complex
MLL2	Mixed lineage lymphoma/ leukemia 2
MLP	Multipotent lymphoid precursors
MMP2	Matrix metallopeptidase 2
mTOR	Mammalian target of Rapamycin
MUM1	Melanoma associated antigen (mutated) 1
MW	Waldenström Macroglobulinemia
MXD1	MAX dimerization protein 1
MYD88	Myeloid differentiation primary response 88
MZ	Marginal zone B cells
NF-κB	Nuclear factor kappa B
NGCB	Non-germinal center B cell like
NHEJ	Non-homologous end-joining
NHL	Non-Hodgkin lymphomas
NK	Natural Killer
NKT	Natural Killer T
NLS	Nuclear localization signal
NR4A	Nuclear Receptor Subfamily 4 Group A Member
$p19^{ARF}$	Protein 19 ADP ribosylation factor
P2RY8	P2Y purinoreceptor 8

p53	Tumor protein 53
PAX5	Paired box 5
PBS	Phosphate-buffered saline
PD1	Programmed cell death 1
PDL1/2	Programmed cell death ligand 1/2
PEL	Primary effusion lymphoma
pGCB	Primary GCB
PI3K	Phosphatidylinositide 3 kinase
PI3P	Phosphatidylinositol (3,4,5) triphosphate
PKB/AKT	Protein kinase B
PKC	Protein kinase C
PLK1	Polo Like Kinase 1
PMBL	Primary mediastinal B cell lymphoma
PPIA	Peptidylprolyl isomerase A
PRDM1/BLIMP-1	PR domain zinc finger protein 1
Ptgs2	Prostaglandin-endoperoxide synthase 2
PTLD	Posttransplant lymphoproliferative disorders
PTPN6	Tyrosine-protein phosphatase non-receptor type 6
PU.1	Spi-1 proto-oncogene
R-CHOP	Rituximab-CHOP
RAG1/2	Recombination activating gene 1/2
RPMI	Roswell Park Memorial Institute Medium
RSK	p90 ribosomal S6 kinase
RSS	Recombination signal sequence
RXR	Retinoid X receptor
S1PR2	Sphingosine-1-phosphate receptor 2
S1pr5	Sphingosine-1-phosphate receptor 5
sBL	Sporadic Burkitt lymphomas
SEM	Standard error of the mean
SHM	Somatic hypermutation
SOD2	Superoxide dismutase 2
SPF	Specific pathogen free
STAT3	Janus kinase (JAK)- signal transducer of activation 3
TACTILE	T cell activation increased late expression
TAM	Tumor-associated macrophage
TBP	TATA-box binding protein
TCF3/E2A	Transcription factor 3
TCR	T cell receptor
T_{FH}	Follicular T-helper cells
tGCB	Transformed GCB
TGFβ	Transforming growth factor β
T_H	T-helper

TH	Triple hit
TIGIT	T cell immunoreceptor with Ig and ITIM domains
TIM3/HAVCR2	T cell immunoglobulin and mucin-domain containing 3
TLR	Toll-like receptor
TNFAIP3/A20	TNF alpha induced protein 3
TNFRSF14	Tumor necrosis factor receptor 14
TNFRSF8	TNF receptor superfamily member 8
TNFSF11	TNF superfamily member 11
TNFα	Tumor necrosis factor α
TRAP220	Thyroid hormone receptor-associated protein 220
TREG	Regulatory T cell
V_H	Variable segments
WHO	World Health Organization
XPO1	Exportin 1

2 List of Figures

3 List of Tables

4 Kurzzusammenfassung

Der nukleäre Weisenrezeptor NR4A1 weist durch pro-apoptotische genomische und nicht genomische Effekte eine tumor-unterdrückende Funktion in der Lymphomentstehung auf. Das Ziel des ersten Teils dieser Arbeit war es, die klinische Relevanz des NR4A1 Proteinexpressionsmusters in einer Kohorte von 60 diffus großzelligen B Zelllymphomen (DLBCL) und nicht-neoplastischen Kontrollen mittels Immunhistochemie zu untersuchen. Diese erste Analyse zeigte eine signifikante Assoziation von zytoplasmatischer NR4A1 Lokalisation mit dem Keimzentrums-DLBCL Subtyp, einem begünstigten erkrankungsspezifischen Überleben, sowie gespaltener Caspase 3. Um mögliche Signalwege zu identifizieren welche an der zytoplasmatischen Lokalisation von NR4A1 beteiligt sind, wurde als komplementärer, funktioneller Ansatz eine Gen Set Anreicherungsanalyse von sogenannten Reactome Signalwegen mittels öffentlich zugänglichen Microarray Daten durchgeführt. Diese Analyse zeigte signifikante Änderungen im ERK1/2 Signalweg, was auch durch semi-quantitative Real-Time PCR nachgewiesen werden konnte. Hier konnte ein hoher zytoplasmatischer NR4A1 Anteil mit einer erhöhten Expression von ERK1/2 Zielgenen assoziiert werden.

Im zweiten Teil dieser Arbeit, wurde der Effekt des *Nr4a1* Verlustes auf die Entwicklung von B Zell Lymphomen in einem *Myc*-gesteuerten Mausmodell untersucht. Daher wurden zuerst *Nr4a1*-/- Mäuse mit *EμMyc* Mäusen gekreuzt. Ein Vergleich der so erhaltenen Mauskohorten zeigte deutlich, daß vor allem *EμMyc Nr4a1*-/- sowie auch *EμMyc Nr4a1*+/- Mäuse, im Gegesatz zu *EμMyc Nr4a1*+/+ Mäusen, eine beschleunigte Tumorentstehung sowie ein verkürztes Überleben aufweisen. Eine Untersuchung des Knochemarkes und der Milz zeigte weiters, daß durch den *Nr4a1* Verlust bereits vor der Lymphomentstehung Defekte in der Apoptose detektierbar sind. Eine anschließende RNA Sequenzierung der *EμMyc Nr4a1*-/- und *EμMyc Nr4a1*+/+ Tumore ergab eine durch den *Nr4a1* Verlust induzierte Anreicherung von Genen welche immunologische und immunoregulatorische Funktionen besitzen. Daher wurden Tumorzellen beider Mauskohorten in C57/Bl6 Wildtyp- und immundefiziente Fox Chase Scid Beige Mäuse transplantiert. Die Resultate unterstrichen deutlich die Annahme, daß die Rolle von *Nr4a1* eine immunologische Komponente beinhaltet da eine Hochregulierung von immunoregulatorischen Genen sowie eine gesteigerte Disseminierung ins Knochenmark von immunkompetenten, aber nicht immundefizienten Mäusen gezeigt werden konnte.

Diese Daten weisen darauf hin, daß ein hoher zytoplasmatischer NR4A1 Proteinanteil durch die Induzierung von Apoptose mit einer günstigen Lymphom-spezifischen Überlebensrate verbunden ist. Gleichermaßen fungiert *Nr4a1* in einem Lymphom Mausmodell durch die Transregulierung von immunoregulatorischen Genen als ein Tumorunterdrücker. Zusammenfassend unterstreichen diese Studien die Wichtigkeit von NR4A1 als möglicher prädiktiver Marker für die Risikoabschätzung in aggressiven Lymphomen.

5 Abstract

The nuclear orphan receptor NR4A1 has been described to possess tumor suppressive functions through pro-apoptotic genomic and non-genomic effects in aggressive lymphomas. In the first part of this project, we aimed to immunohistochemically characterize the clinico-pathological relevance of NR4A1 protein expression patterns in a cohort of 60 diffuse large B cell lymphoma (DLBCL) patients and non-neoplastic lymph nodes. We observed that high cytoplasmic NR4A1 was significantly associated with favorable cancer-specific survival, the germinal center B cell-like subtype and cleaved caspase 3. Complementary, functional profiling using gene set enrichment of Reactome pathways based on a publicly available microarray data was applied to determine pathways potentially implicated in cytoplasmic localization of NR4A1 and validated by means of semi quantitative real-time PCR. The pathway analysis revealed changes in the ERK1/2 pathway, and this was corroborated by the finding that high cytoplasmic NR4A1 was associated with higher expression of ERK1/2 targets in our cohort.

In the second part of this project, the effects of *Nr4a1* loss on B cell lymphoma development were determined in a mouse model of *Myc*-driven lymphomagenesis. Therefore, first the *EμMyc* mouse was crossed with the *Nr4a1*-/- mouse. The generated mouse cohorts comprising of *EμMyc Nr4a1*+/+, *EμMyc Nr4a1*-/- and *EμMyc Nr4a1* +/- mice were compared with respect to tumor formation and survival and results demonstrated accelerated tumor formation and reduced survival upon loss of *Nr4a1*. Moreover, investigation of bone marrow and spleen of mice at the premalignant stage revealed defects in apoptotic potential. RNASeq of tumors from *EμMyc Nr4a1*-/- mice and *EμMyc Nr4a1*+/+ mice showed that genes involved in immune function and/or immune regulation were induced by *Nr4a1* loss. Hence, tumor cells of both mouse cohorts were transplanted into C57/Bl6 and immunocompromised Fox Chase Scid Beige recipients. Results from the transplantation of *EμMyc Nr4a1*-/- derived tumors clearly demonstrated an upregulation of immunoregulatory molecules upon loss of *Nr4a1* only in immunocompetent mice. Furthermore, transplantation of the same tumors led to an enhanced dissemination potential to the bone marrow of immunocompetent but not immunodeficient mice.

These data indicate that high cytoplasmic NR4A1 is associated with a favorable lymphoma-specific survival in DLBCL patients by induction of apoptosis. Likewise, in a

lymphoma mouse model, it functions as a tumor suppressor by transregulating immunemodulatory genes. Collectively, these studies underpin the importance of NR4A1 as potential prognostic marker for risk assessment in aggressive lymphomas.

6 Introduction

6.1 B Cells and Malignant Transformation

6.1.1 B Cell Development

B cells form an integrate part of humoral immunity and are the main line of defense against extracellular pathogens. There exists an almost infinite repertoire of antibodies produced as immunoglobulins by B cells targeting their cognate antigen. The generation of B cells occurs throughout life and encompasses several checkpoints and stages. B cell generation starts in the bone marrow, where cells progress through pro-B cell and pre-B cell developmental stages. At the next differentiation step as immature B cells, they acquire antigen specificity by expression of a functional B cell receptor (BCR), thereby representing the first key check point in B cell development. Cells which successfully transverse this process enter the periphery as transitional B cells and migrate to the spleen, where they complete their development by differentiation into naïve, follicular, or marginal B cells (1-4). For the expression of functional BCR and formation of antigen-specific mature B cells, several rearrangement processes are necessary. Malfunction in one or more of these pathways leads to development of lymphoid neoplasms, autoimmune disorders, allergies and immunodeficiencies, respectively.

6.1.2 B Cell Development in the Bone Marrow

B cell development from hematopoietic stem cells (HSC) starts prenatally in the liver and is then outsourced to the bone marrow (BM) as primary lymphoid tissue for the rest of a mammals' lifetime. Various transcription factors drive development and maturation of B cells in the BM. The entire process is characterized by rearrangement processes of deoxyribonucleic acid (DNA) segments encoding the heavy- and the light-chain regions of variable (V_H), diversity (D_H) and joining (J_H) segments of immunoglobulins, and expression of accessory molecules on the cell surface. The finally resulting BCR complex is indispensable for positive selection of developing B cells and migration of these cells to secondary lymphoid organs for further maturation (1)

Development starts with pluripotent HSCs, which differentiate to multipotent lymphoid precursors (MLPs) and common lymphoid precursor cells (CLP). From there on, several

transcription factors guide development of B cells from the pre-pro B cells state to the pro-B cell state - expressing CD19 - and pre-B cells, having already upregulated the pre-BCR on the cell surface (5). The transcription factor *Spi-1 proto-oncogene* (*PU.1*) is expressed at very early developmental stages (6). Its low expression favors B cell development by its ability to modify the chromatin structure of its target genes (7). Among them components of the pre-BCR (*Ig-α*, *Ig-β*, *VpreB*, *λ5*), *interleukin* (*IL*) *7 receptor α* (*IL7Rα*), *early B cell factor* (*EBF*) and *recombination activating gene 1/2* (*RAG1/2*), all indispensable for B cell maturation (5). *EBF*, induced by *PU.1*, positively regulates expression of *transcription factor 3* (*TCF3; E2A*), both being essential *for paired box 5 (PAX5)* expression (8-11). The main processes of B cell development in the BM- VDJ recombination, expression of the pre-BCR complex and fate to the B cell lineage- are synergistically regulated by these three factors. VDJ recombination is initiated early in CLP by *PU.1* expression (7, 12). Recombination signal sequences (RSS) flank the *V*, *D* and *J* gene segments and are recognized by RAG1/2, which introduces DNA double strand (ds) breaks that are finally resolved by non-homologous end-joining (NHEJ) DNA repair mechanisms (13-18). First, rearrangement of the D_H and J_H segments occurs followed by further joining of an upstream V_H to the D_HJ_H segment, so that CD19 positive pro-B cells express a recombined heavy chain. Next, functional *VDJ-*C_H heavy chains form the pre-BCR complex by pairing with *VpreB* and *λ5*. Signals transmitted by the pre-BCR complex induce a shutdown of *RAG1/2* expression, thereby inhibiting recombination of another *H-chain* allele in pre-B cells. Finally, cell division and rearrangement of the *L-chain* segments encoding the *λ*- or *κ-chain* occurs which is facilitated by re-induced *RAG1/2* expression. Successfully rearranged *κ*- or *λ*-chains ultimately replace the *VpreB* and *λ5* chains of the pre-BCR to form a functional immunoglobulin M (IgM) molecule on the cell surface of immature B cells, which in the next step enter the spleen to undergo further maturation processes (5, 19-22).

6.1.3 B Cell Development in Secondary Lymphoid Organs and the Germinal Center Reaction

After leaving the bone marrow, immature B cells expressing IgM and IgD enter the spleen as transitional B cells where they differentiate into marginal zone (MZ) – or follicular (FO) B cells, depending on the specificity of their B cell receptor. Upon antigen contact, MZ differentiate further into short-lived plasma cells, while FO cell take part in the germinal center reaction (1). Germinal centers (GCs) of secondary lymphoid organs like lymph nodes and spleen provide the places for B cell affinity maturation upon encounter of foreign antigen. Germinal centers can be divided in distinct zones harboring specialized cells and forming definable structures for differentiation of B cells into antibody-producing plasma cells and memory B cells (23) (Figure 1). Secondary follicles, where the germinal center reaction takes place, develop from primary follicles with naïve B cells (24, 25). Primary lymphoid follicles are separated by interfollicular regions and surrounded by T cell rich zones (26, 27). Follicular dendritic cells (FDCs), residing in the center of the follicles, are responsible for initiation of the germinal center reaction by antigen presentation and thus activation of naïve B cells (28-30). Antigen-activated B cells move to the borders of the follicles where they interact with follicular T Helper cells (T_{FH}) (31, 32). Activated B cells can be distinguished by naïve B cells by increasing size, altered morphology, higher proliferation rate as well as upregulation of distinct marker molecules on the cell surface and a changed genetic program (33-40). Approximately four to six days after antigen encounter, germinal centers begin to form surrounded by a mantle zone consisting of naïve B cells displaced by the expanding germinal center B cells (25, 41). The after seven days fully established GC, can at this timepoint be subdivided in two microscopically distinct zones. The dark zone (DC) is characterized by expansion and somatic hypermutation (SHM) of expanding B cells termed centroblasts, while in the light zone (LZ) B cells termed centrocytes undergo antigen selection and class switch recombination (CSR) (33, 42-45) (Figure 1) .

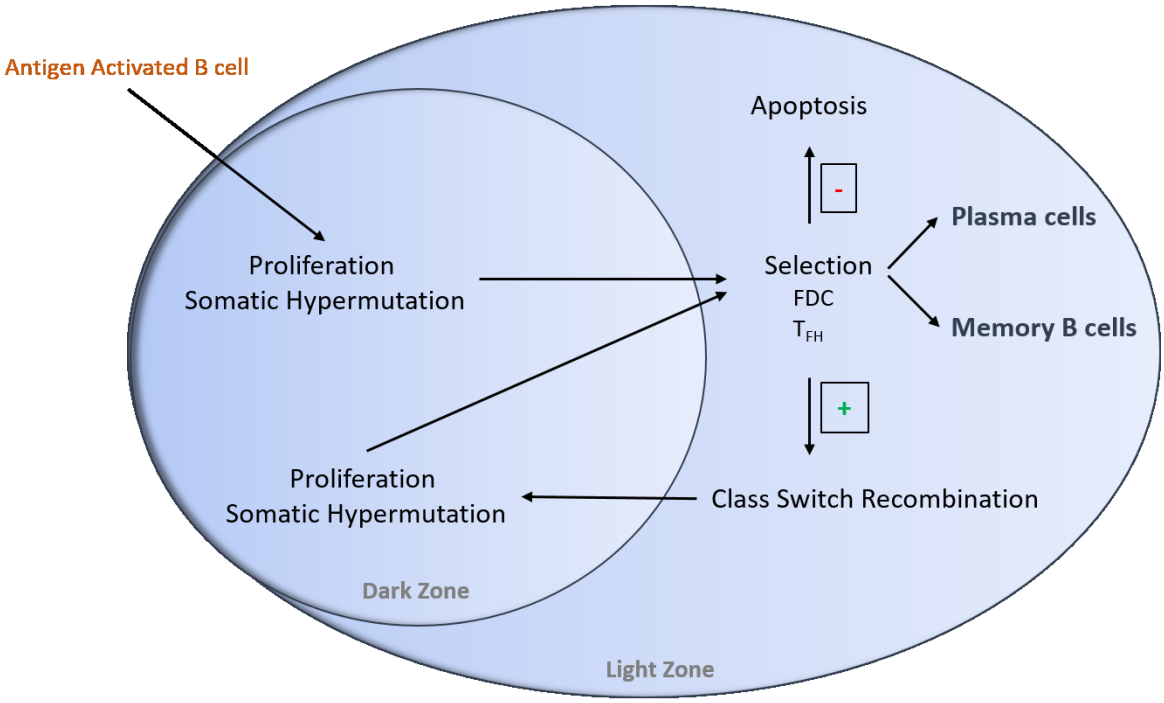

Figure 1: The Germinal Center Reaction

Adapted by permission from Springer Nature Customer Service Centre GmbH: Spinger Nature. Nature Reviews Immunology. Dynamics of B cells in germinal centres. De Silva NS, Klein U (24). ©Springer Nature. 2015

Although being restricted to different zones within the germinal center, SHM and CSR are both independent of RAG1/2 but dependent on activation-induced deaminase (AID). Somatic hypermutation of the rearranged V_H,D_HJ_H and V_LJ_L genes by insertion of point mutations in mainly the variable regions provides antibody mutants with higher affinities for the antigen and thus contributes to affinity maturation of the humoral immune response. In contrast, class switch recombination affects the constant region of the antibody, thereby changing the effector functions in humoral immunity by producing IgE, IgA and IgG, respectively. In humans the eight C_H heavy chain genes (C_μ, C_δ, $C_{\gamma 3}$, $C_{\gamma 1}$, $C_{\alpha 1}$-E_α-$C_{\gamma 2}$, $C_{\gamma 4}$, C_ε and $C_{\alpha 2}$) lie downstream of the *VDJ* segments. So-called switch (S) regions are located upstream of C_H except C_δ. AID introduces breaks in two S regions leading to exertional deletion of the intervening region together with C_μ, so that only C_α, C_γ and C_ε regions remain (46, 47). Reticular cells in the DZ lead to attraction of B cells via the C-X-C Motif Chemokine Receptor 4 - C-X-C Motif Chemokine Ligand 12 (CXCR4-CXCL12) axis compared to the LZ, where immune cells like follicular T-helper cells (T_{FH}), macrophages and FDCs reside (48). Intravital microscopy showed that the process of affinity maturation

is a dynamic one where lymphocytes travel from the dark to the light zone and vice versa. Thereby, they undergo several rounds of proliferation and SHM to generate high affinity clones. These clones are then positively selected in the light zone by either competing for antigen binding or T cell help (34, 42, 49-52) (Figure 1).

6.1.4 Gene Expression Programs Regulating the Germinal Center Reaction

Distinct gene expression programs direct B cell development from GC formation, recirculation between the light and the dark zone to exit of mature B cells as antibody producing plasma cells or long-lived memory B cells (24).

B Cell CLL/Lymphoma 6 (*BCL-6*) is indispensable for initiating the germinal center reaction by controlling migration of activated B cell precursors towards the center of the follicle and is expressed throughout the GC reaction. Furthermore, *BCL-6* is essential for controlling genetic programs of somatic hypermutation in the dark zone (26, 27, 53). *Myocyte–specific enhancer factor 2B* (*MEF2B*) shows a similar expression pattern to *BCL-6* and directly activates *BCL-6* transcription in GC B cells. In contrast, *myocyte–specific enhancer factor 2B* (*MEF2C*) is expressed in B cells upon antigen encounter and stimulates proliferation during the early phase (54, 55). *Interferon regulatory factor 4 (IRF4)* has a dual function in the GC reaction. *IRF4* expression is positively regulated by *nuclear factor kappa B (NF-κB)* and drives early GC formation in B and T cells. In this phase it also synergizes with *MEF2B* in inducing *BCL-6* expression. In contrast, *IRF4* functions as a negative regulator of *BCL-6* expression in light zone B cells and drives class-switch recombination and differentiation of B cells into plasma cells (56-59). *Myelocytomatosis oncogene cellular homolog (c-MYC)* is expressed during antigen activation of B cells but repressed by *BCL-6* during the phase of appearance of early to mature germinal centers. Once the germinal center formation has taken place, *c-MYC* is re-expressed in a subset of light zone B cells in mature germinal centers and regulates the light zone-dark zone recirculation of activated B cells (60, 61). Last, *myeloid cell leukemia sequence 1* (*BCL-2-related*) (*MCL1*) regulates in accordance with *c-MYC* germinal center formation by negatively regulating apoptosis of B cells during the early phase throughout the establishment of germinal centers (62).

The fate of mature B cells towards the plasma cell or memory B cell lineage is mainly determined by gene expression profiles and affinity maturation. B cells differentiating into

plasma cells harbor high affinity receptors for the respective antigen. *NF-κB*-driven induction of *IRF4*, which in turn suppresses *BCL-6* expression and induces *PR domain zinc finger protein 1* (*PRDM1* also known as *BLIMP-1*), furthermore contributes to production of plasma cells upon antigen encounter (57, 63) In contrast, commitment to the memory compartment can happen without T cell help and even without GC formation. Nevertheless, the majority of memory cells arise after T cell help to B cells in germinal centers and their development seems to depend on the presence of interleukin 21. These memory cells exhibit hypermutated immunoglobulin genes, though with lower antigen affinities as opposed to plasma cells (63-66).

6.2 Lymphomas

6.2.1 What are Lymphomas?

The World Health Organization (WHO) classification of neoplasms of the hematopoietic and lymphoid tissue combines morphology, immunophenotype, genetic, molecular, and clinical features to stratify these malignancies according to their cell of origin and maturation state (67). Lymphomas originate from lymphoid cells and comprise a very heterogenous type of cancer with a predominant localization in lymphoid tissues and to a lesser extent at extranodal sites (68). Included in this classification are mature B cell malignancies, T- and Natural Killer (NK) cell neoplasms, Hodgkin lymphomas (HL), histiocytic and dendritic cell neoplasms, and posttransplant lymphoproliferative disorders (PTLD). The great clinical and pathological diversity of B cell lymphomas can be subdivided into HL and non-Hodgkin lymphomas (NHL). NHL may show an indolent or aggressive course, resulting in a further classification into one of the two subtypes. (69, 70).

6.2.2 Indolent B Cell Lymphomas

Indolent lymphomas account for almost 40% of all non-Hodgkin lymphomas worldwide, whereby follicular lymphoma (FL) represent the third most common type of non-Hodgkin lymphomas in the Western world (71-73). An overview of indolent B cell lymphomas and their frequencies is depicted in Table 1.

Table 1: Worldwide occurrence of indolent B cell lymphomas.

Republished with permission of American Society of Hematology. From Hematopathology Approaches to Diagnosis and Prognosis of Indolent B-Cell Lymphomas. Randy D. Gascoyne, 2005, 299-306. © 2005; Permission conveyed through Copyright Clearance Center, Inc. (73)

Lymphoma Subtype	Frequency
Follicular lymphoma, grade 1-3A	22%
Extranodal marginal zoine B cell lymhoma, MALT-type	8%
Small lymphocytic lymphoma/ CLL	7%
Nodal marginal zone lymphoma	2%
Lymphoplasmacytic lymphoma	1.2%
Splenic marginal zone lymphoma	<1%

6.2.2.1 Follicular Lymphomas

Follicular lymphoma is the third most common type of non-Hodgkin lymphomas in the Western world (71, 72). FL represents the prototype of an indolent clinical course with slow progression, whereby the majority of patients already suffer from advanced stage disease at time of presentation and diagnosis, with approximately 70% showing bone marrow involvement. Similar to chronic lymphocytic leukemia (CLL), the median age at time of diagnosis is elevated with around 60 years, however there exist around 25% of patients being 40 years or less (74). A hallmark of follicular lymphomas is the t(14;18) (q32:q21) translocation, present in 80-90% of all cases, leading to overexpression of *B Cell CLL/Lymphoma 2* (*BCL-2*) having anti-apoptotic effects. Nevertheless, this mutation is considered to be not enough for the full development of FLs, as other genetic (75, 76) and epigenetic factors (77, 78) as well as the microenvironment (79, 80) seem to play a substantial role in the development of disease.

6.2.2.2 Mucosa-Associated Lymphoid Tissue Lymphomas

Mucosa-associated lymphoid tissue (MALT) lymphomas represent around 8% of all non-Hodgkin lymphomas. They usually arise at extranodal sites with a distribution from the stomach (70%), lung (14%), ocular adnexa (12%), thyroid (4%) and small intestine (1%) (81). Histologically MALT lymphomas infiltrate the marginal zone and spread diffusely into the surrounding tissue. Their immunophenotype is CD20+, CD21+, CD35+, IgM+, IgD- (67). Usually MALT lymphomas show a very indolent disease course with a ten-year survival of 90% and a disease-free survival of 70% (82). However, in some cases, MALT lymphomas can progress and transform into aggressive extranodal diffuse large B cell lymphoma (eDLBCL) with a ten-year survival rate of approximately 42% (82). The different mechanism responsible for development of MALT lymphomas include translocations, trisomies, deletions, somatic mutations and chronic infections (83).

6.2.2.3 Chronic Lymphocytic Leukemia

According to the WHO, chronic lymphocytic leukemia is classified as mature B cell neoplasm characterized by an accumulation of monoclonal, small, mature CD5+ B lymphocytes - co-expressing CD19, CD20 and CD23 as well as low levels of surface

immunoglobulin - in blood, bone marrow and other lymphoid tissues (67, 72, 84, 85). CLL is in many cases an age-related disease with a median age of 70 years, whereby the molecular mechanisms still remain unknown with most of the cases being sporadic ones (72, 86, 87). The clinical course of CLL is extremely heterogeneous. Accordingly, survival of patients with CLL ranges from less than 1-2 years to over 15 years (88), with patients showing a greater proliferation rate have been found with a more aggressive disease (89) also presenting symptoms including fever, fatigue, weight loss and night sweats (90).

6.2.2.4 Morbus Waldenström

Waldenström Macroglobulinaemia (MW) or Morbus Waldenström is a type of indolent lymphoma first described in 1944 by a Swedish physician, who also acts as eponym of the disease. Characteristics of the disease are accumulation of monoclonal IgM positive B cells. Patients usually also present with bone marrow, lymph node and spleen involvement. Malignant B cells arise from memory B cells and express the pan B cell markers CD19, CD20, CD22 and CD79a, while CD5, CD10 and CD22 are missing. Genetic aberrations affecting the t(9;14) loci as well as rearrangements and mutations in *PAX5*, *CXCR4*, and *myeloid differentiation primary response 88* (*MYD88*) are hallmarks of this disease (67, 91, 92).

6.2.3 Aggressive B Cell Lymphomas

The most common types of hematological neoplasms in adults are aggressive B cell lymphomas. Aggressive B cell non-Hodgkin neoplasms include several subtypes of DLBCLs, Burkitt lymphomas (BL), follicular lymphomas grade IIIb, mantle cell lymphomas (MCL), B cell lymphoma unclassifiable with features intermediate between DLBCL and BL, and primary effusion lymphoma (PEL), whereby the first four types account for almost 50% of all lymphomas (70).

6.2.3.1 Mechanisms of Aggressive B Cell Lymphoma Development

Most B cell lymphomas arise from a malignant transformed and clonally expanded B cell in the germinal centers of secondary lymphoid follicles (93). This entails that B cells undergoing maturation processes are also prone to errors made during these processes, which ultimately give rise to malignant clones driving together with microenvironmental factors lymphomagenesis. The cellular origin represents an important feature of malignant B cells and is used for their classification. For instance, germinal center B cell like (GCB-DLBCL) show, like Burkitt lymphomas and follicular lymphomas, a gene signature representative of germinal center B cells (GC-B cells), while other activated B cell like/ non-germnial center B cell like (ABC-DLBCL/ NGCB-DLBCL) resemble activated B cells. Another important mechanism resulting in B cell lymphomagenesis are transformation events occurring during VDJ recombination, SHM, and CSR ultimately leading to juxtaposition of Ig loci to proto-oncogenes. Other genetic causes of lymphoma development include mutations in tumor suppressor genes like *tumor protein 53* (*p53*), amplifications and translocations not affecting immunoglobulin loci. Furthermore, viruses like Epstein-Barr virus (EBV) and human herpes virus 8 (HSV8) are implicated in lymphomagenesis. Last, BCR signaling and the tumor microenvironment contribute to the development of lymphoid neoplasms. While some lymphomas show dependence on the BCR or exhibit a chronic active BCR signaling, others do not express a functional BCR at all. Likewise, the surrounding cells influence lymphoma development depending on the subtype. In HL the microenvironment is indispensable for lymphomagenesis and forms the main part of tumor mass, while DLBCLs seem to be less dependent on the surrounding microenvironment (94, 95).

6.2.3.2 Diffuse Large B Cell Lymphomas

Diffuse large B cell lymphoma is the most common subtype of NHL, accounting for 30%-40% of all NHL cases in adults. Even though DLBCL occurs predominately at higher ages, a considerable part of children and adolescents also account for the high percentage of people developing DLBCL. With standard immunochemotherapy, aggressive B cell lymphoma, even at the advanced stage, is in many instances a curable disease. Nevertheless, around 40% of patients experience a relapse (96). DLBCL can develop *de*

novo or by transformation of indolent lymphomas like follicular lymphomas and CLL (97). Immunohistochemically, DLBCL cells express pan B cell markers like CD19, CD20, CD22, CD79a and PAX5. Other markers important for classification and risk stratification include CD10, BCL-6, BCL-2, CD5, CD30 CD43, IRF4/ melanoma associated antigen (mutated) 1 (MUM1), p53 and MYC (97). The hallmarks of DLBCL are chromosomal translocations and aberrant somatic hypermutation (ASHM) occurring during SHM and CSR in the GC reaction. Gene expression profiling of DLBCL samples showed that DLBCL can be subdivided in three different subtypes based on similarity in expression pattern to the cell of origin (COO); GCB-DLBCL, ABC-DLBCL, or in case of usage of an immunohistochemical algorithm NGCB-DLBCL, and primary mediastinal B cell lymphoma (PMBL) (98). While both GCB- and ABC-/NGCB-DLBCL cells originate from light zone B cells, GCB-DLBCL cells express higher levels of BCL-6 and CD10, lack IRF4 expression and show high SHM. In contrast, the ABC-/NGCB-DLBCL subtype lacks SHM and rather resembles more activated or plasmablastic B cells undergoing terminal differentiation (99, 100). Genetic inactivation of the histone modifying enzymes *CREB Binding Protein* (*CREBBP*) in 40% of all cases, of *mixed lineage lymphoma/ leukemia 2* (*MLL2*) in 30% of DLBCL cases, and to a lesser extent of *E1A Binding Protein P300* (*EP300*) are common for both subtypes. Mutations in *CREBBP* and *EP300* affect only one allele in the majority of cases and lead to impairment of *BCL-6* downregulation and *p53* activation. Thereby, favoritism of enhanced genomic instability occurs by constitutive *BCL-6* activation and repression of the anti-oncogenic effect of *p53* (101, 102). Mutations in *MLL2* are less well characterized and seem to have a broad effect on epigenetic regulatory mechanisms. Interestingly, genetic modifications of *MLL2* together with mutations in *CREBBP* are characteristic for transformed FL even before the transformational event occurs (103, 104). Another hallmark of DLBCL is deregulation of *BCL-6*. Several direct and indirect mechanisms target *BCL-6* and thus lead to its dysfunction. First, around 35% of patients harbor chromosomal rearrangements of *BCL-6* resulting in its expression instead of downregulation during the late phase of the GC reaction. Even though this type of mutation affects both subtypes, the frequencies of *BCL-6* chromosomal translocations are higher in the ABC-/ NGCB-DLBCL subtype. In contrast, point mutations, seen in >70% of cases are rather observed in the GCB-DLBCL subtype (105). Mutations occurring during SHM may on the one hand disrupt the negative

autoregulation of *BCL-6* itself or on the other hand prevent binding and transcriptional repression of *IRF4* in the CD40 signaling pathway (57, 106). As above mentioned, *CREBBP/EP300* loss indirectly affects *BCL-6* downregulation. Furthermore, gain-of-function mutations in *MEF2B* and loss-of-function mutations in *F-Box Protein 11* (*FBXO11*) give indirectly rise to higher *BCL-6* expression levels (99). Other genetic lesions shared between GCB- and NGCB-DLBCL are mutations in *p53* (103) and *Forkhead Box O1* (*FOXO1*), both being of prognostic value for risk assessment (107). Importantly, more than 60% of DLBCL cases lack cell surface expression of major histocompatibility complex (MHC) class I molecules. In this setting, inactivation of *β2 Microglobulin* (*β2M*), *CD58* and other genes encoding *human leukocyte antigen* (*HLA*) molecules occurs together with insufficient transport of these molecules to the cell surface. As a consequence, the lack of co-stimulatory molecules gives rise to immune escape of DLBCL cells from NK- and T cells (108). The GCB-DLBCL subtype is less well characterized regarding key lesions associated with disease. Chromosomal translocations of *MYC* (10% of cases) and *BCL-2* (40% of cases) analogous to those occurring in BL and FL are of poor prognosis if occurring together. Likewise, so called double hit (DH) or triple hit (TH) lymphomas affecting chromosomal translocations of *MYC*/*BCL-2* or to a lesser extent *MYC*/*BCL-6* and *MYC*/*BCL-2*/*BCL-6*, respectively, are restricted to the GCB-DLBCL subtype (109, 110). Additionally, around 20% of GCB-DLBCL patients harbor mutations in the *Enhancer of zeste homologue 2* (*EZH2*) gene. *EZH2* functions as a transcriptional repressor of genes involved in GC proliferation and gain-of-function mutations thus lead to impaired post-GC differentiation (111). Last, hindrance of cell migration out of the germinal center favors lymphomagenesis. Mutations in *Sphingosine-1-Phosphate Receptor 2* (*S1PR2*), *P2Y Purinoreceptor 8* (*P2RY8*), *G Protein Subunit Alpha 13* (*GNA13*), and *Rho Guanine Nucleotide Exchange Factor 1* (*ARHGEF1*) of the G protein α13 (Gα13) pathway result in its inactivation and restriction of B cells to the GC (112). In the ABC-/ NGCB-DLBCL subtype two important mechanisms contributing to lymphoma development have been characterized. Constitutive activation of the NF-κB pathway is representative for NGCB-DLBCL cells. Chronic active BCR signaling, mutations in the Toll-like receptor (TLR) pathway and mutations in negative regulators of NF-κB all converge in a deregulation of NF-κB. Chronically active BCR signaling requires activating mutations in the *caspase recruitment domain-containing protein 11* (*CARD11*).

Furthermore, mutations in the BCR receptor complex components *CD79B* and *CD79A* are present in 20% of ABC-/ NGCB-DLBCL cases and lead to attenuation of the BCR signaling pathway (113). Additionally, 30% of ABC-/ NGCB-DLBCL patients carry mutations in *MYD88* - a gene being involved in the TLR pathway. This mutation leads to spontaneous assembly of a protein complex containing the two kinases interleukin-1 receptor-associated kinase 4 (IRAK1) and IRAK4, thereby activating NF-κB. Moreover, this assembly leads to activation of the Janus Kinas (JAK)-signal transducer of activation 3 (STAT3) pathway, a typical type I interferon pathway (114). *TNF Alpha Induced Protein 3* (*TNFAIP3*, *A20*), which functions as a negative regulator of the NF-κB pathway, is found to be inactivated in around one third of NGCB-DLBCL samples and consequently leads to prolonged activity of the transcription factor (115). A further hallmark of ABC-/ NGCB-DLBCL cells is the prevention terminal differentiation. Mutually exclusive bi-allelic inactivation of *PRDM1*, acting as the master regular of terminal differentiation into plasma cells, or *BCL-6* translocations, mediating *PRDM1* repression, both can lead to inhibition of *PRDM1* function and thus blocked differentiation to antibody producing B cells (116, 117). These subtypes of DLBCLs are associated with distinctly different overall survival rates after chemotherapy (i.e Cyclophosphamide-Doxorubicin-Vincristine-Prednisone (CHOP) alone or immunochemotherapy based (i.e. Rituximab (R)-CHOP) regimens. While GCB-DLBCL patients show a favorable overall survival, patients with ABC-/ NGCB-DLBCL have worse prognosis (118, 119).

6.2.3.3 Burkitt Lymphomas

Dennis Burkitt first described the prevalence of rapidly growing tumors of the jaw and abdomen in children infected with malaria, what he at that time supposed to be round-cell sarcomas. Some years later it became clear that these malignancies were indeed lymphomas. The WHO currently classifies Burkitt lymphomas into three different clinical variants: the specific geographical variant of endemic (African) Burkitt lymphomas (eBL) and sporadic Burkitt lymphomas (sBL) occurring elsewhere. Compared to endemic BL, which are almost to 100% EBV positive, only 10-20% of sBL carry viral DNA. The third BL variant is related to human immunodeficiency virus (HIV) infections and thus termed immunodeficiency-related BL. In this variant around 40% of patients shows EBV infections. The annual incidence of eBL is 40-50 cases per million children under 18 and

represents up to 90% of all newly diagnosed lymphomas, while sBL have an incidence of 2 cases per 1 million children (120, 121). Burkitt lymphomas express CD20, CD79a as well as CD10 and BCL-6, whereas BCL-2 is usually not expressed (120). They arise from GC-B cells and show an extremely high proliferation rate with a doubling time of 24-48 hours. Expression of AID leads like in normal GC-B cells, to somatic hypermutation and class switch recombination. The hallmark of BL is the t(8;14) translocation juxtaposing *c-MYC* to the immunoglobulin heavy chain promotor leading to constitutive *c-MYC* expression. The t(8;14) translocation involves immunoglobulin switch regions indicating that the translocation arises from CSR (122, 123). While *c-MYC* is mutated in 70% of cases, mutations increasing the protein stability of *cyclin D3* (*CCND3*) are present in 38% of sBL but only 2% of eBL. Another important pathway in BL is the TCF3-Inhibitor of DNA Binding 3, HLH Protein (ID3) axis. *E2A* or its negative regulator *ID3* are mutated in 70% of sBL cases. TCF3 directly transactivates *CCND3* resulting in increased cell cycle progression and promotion of BCR signaling by immunoglobulin expression and *tyrosine-protein phosphatase non-receptor type 6 (PTPN6)* suppression. Furthermore, inactivating mutations in *p53* in 35% of all cases and BCR signaling involving phosphatidylinositide 3 kinase (PI3K) are common in Burkitt lymphomas (121, 123, 124). Clinical outcome is favorable in young people treated with high dose chemotherapy. Nevertheless, elderly people poorly respond to this therapeutic strategy so that currently new efforts like the use of BCR and PI3K inhibitors are under investigation (121).

6.3 The *EμMyc* Lymphoma Mouse Model

The *EμMyc* mouse model, first described in the mid-80s, is based on the genetic transfer of the proto-oncogene *c-Myc* coupled to the immunoglobulin heavy chain enhancer into the genome of C57BL/6Jx SJL/JF_2 recipients. Through mimicking the t(8;14) translocation present in Burkitt lymphomas, follicular lymphomas and CLL, this model recapitulates important features of human lymphomagenesis (125). Though being a spontaneous tumor model, mice develop rapidly malignant monoclonal lymphomas with a median of 12-16 weeks and besides, however to a lesser extent, lymphoid leukemias. Transgene expression is almost exclusively restricted to B cells of the pre-B cell lineage and to a lesser extent to mixed pre-B/ B cells and more mature IgM expressing B cells, respectively. Lymphomagenesis is characterized by enhanced *c-Myc*-driven B cell proliferation and concomitant enlargement of B cells, even ahead of birth. Pathologically, mice show disseminated lymphomas with enlarged spleens and lymph nodes, detectable already before disease onset. Notably, they develop thymomas originating solely and exclusively from B cells. Furthermore, dissemination into the lung and liver as well as swelling along the vertebral column are characteristic for this mouse model (126-128).

Despite acting as a proto-oncogene, *c-Myc* induced transformation is usually counterbalanced by either accumulation of p53 via the protein 19 ADP ribosylation factor ($p19^{ARF}$)-mouse double minute 2 (Mdm2)-p53 pathway or suppression of the anti-apoptotic genes like *Bcl-2* and *Bcl-2-Like 1* (*Bcl-xL*), both resulting in stimulation of apoptosis. As a consequence, a second hit, interfering with or disrupting these pathways is necessary to make *c-Myc* a driver of lymphomagenesis. In this setting, the $p19^{ARF}$–Mdm2-p53 pathway is inactivated by mutations arising in $p19^{ARF}$ and *p53* as well as overexpression of *Mdm2* (129). Furthermore, *c-Myc* cooperates independently with *Bcl-2*, *Bcl-xL* and other pro-apoptotic genes leading to hyperproliferative stimuli during early stages of B cell development (130-132).

6.4 Tumor immunology

6.4.1 The Immune System and its Components

The immune system serves to counteract invading pathogens thereby mediating immunity to the host. This comprises the concerted action of cells from the innate and adaptive immune system thereby leading to an appropriate immunological response. Discrimination of self and nonself is a key feature of innate and adaptive immunity. In contrast, these two systems differ in their specificity, receptors and cells involved in immune response.

6.4.2 Innate Immunity

The innate, or native, immune system is always present and responds to microbial pathogens, whereas nonmicrobial pathogens are not recognized by this system. The components of innate immunity recognize so called 'molecular patterns' for structures shared by several classes of microbes (pattern recognition receptors). Among them are the TLRs binding e.g. to bacterial products and double-stranded RNA (ds-RNA). The receptors involved in recognition are encoded in the germline and thus a specific cell line expresses the same receptors. This renders the innate immune systems a system with limited diversity and efficiency considering the sheer endless number of pathogens, however, makes it indispensable in the first line of defense upon pathogen encounter and stimulation of the adaptive immune system (133, 134).

6.4.2.1 Neutrophils

Neutrophils are myeloid cell-derived phagocytes produced continuously in the bone marrow and usually circulating through the blood with a short half-life. Upon microbial infection, they are recruited to sites of infection by chemo attractants, become attached through binding to endothelial adhesion molecules and transmigrate through the endothelium.

Recognition of microbial structures, especially those of bacteria and fungi, leads to activation, ingestion and killing of microbes. Traditionally neutrophils were thought to be just specialized in killing extracellular microbes, however, recent work showed that they play also a role in combating intracellular microbes, e.g. those infecting macrophages, and antigen trafficking. Neutrophils use oxygen independent molecules like lysozyme,

proteases and defensins as well as secretion of reactive oxygen and nitrogen species (respiratory burst). In order to avoid overwhelming immune reactions, they are subjected to apoptosis and subsequently ingested by macrophages. Lack or excess of neutrophil recruitment and activation leads to deficient or exacerbated immune responses. Hence, activation, secretion and elimination have to be tightly regulated (135-137).

6.4.2.2 Monocytes

Like neutrophils, monocytes derive from the myeloid lineage of hematopoietic precursors from the bone marrow. They circulate in blood and are recruited rapidly to sites of inflammation and also directly to lymphoid organs. Circulating monocytes have a reduced lifespan which is regulated by induction of apoptosis. Augmentation of monocyte lifespan can be induced upon differentiation into macrophages and dendritic cells. In homeostatic conditions and upon inflammatory stimuli like cytokines and microbial products monocytes get recruited, transmigrate through the endothelium, and differentiate into distinct cell populations depending on the surrounding cytokine milieu. Differentiated monocytes populate lymphoid and nonlymphoid tissue thereby exerting diverse roles in homeostasis, inflammation, and chronic disease. (138-140).

6.4.2.3 Macrophages

Macrophages derive from monocytes and together with them they are often called the mononuclear phagocyte system. They have, compared to monocytes, a longer lifespan and altered morphology and are found in connective tissue where they play an important role in host defense against pathogens, stimulation of the adaptive immune system and tissue remodeling (133, 141). Macrophages are cells involved in professional phagocytosis, antigen presentation to T cells and tissue repair. Expression of receptors specific for apoptotic cells and various pathogens like viruses, fungi and bacteria leads to their recognition and ingestion. Phagocytosis involves production of hydrogen peroxide (H_2O_2), reactive oxygen species and proteins i.e. cytokines and chemokines involved in the inflammatory response. Processed pathogens are transported and integrated in the macrophages cell membrane as MHC class II peptide complexes. This initiates cell-mediated immunity by antigen presentation to T cells. Activated macrophages secrete pro-

inflammatory cytokines like tumor necrosis factor α (TNFα), IL-6, IL-1 and Type I Interferons leading to enhanced inflammatory response and stimulation of the adaptive immune system in a feedback mechanism enhancing their proper activation (133, 139, 142).

6.4.2.4 NK cells

NK cells comprise about 15% of lymphocytes in blood and lymphoid organs. They resemble cytotoxic CD8+ T cells regarding their potent lysis of virus-infected or transformed cells. Development of NK cells is not dependent on the thymus, they lack - in contrast to Natural Killer T (NKT) cells - the T cell marker CD3, and activation and target cell killing is rather mediated by the concerted action of activating and inhibitory receptors expressed on the cell surface. In contrast to cytolytic T cells, NK cells are inhibited by expression of MHC I molecules. Downregulation of MHC I molecules is a common mechanism used by tumors and virus-infected cells in order to evade cytolysis by the adaptive immune system, rendering NK cells a potent counterpart of T cells in cell-mediated cytotoxicity. NK cell mediated killing is accomplished by exocytosis of cytoplasmic granules containing perforin and granzymes inducing apoptotic cell death of target cells. Furthermore, there exists a crosstalk between NK cells and other cell types. Production of interferon γ (IFNγ), TNFα and granulocyte−macrophage colony stimulating factor (GM-CSF) activates macrophages to effectively ingest and kill microbes. Activated macrophages produce IL12 in turn stimulating IFNγ production by NK cells. Immature dendritic cells (DC) are killed by NK cells in order to avoid improper stimulation of T cells and DCs in turn promote NK cell activation and cytolytic activity (133, 143, 144).

6.4.2.5 γδ-T lymphocytes

γδ-T cells build a bridge between innate and adaptive immunity and even though belonging to the T lymphocyte lineage they represent a counterpart to αβ-T cells. They comprise 1-10% of nucleated cell in blood (Vγ9Vδ2 cells) and are abundant in epithelial layers (Vγ9Vδ1). Blood γδ-T cells recognize low-molecular-weight compounds called phosphoantigens in an MHC-unrestricted manner. Intermediates of the 2-C-methyl-D-erythritol 4 phosphate (MEP) pathway of microbial isoprenoid synthesis as well as

aminobisphosphonates of the mevalonate pathway of eukaryotic isoprenoid synthesis, alkylamines and tumor cells activate γδ cells (145-149). Bisphosphonates like zoledronate and pamidronate are currently used in clinics to boost γδ-T cell responses against tumors (150, 151).

6.4.3 Adaptive Immunity

There exist two types of adaptive immunity protecting the host either from intra- or extracellular microbes. Cell-mediated immunity is carried out by T lymphocytes killing intracellular microbes while humoral immunity is mediated by antibodies produced by B cells against extracellular pathogens, thus preventing microbes to enter host cells. Several features distinguish the adaptive from the innate immune system. First, the adaptive immune response is specific. This is achieved by clonal selection of antigen receptors, each one specific for an antigen. Second, antigen encounter leads to clonal expansion of lymphocytes producing clones of the same cell. Third, memory lymphocytes mediate a more rapid and larger immune response upon repeated encounter of a certain antigen (133, 134).

6.4.3.1 αβ-T lymphocytes

αβ-T lymphocytes develop in the thymus by positive and negative selection to ensure elimination of T lymphocytes with too weak or too high binding affinities to self-MHC molecules. Antigen specificity is achieved by somatic recombination of T cell receptor genes during maturation. The antigen binding site consists of the variable regions of the α- and β-chains, respectively, while the constant domains of both chains are responsible for signal transduction and effector functions. In case of αβ-T lymphocytes efficient T cell development and function are mediated by association of the T cell receptor (TCR) with the CD3 complex, containing six chains termed ε-, δ- γ- and ζ, to form the TCR-receptor-complex. Recognition of antigen by T cells depends on binding of co-stimulatory molecules to MHC molecules expressed on cells harboring pathogens in their cytosol or cytoplasmic particles. CD8 or CD4 co-receptors on T cells bind to MHC class I or MHC class II molecules on infected cells, professional antigen presenting cells (APCs) and B cells, respectively, which present peptide fragments after prior internalization and

procession. This feature elicits specific immune responses adjusted to distinct kinds of pathogens. Likewise, proliferation and differentiation into cytotoxic effector cells needs co-stimulation by molecules expressed on APCs. Among those are the expression of B7.1 (CD80) and B7.2 (CD86) binding to CD28 on T cells. Following activation T cells express several stimulating and inhibitory molecules like IL2 and cytotoxic T-lymphocyte-associated antigen 4 (CTLA4), respectively, responsible for clonal expansion and conversion into effector cells. In contrast to strict co-stimulatory requirements before clonal expansion proliferating T cells differentiate without co-stimulation increasing their effector potential.

Specialization of αβ-T lymphocytes mediated immunity is furthermore achieved by specialization on distinct types of pathogens. CD8+ effector cells differentiate into cytotoxic lymphocytes whose primary function is to kill mainly virus infected cells in order to irradiate the origin of infection. Lysis of target cells is mediated mainly by cytoplasmic granules containing perforin, granzymes and Fas-Ligand (FasL) leading to apoptotic cell death. Contrary, the fate of CD4+ effector cells to differentiate into T_H1-, T_H2- or T_H17- T-helper lymphocytes is more likely determined by the kind of pathogen and surrounding inflammatory cytokine milieu. Both have in common that they recognize pathogens and its products processed in cytoplasmic particles. The principal function of T_H1-cells is to activate macrophages to kill ingested bacteria while T_H2-cells stimulate i.e. B cells to perform humoral immunity. Cytokines important for CD4+-mediated immunity regulate and fine-tune the immune system. Important cytokines and membrane bound proteins that mediate CD4+ effector functions are CD40-Ligand (CD40-L), GM-CSF, TNFα and IFNγ, which are also expressed by CD8+ T cells, as well as IL4, IL5 and IL-10 secreted by T_H2- cells (134, 152, 153)

6.4.3.2 B Lymphocytes

Arising from the same hematopoietic precursor as T lymphocytes, B cells mature in the bone marrow with the help of stromal cells. As their lymphoid counterparts their differentiation includes somatic recombination of immunoglobulin chains, negative-selection of self-recognizing B cells and ultimately migration to peripheral lymphoid organs (in detail described in chapter 6.1). The receptor of B cells resembles the T cell receptor, however, it can be secreted and shows variety in the constant regions. The

secreted form of the B cell receptor is called antibody. In the membrane bound form the B cell receptor binds to one Igα and one Igβ-chain responsible for signal transduction of the BCR-receptor-complex. Mature B cells express IgM on their surface. Antigen stimulation leads to differentiation to plasma cells accompanied by isotype switch with consequent production of membrane-bound and soluble immunoglobulins of different classes (IgM, IgD, IgE, IgA and IgG). Activation is regulated by T_H1 cells and recognition of antigen without need of prior procession. Antibodies secreted by plasma cells are responsible for neutralization of pathogens and opsonization stimulates phagocytosis of pathogen, while formation of memory B cells mediates a rapid response upon repeated encounter with an antigen (134).

6.4.4 Immunoregulation

During the past decades cancer epidemiologists have identified several major risk-factors contributing to cancer development and progression, thereby giving insight not only into the genetic predisposition of cancer development but also highlighting environmental and lifestyle caused factors (154). In the 1980s, the discovery of Warren and Marshall, who showed that chronic *Helicobacter pylori* infection may cause gastric cancer shed light on the connection between chronic infection and inflammation and cancer development (155). The concept that the immune system recognizes and eliminates transformed cells was first postulated by Paul Ehrlich in 1909 (156) and not modified until the late fifties with the upcoming field of immunology. Burnet and Thomas were the ones who proposed in 1957 and 1959, respectively, that the primary function of the immune system is to protect from cancerous cells through a immunosurveillance mechanism (157, 158). However, this theory was discarded again in the 1980s where studies from Stutman and others showed that there was no difference in tumor development between wildtype and athymic nude mice, which to that time point apparently were lacking T- and B cells (159-161). Resumption of the theory and final evidence that the immune system is indispensable for the elimination of cancer cells came by the generation *Rag-1* and *Rag-2* knockout mice, respectively, which completely lack NKT cells, T- and B cells (162). Two studies clearly demonstrated that mice lacking these immune cells are more likely to develop chemically induced and, importantly, spontaneous tumors and that different cells of the immune system have a synergistic effect in cancer immunosurveillance (163, 164). Recent data led

to refinement of the cancer immunosurveillance theory now known as cancer immunoediting. The process involves three phases defined as elimination, equilibrium, and escape. During the elimination phase cells of innate and adaptive immunity efficiently target and lyse tumor cells. During the equilibrium phase tumor cells develop mechanisms by which several tumor variants show increased resistance to immune attack while others are eliminated by the immune system, thereby giving rise to tumor persistence under the regulatory control of the immune system. In the final phase, tumor cells expand in an uncontrolled manner and actively disable recognition by the immune system. Tumors have evolved several mechanisms by which they try to evade the immune system. Among them are downregulation of the antigen processing machinery and antigen expression on the cell surface. Generally, tumors create a tolerogenic environment in order to suppress recognition and elimination by the immune system. Promotion of regulatory T cells (Tregs), suppressing cytotoxic T cell functions and APCs, attraction of myeloid-derived suppressor cells (MDSC) and tumor-associated macrophages (TAMs) all serve the tumor to evade the host's immune system (165-167). In humans, participation of the immune system in malignant transformation of cells was first described in immunosuppressed patients and people suffering from immunodeficiencies who showed a higher risk of viral-associated tumors (168). Furthermore, evaluation of *de novo* malignant transformations in transplant patients clearly demonstrated the higher prevalence of tumor formation without any known viral etiology in immunosuppressed individuals, thereby confirming the role of immunosurveillance in cancer epidemiology (169, 170).

6.4.5 Immune Checkpoints in Health and Disease

One important group of immunostimulatory molecules is represented by the CD80/CD86–CD28/CTLA4 superfamily. In T cell physiology, this family is one of the prime examples of how coreceptor-ligand binding regulate T cell activation and repression. While CD28 is constitutively expressed on T cells and functions as a co-activator during T cell activation, its counterpart CTLA4 is upregulated upon T cell stimulation and inhibits prolonged responses by competing with CD28 for the same two ligands CD80 and CD86 (171, 172). Moreover, inducible T cell costimulator (ICOS) and inducible T cell costimulator ligand (ICOSL) (173)- both members of the CD28-B7 superfamily – enhance T cell activation. ICOS, present on T-helper type 1 and 2 (T_H1 and T_H2) cells is expressed upon TCR

engagement and important for co-stimulation of naïve and especially antigen experienced T cells (174-176). ICOS also participates in the germinal center reaction of T cell help to B cells and antibody class switch in humoral immune responses (177). CD25, the interleukin 2 receptor α chain, was first described in 1976 and forms part of a multi-subunit complex consisting of the interleukin 2 receptor α (IL2Rα), IL2Rβ (CD122) and γc (CD132) receptor subunits. Chrystal structure analysis revealed that binding of IL2 to CD25 leads to assembly and formation of the fully active receptor complex. CD25 is not expressed on resting but activated T cells and acts as a key molecule in transmitting pro-survival signals to proliferating T cells and other cells of the hematopoietic lineage. Nevertheless, its presence together with forkhead box P3 (FoxP3) is also a hallmark of Tregs, thereby preventing autoimmune reactions but also immunological reactions towards cancerous cells (178-180). Similarly, IRAK4, being part of the TLR/ interleukin 1 receptor signaling pathway, is important for proper immune function. Mutations in the IRAK4-dependent signaling pathway have been shown in ABC-DLBCL and Waldenström's Macroglobulinaemia (181, 182). In analogy to the CD28/CTLA4 pathway, CD226/ CD96/ T cell immunoreceptor with Ig and ITIM domains (TIGIT) form a way of activating and inhibiting T cell responses by competing with each other for the same ligands CD155 and CD112 with different affinities. Akin to CD28 and CTLA4, CD226, CD96 as well as TIGIT bind to CD155 while CD112 is bound solely by TIGIT and C226 (183). TIGIT is expressed on conventional $\alpha\beta$-T lymphocytes, various T cell subpopulations and NK cells, where it exerts an inhibitory function (184-186). Likewise T cell activation, increased late expression (TACTILE), also termed CD96, present on T-, NK- and NKT cells, has been identified as an immunosuppressive marker (187). In contrast, CD226 shares similarities with CD28 in boosting immune responses (188, 189). Further inhibitory signals playing a role in T- and B cell mediated immunity can be induced by binding of the tumor necrosis factor receptor 14 (TNFRSF14), better known as herpesvirus entry mediator (HVEM) (190), to its inhibitory receptors B- and T lymphocyte attenuator (BTLA, CD272) and CD160 (BY55). Two reports independently identified BTLA as the co-inhibitory receptor for HVEM (191, 192). The expression of BTLA is widespread on immune cells like B cells and T cells as well as antigen presenting cells and natural killer (T) cells, while CD160 expression is restricted to cytotoxic cells but not B cells or cells of the myeloid lineage (193-195). The ligand HVEM is expressed on almost all hematopoietic cells and

transmits inhibitory signals to cells upon binding to the aforementioned receptors (194, 196). Other important inhibitory pathways, which have already gained broad attention in clinic or are on the way of doing so are represented by programmed cell death 1 (PD1), binding to its ligands programmed cell death ligand 1 and 2 (PDL1 and PDL2), respectively, and T cell immunoglobulin and mucin-domain containing-3 (TIM3) binding to its ligand Galectin 9 (GAL9) (197-200). The immunosuppressive functions of TIM3 has first been identified on IFNγ secreting T_H1 and cytotoxic CD8+ T cells (201). Meanwhile it has been shown to be expressed on many solid and hematological neoplasms, where it is targeted together with other checkpoint inhibitors to restore exhausted cytotoxic T cells (202, 203). Besides, it has been shown to not solely inhibit T cells by additionally inhibiting tumor-infiltrating dendritic cells (204). The function of GAL9 in cancer is not restricted to binding of TIM3 but rather affects other mechanisms including apoptosis, cell cycle control, migration and metastases (205). Furthermore, lymphocyte activating gene 3 (LAG3, CD223), first isolated from an IL2-dependent NK cell line (206) is upregulated on activated T cells and furthermore expressed on plasmycytoid dendritic cells. In contrast to other immune checkpoints, LAG3 binds to MHC class II molecules, thereby resembling CD4 T cells with which it shares a similar structure. Nevertheless, it also associates with the CD3 receptor complex and is present on CD8 T cells (207, 208). Apart from the interplay of receptors and ligands expressed on immune cells and other cells of non-hematopoietic origin, cytokines play a key role in cell migration and cellular crosstalk. Interleukin 10 is an immunosuppressive cytokine produced by almost all lymphocytes and myeloid cells. Equally, it suppresses innate and adaptive immune responses by inhibiting proliferation of cells, antigen presentation and cytotoxic effector functions. IL10 plays important roles in autoimmune disorders and viral infections. Targeting IL10 to enhance immune reactions proved to be difficult due to its diverse sources and target cells (209, 210). Likewise, the transcription FoxP3 is characteristic for immunosuppressive processes. Natural and induced Tregs, expressing high levels of CD25 and FoxP3 (211), are indispensable for maintaining peripheral tolerance and inhibiting autoimmune reactions. Both belong to the CD4 T cell compartment and their regulatory function is based on direct and indirect interactions leading to suppression of effector T cells. Direct effects are mediated by deprivation of IL2 and production of IL10 and transforming growth factor β (TGFβ), while they indirectly suppress T cells by interaction with dendritic cells (212-

215). In contrast, IFNγ, a type II interferon, functions as one of the first cytokines produced in adaptive immunity to enhance cellular and humoral cytotoxicity (216). With respect to other cytokines and interleukins, members of the interleukin 12 family of cytokines consisting of interleukin 12, interleukin 23, and interleukin 27 share functional and structural aspects. Though all of the members being proinflammatory cytokines, their modes of action differ during infections, autoimmune disorders, and tumor development. All of them are multimeric proteins being formed by distinct subunits to be fully active. The IL-12p40 subunit is part of IL12 and IL23 and forms together with IL-12p35, the active form of IL12, while covalent linkage to IL-23p19 gives rise to IL23. IL27 is also a heterodimeric protein build of the two subunits IL-27p28 and Epstein Barr virus induced gene 3 (EBI3). The main function of IL12, produced by myeloid cells like DCs, macrophages as well as B lymphocytes upon TLR ligation is to enhance cellular cytotoxicity mediated by NK cells and T lymphocytes, their IFNγ production as well as differentiation of naïve T cells towards T_H1 cells (217, 218). IL12 represents an important bridge connecting innate and adaptive immune responses and is negatively regulated by other immunosuppressive cytokines like IL10 and TGFβ (219). In contrast, naïve T cells do not respond to IL23, which rather enhances a skewing of immune responses towards CD4+ memory cells. Furthermore, NK cells, monocytes and macrophages respond to IL23 (220, 221). Generally, its effects are similar to IL12, albeit the main difference between these two cytokines is the central role of IL23 in inducing differentiation of naïve CD4+ T cells into T_H17 cells producing high levels of interleukin 17A and IL17F. T_H17 cells are important for host defense against microbial pathogens but also major contributors to autoimmune diseases (222, 223). IL27, sharing similarities with IL12 and IL23 possesses furthermore structural relationship to the interleukin 6 family of cytokines (224, 225). Following IL6 signaling pathway, the IL27 receptor is composed of the gp130 subunit, like the interleukin 6 receptor, bound to WSX-1. The actions of IL27 resembles more those of IL12 than IL23. Il27 induces proliferation of CD4 cells, induces together with IL12 the production of IFNγ in naïve T cells and supports differentiation into the T_H1 lineage, which is enhanced upon TLR ligation on myeloid cells(226-228). Interleukin 21 regulates the function of lymphoid cells, NK cells and myeloid cells and is highly expressed on B cells whose differentiation and activation are highly regulated by this cytokine. IL21 enhances differentiation of B cells into plasma cells, its activation by anti-CD40 antibodies and

promotes class switch recombination to IgG1 (229, 230). Last, interleukin 16 was first identified to act as a chemoattractant produced by blood mononuclear cells. It is produced by T cells, DCs and eosinophils in a pro-form and cleaved by caspase 3 in an apoptosis-independent manner into a pro-molecule and mature part which is further secreted to bind to CD4 (231-233).

6.4.6 The Tumor Microenvironment in B Cell Lymphomas

A particular feature of tumor immunosurveillance and prevention of autoimmunity is the expression of inhibitory receptors - referred to as "immune checkpoints" - and their corresponding ligands (Figure 2) on distinct cell types of the immune system. The so-called tumor microenvironment, composed of tumor cells, surrounding immune cell infiltrates, extracellular matrix, stroma, and blood vessels modulates or suppresses immune cell function in order to preserve immune responses while preventing autoimmunity. Considerable improvements have been made in order to dissect the role of immune checkpoints in disease development. In many neoplasms, the tumor microenvironment is nowadays regarded rather a putative driver of cancer progression than a positive contributor to tumor cell clearance. Immune checkpoint blockade (ICB) using therapeutic antibodies targeting immune checkpoint inhibitors has led to enormous improvements in survival of patients, especially those suffering from diseases with high mutational load like melanomas, lung cancer and bladder cancer, where two of the inhibitory receptors, CTLA4 and PD1, were found to exhibit critical inhibitory effects on T cells. In the last years, novel "immune checkpoints" and their ligands (shown in Figure 2) have been identified, nevertheless many of them are remaining less well characterized (234-239).

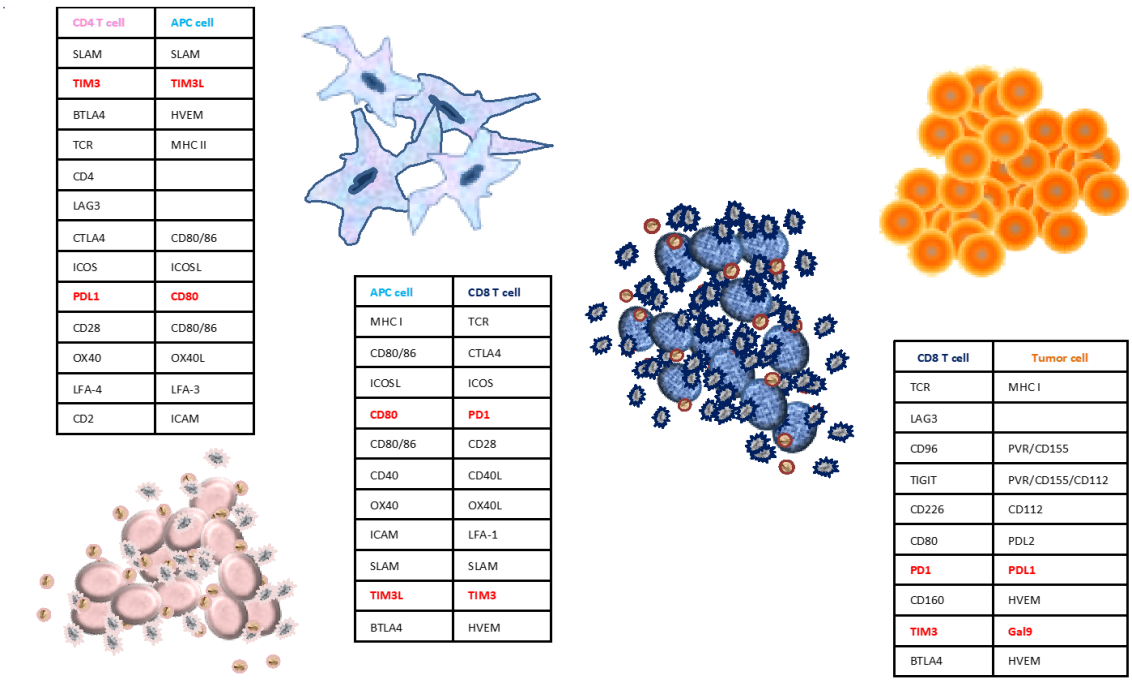

Figure 2: Immune checkpoints expressed on immune and tumor cells.

Adapted by permission from Springer Nature Customer Service Centre GmbH: on behalf of Cancer Research UK: :Spinger Nature. British Journal of Cancer. Hallmarks of response to immune checkpoint blockade. Cogdill AP, Andrews MC, Wargo JA (234). ©Springer Nature. 2017

The influence of the tumor microenvironment on disease development in solid and hematological neoplasms is defined by the genetic aberrations of tumor cells, the dependence of tumor cells on external stimuli and the hosts' immune response. In B cell lymphomas, three patterns have been described to contribute differentially to disease progression. Re-education is a process characterized by dependence of lymphoma cells on pro-survival and proliferation signals provided by the tumor microenvironment. This is exemplified in FLs, where low expression of PD1, high Treg cell infiltrates, and increased numbers of TAMs lead to exhaustion of infiltrating immune cells and thus negatively contribute to disease outcome, while maintaining a rather normal tissue distribution (240-242). Another process termed recruitment is a hallmark of classical Hodgkin lymphomas. In this tumor type, malignant Hodgkin Reed-Sternberg (HRS) cells account for only <5% of the tumor, while the remaining tumor mass is composed of immune cells, resulting in a

distinct tissue composition as opposed to FLs. Third, effacement is seen in BLs and also DLBCL. Here, genetic alterations lead to a rather tumor microenvironment-independent proliferation of malignant cells (68, 95). Hence, based on the curative potential of adoptive immunotherapy through allogenic stem cell transplantation in hematologic neoplasms, clinical trials of ICB are currently ongoing, especially in the context of B cell lymphomas (243). In follicular lymphomas, high numbers of PD1 expressing regulatory lymphocytes were associated with a good prognosis (240). While PD1 is expressed on T cells, PDL1 is typically expressed on tumor cells (197, 234). Importantly, PDL1 expression has been shown recently for DLBCL cells and its expression was associated with the more aggressive NGCB subtype (244, 245). Blockage of the PD1 pathway was associated with high response rates seen in heavily pretreated Hodgkin B cell lymphoma patients (243), based on a frequent amplification of the gene locus (9p24.1) causing *PDL1* and/or *PDL2* overexpression (246). Moreover, *PDL1* and *PDL2* are overexpressed by *Janus kinase/ signal transducer and activator of transcription* (*JAK/STAT*) amplification (246) or by EBV infection in Hodgkin B cell lymphoma (247). In DLBCL, *PDL1* but not *PDL2* is overexpressed due to genetic alterations affecting the 9p24 locus (244, 248). Though being obviously less dependent on the tumor microenvironment compared to FL or HL, promising results have been published in early phase clinical trials targeting immune checkpoints in DLBCL (181, 200, 249, 250). Blockade of PD1 with Pidilizumab, Nivolumab and Pembrolizumab – alone or in combination therapy - shows promising results in clinical trials targeting diffuse large B cell lymphomas of nodal and extranodal origin as well as those lymphomas developed from indolent CLL by Richter Transformation (200, 249-252).

6.5 The Nur77-Family

The *Nur77*-family of nuclear orphan receptors is comprised of the three members *Nuclear Receptor Subfamily 4 Group A Member 1* (*NR4A1, Nur77*), *NR4A2* (*Nurr1*), and *NR4A3* (*Nor-1*). All members have a homologous amino acid sequence with an N-terminal activation function domain (AF-1), a subsequent DNA binding domain (DBD), and the ligand binding domain (LBD). The C-terminal domain harbors a second but dispensable activation function domain (AF-2). While the amino acid sequence of the DBD (91-95%) and LBD (60%) is well conserved among the three members, AF-1 mediating transactivation shows a variant sequence. NR4A1, NR4A2, and NR4A3 have a diverse expression pattern in distinct tissues like skeletal muscle, adipose tissue, heart, kidney, brain, and T cells. As immediate early- or stress response genes *Nur77* family members become activated by several external physiological stimuli like stress, prostaglandins, inflammatory responses, hormones, neurotransmitters, growth factors, and calcium. Nevertheless, no specific endogenous ligand has been characterized yet, so that the family members are specified as orphan receptors of the superfamily of steroid nuclear hormone receptors. The DNA binding domain contains a nuclear localization signal (NLS) thereby leading to nuclear localization of NR4As. Expression of target genes is mediated by binding of the DBD to the DNA consensus sequence AAAGGTCA termed NRBE or NGFI-B-responsive element as a monomer. Alternatively, the DBD can bind as dimer (homo- or heterodimer) to the sequence AAAT(G/A)(C/T)CA termed NurRE or Nur-responsive element (253-258). Transactivation of *Nur77* family members leads to diverse processes like regulation of apoptosis, inflammation, cell cycle control, metabolism, DNA repair mechanisms as well as tumor development in a cell context-dependent manner. The opposing roles of NR4As in pro-survival versus pro-apoptotic stimuli can be attributed to three different biological properties of these transcription factors: (1) Transactivation might lead to upregulation of target genes involved in survival and proliferation or (2) contrary to apoptosis. (3) Furthermore, translocation from the nucleus to the cytoplasm leads to mitochondrial targeting triggering apoptotic pathways (258-263).

6.5.1 NR4A1

Overexpression of *NR4A1* and its related transcriptional activity can lead to proliferation and malignant transformation in cancer cells (264-266). In contrast, NR4A1 can also exert pro-apoptotic functions. In T cells, *NR4A1* is induced upon TCR-mediated stimulation leading to apoptosis of T cells (262). Moreover, NR4A1 possesses non-genomic functions. These are based on the translocation of NR4A1 from the nucleus to the cytoplasm, where it binds to the hydrophobic groove. This in turn leads to a change in the conformation of BCL-2 converting it from an anti-apoptotic to a pro-apoptotic protein triggering cytochrome C release and apoptosis (267). Subcellular localization is regulated by posttranslational phosphorylation of NR4A1. While hyperphosphorylated NR4A1 is found in the cytoplasm, its hypophosphorylated counterpart is present in the nucleus (268). C-Jun terminal kinase (JNK), extracellular signal-regulated kinases 2 and 5 (ERK2, ERK5), protein kinase C (PKC), mitogen-activated protein kinases (MAPK), p90 ribosomal S6 kinase (RSK), protein kinase B (PKB, AKT), glycogen synthase kinase 3 (GSK3) as well as the DNA-dependent protein kinase are all able to phosphorylate NR4A1 within different positions of the amino acid sequence (258). Positive regulation of NR4A1 translocation to the cytoplasm is achieved via phosphorylation of its N-terminal residues by JNK (269), at Ser105 within the MAPK pathway (270), by ERK5 (271), and at Ser351 by AKT (272), which results in inhibition of its DNA binding ability and consequently to translocation of NR4A1 to the cytoplasm. Contrary, phosphorylation at Thr142 by ERK2 leads to retention of NR4A1 in the nucleus (273). Other important transcriptional and post-transriptional regulatory mechanisms affect NR4A1 expression levels. Apart from phosphorylation, protein interactions of NR4A1 with retinoid X receptor (RXR), hypoxia-inducible factor 1 α (HIF1α), NF-κB and thyroid hormone recptor-associated protein 220 (TRAP220) regulate *NR4A1* expression. Transcriptional control of *NR4A1* is influenced by histone deacetylases, acting as co-repressors of *NR4A1*. Repression is positively regulated by calcium flux, ERK5 and cyclic adenosine monophosphate/ cAMP response element-binding protein (cAMP/CREB). Furthermore, the Fos proto-oncogene c-FOS and positively affect *NR4A1* expression by binding to the AP-1 binding site of *NR4A1* (258, 274, 275).

6.5.2 NR4A1 and NR4A3 in Hematological Neoplasms

Involvement of NR4As in human diseases has been described for inflammatory and neurodegenerative diseases (253, 276). Moreover, they have been shown to be implicated in tumor development. Overexpression of NR4A3 caused by translocation has been detected in extraskeletal myxoid chondrosarcoma and in addition in transformed HeLa cells (277, 278). Contrary, in a murine model, *Nr4a1*/*Nr4a3* double knockout mice rapidly developed acute myeloid leukemia (AML) characterized by an increased expansion of hematopoietic precursor cells and decreased expression of *JunB proto-oncogene* (*JunB*) and *Jun proto-oncogene* (*cJun*). In human AML, these results could be confirmed as *NR4A1* and *NR4A3* were downregulated in leukemic blasts irrespective of karyotype (279). Another study confirmed these results using hypo allelic (*Nr4a1*+/- *Nr4a3*-/- and *Nr4a1*-/- *Nr4a3*+/-) mice. Mice with reduced gene dosage developed chronic myeloid malignancy recapitulating mixed myelodysplastic/ myeloproliferative neoplasm (MDS/MPN) in humans (280). Likewise, reduced *NR4A1* and *NR4A3* expression levels were found in solid tumors like follicular thyroid carcinomas and melanomas (281, 282). In lymphoid neoplasms, high expression of NR4A3 was shown in treated DLBCL patients with good response rates compared to those who were refractory to CHOP treatment (283). Furthermore, both transcription factors were found to be downregulated in indolent (CLL and FL) and aggressive (DLBCL and FLIIIb) lymphomas. Induction and/or overexpression of either factor, led to induction of apoptosis in tumor cells *in vivo* and *in vitro* and expression levels correlated to those of pro-apoptotic genes (258, 284, 285).

7 Material and Methods

7.1 Part I (reproduced and modified from Fechter K. *et al.* (286) with permission of Scientific Reports)

7.1.1 Patient Samples

Tumor specimens of 60 patients with DLBCLs, including 37 *de novo* and 23 transformed lymphoma samples, receiving a Rituximab containing regimen at the Division of Hematology, Medical University of Graz between 2000 and 2010 (with follow-up until May 2016, median follow up time: 5.84 years) were obtained from the Institute of Pathology, Medical University of Graz. All samples represented DLBCLs using the WHO classification (67). Based on the immunohistochemistry (IHC) profiles according to the Hans algorithm (287), all cases were classified as follows: 12 cases were categorized as germinal center subtype, 22 as non-germinal-center B cell like, and three as non-classifiable. In these three cases, re-classification was not possible because of lacking tumor material. As transformed DLBCL samples originating from FLs exhibited a similar expression pattern as GCB-DLCBL samples (288), 23 transformed DLBCL samples were added to this subtype (Table 7). For this retrospective study, we used patient specimens obtained for routine diagnostic procedures. Hence, no written informed consent of patients was obtained. This consent procedure was approved by the Ethical Committee of the Medical University Graz (No. 28-517 ex 15/16).

7.1.2 Survival Analysis

To test whether different levels of NR4A1 in the cytoplasm influence clinical outcome, we analyzed the association between histological NR4A1 abundance and clinical data of histologically-confirmed aggressive lymphoma patients (summarized in Table 7). Patients were categorized into two groups using as a cutoff the median percentage of lymphoma cells exhibiting NR4A1 in the cytoplasm (in the following termed low and high cytoplasmic NR4A1 expression). Survival analysis was performed in R 3.3.3 (289) using the R package 'survival' (290). Patients' cancer-specific survival was calculated with the Kaplan-Meier method, compared by the log rank test. Survival curves were visualized using the R package 'survminer' (291). P-values <=0.05 were considered as significant.

The Cox proportional-hazards model was applied to investigate the association between the survival time and clinico-pathological variables (cytoplasmic NR4A1 level, age, sex, and stage – univariate and multivariate analysis), thereby determining Hazard ratios (HRs), corresponding 95% confidence intervals (CIs) and p-values. The validity of the Cox proportional-hazards model (assessing the assumption of proportional hazards as well as testing for non-linearity) was checked using the R package 'survival' (290), survminer' (291) and 'Greg' (292). P-values <= 0.05 were considered as significant.

7.1.3 Immunohistochemistry

Formalin-fixed paraffin embedded tissue was stained after pre-treatment with Target Retrieval Solution (Dako, Glostrup, Denmark) using the staining kit K5001 (Dako, Glostrup, Denmark) and the automated stainer intelliPATH FLX® (Biocare Medical, Pacheco, CA, USA). Primary antibody to NR4A1 (clone E-6, 1:200, #sc-166166) was purchased from Santa Cruz (Dallas, TX, USA) and primary antibody to cleaved caspase 3 (clone 5A1E, #9664L) from Cell Signaling (Leiden, The Netherlands). To determine the IHC profiles according to the Hans algorithms, primary antibodies to CD10 (clone 56C6, 1:6, # NCL-CD10-270, Novocastra, Leica Biosystems, Wetzlar, DE), MUM1 (clone MUM1p, 1:50, #M7259, Dako, Glostrup, Denmark) and BCL-6 (clone GL191E/A8, 1:100, #227M-96, Cell-Marque, Newcastle Upon Tyne, United Kingdom) were applied. For control purposes, tissues known to contain the respective antigens were included (positive controls). Replacement of the primary antibody by normal serum always revealed negative results (negative controls). The percentage of lymphoma cells exhibiting cytoplasmic NR4A1 expression was independently determined by two pathologists. For cleaved caspase 3, positive cells were defined as positive cells per mm^2.

7.1.4 Isolation of Germinal Center B Cells as Non-Neoplastic Controls

Tonsils from young patients undergoing routine tonsillectomy were disaggregated and separated by Ficoll (GE Healthcare, USA). The specific monoclonal antibodies used were anti CD20-APC (clone 2H7, #559776, BD Biosciences, San Jose, CA, USA) and anti CD77-FITC (clone 5B5, #551353, BD Biosciences, San Jose, CA, USA).

Cells were sorted using the FACSAria (BD Biosciences, San Jose, CA, USA) into germinal center B cells (GC-B, CD20+, CD77+).

7.1.5 RNA Extraction

Total RNA was extracted using Trizol (Invitrogen, Thermo Fisher Scientific, Waltham, MA, USA) according to the manufacturer's protocol. cDNA was synthesized using the RevertAid™ H Minus First Strand cDNA Synthesis Kit (Fermentas, Thermo Fisher Scientific, Waltham, MA, USA).

7.1.6 Microarray Analysis

The dataset E-GEOD-10846 (Affymetrix GeneChip Human Genome U133 Plus 2.0) (293) was downloaded from ArrayExpress and analyzed in R 3.3.3 (289). By applying rma, the data was preprocessed with the R package 'affy' (294, 295), and the 200 clinical samples from R-CHOP-treated patients diagnosed with NGCB- or GCB-DLBCL were used for the analysis. The R package 'limma' (296) was applied to compute differentially expressed genes between the NGCB- and GCB subtypes, and the resulting p-values were adjusted for multiple testing with Benjamini and Hochberg's method to control the false discovery rate (297).

Genes with an adjusted p-value <= 0.05 and abs(log2FC) > log2(1.5) were used as input for the Gene Ontology (GO) analysis (959 unique genes with Entrez IDs). The R package 'GOstats' v.2.40.0 (298) was applied to compute hypergeometric p-values for overrepresentation of each GO term (biological process). Terms with a p-value <= 0.01 were considered as significantly enriched. Terms were filtered based on the distance to the root (>=14) to obtain informative terms. Pathway analysis based on a gene set enrichment analysis (GSEA) was conducted using the R package 'ReactomePA' v.1.18.1 (299) and Reactome pathways (v.1.58.0) with a p-value <= 0.05 were considered as significantly enriched.

7.1.7 Semi-Quantitative Real Time PCR

Semiquantitative real-time polymerase chain reaction (RQ-PCR) was done with the QuantiNova SYBR Green PCR Kit using an ABI Prism 7000 Detection system (Applied Biosystems, Foster City, CA, USA). QuantiTect primers assays depicted in Table 3 were bought from Qiagen (Hilden, Germany). *Glyceraldehyde 3-phosphate dehydrogenase* (*GAPDH*), *hypoxanthine-guanine phosphoribosyltransferase* (*HPRT*) and *peptidylprolyl isomerase A* (*PPIA*) served as housekeeping genes. Results are expressed as fold changes based on calculation $2^{-\Delta\Delta CT}$ and normalized to the geometric mean of the housekeeping genes. The cycling protocol included 34 cycles with activation at 95°C, followed by a denaturation step for 5 seconds at 95°C and an annealing/extension step for 10 seconds at 60°C. Melt curve analysis served to identify the different reaction products including nonspecific products.

Table 2: Thermal cycler amplification program for Real-Time PCR.

Step	Time	Temperature [°C]	Amplification Cycle
PCR initial activation step	2 min	95°C	1
DNA denaturation	5 sec	95°C	34
Combined annealing/extension	10 sec	60°C	
Melt curve analysis	5 sec	95°C	1
Melt curve analysis	5 sec	60°C	1

Table 3: Oligonucleotide sequences of primers for RQ-PCR.

Gene	Alternative Name	Assay Name	Reference
GAPDH3428-f *GAPDH3428-r*	Glyceraldehyde 3-phosphate dehydrogenase		AAG GTC GGA GTC AA C GGA TTT ACC AGA GTT AAA AGC AGC CCT G
HPRT1-f *HPRT1-r*	Hypoxanthine-guanine phosphoribosyltransferase		ATG GGA GGC CAT CAC ATT ATG TAA TCC AGC AGG TCA GCA A
PPIA-f	Peptidylprolyl isomerase A		CTC CTT TGA GCT GTT TGC AG
PPIA-r			CAC CAC ATG CTT GCC ATC C
ElF4E-f	Eukaryotic Translation Initiation Factor 4E		TGC GGC TGA TCT CCA AGT TTG
EIF4E-r			CCC ACA TAG GCT CAA TAC CAT C
ElF4EBP1-f	Eukaryotic Translation Initiation Factor 4E Binding Protein 1		CAC CCC GGG AGG TAC CAG GAT C
EIF4EBP1-r			CGC CCG CCC GCT TAT CTT CT
XPO1	Exportin 1	HS_XPO1_1_SG	#QT00045528
CDKN1B	Cyclin Dependent Kinase Inhibitor 1B	Hs_CDKN1B_2_SG	#QT00998445
CDKN1A	Cyclin Dependent Kinase Inhibitor 1A	Hs_CDKN1A_1_SG	#QT00062090
GADD45	Growth Arrest And DNA Damage Inducible Alpha	Hs_GADD45A_1_SG	#QT00014084
BCL6	B cell CLL/ Lymphoma 2	Hs_BCL6_1_SG	#QT00079233
CCNG2	Cyclin G2	Hs_CCNG2_1_SG	#QT00998193
CCNB1	Cyclin B1	Hs_CCNB1_1_SG	#QT00006615
CAT	Catalase	Hs_CAT_1_SG	#QT00079674
SOD2	Superoxide Dismutase	Hs_SOD2_1_SG	#QT 01008693
PLK1	Polo Like Kinase 1	Hs_PLK1_1_SG	#QT00049749
EGR3	Early Growth Response 3	Hs_EGR3_1_SG	#QT00246498
cFOS	Fos Proto-Oncogene, AP-1 Transcription Factor Subunit	Hs_FOS_1_SG	#QT00007070
BUB1	BUB1 Mitotic Checkpoint Serine/Threonine Kinase	Hs_BUB1_1_SG	#QT00082929
MXD1	MAX Dimerization Protein 1	Hs_MXD1_1_SG	#QT00082915
JUNB	JunB Proto-Oncogene, AP-1 Transcription Factor Subunit	Hs_JUNB_1_SG	#QT00201341
cJUN	Jun Proto-Oncogene, AP-1 Transcription Factor Subunit	Hs_JUN_1_SG	#QT00242956
ETV5	ETS Variant 5	Hs_ETV5_1_SG	#QT00009485

Gene	Alternative Name	Assay Name	Reference
DUSP1	Dual Specificity Phosphatase 1	Hs_DUSP1_1_SG	#QT00036638
CCL22	C-C Motif Chemokine Ligand 22	Hs_CCL22_1_SG	#QT00089817
CCR7	C-C Motif Chemokine Receptor 7	Hs_CCR7_2_SG	#QT01666686
CD44	CD44 Molecule (Indian Blood Group)	Hs_CD44_1_SG	#QT00073549
IL10	Interleukin 10	Hs_IL10_1_SG	#QT00041685
MMP2	Matrix Metallopeptidase 2	Hs_MMP2_1_SG	#QT00088396
FN1	Fibronectin 1	Hs_FN1_1_SG	#QT00038024
COL1A	Collagen Type I Alpha 1 Chain	Hs_COL1A1_1_SG	#QT00037793
CFLAR	CASP8 And FADD Like Apoptosis Regulator	Hs_CFLAR_1_SG	#QT00064554
ADARB	Double-stranded RNA-Specific Editase B	Hs_ADARB1_1_SG	#QT00081655

7.1.8 Statistical Analysis

Statistical analysis was performed using the IBM SPSS Statistics 23.0 (IBM, Vienna, Austria). P-values < 0.05 were considered statistically significant. The non-parametric Mann–Whitney U-test was used to analyze differences in the expression analysis. Fisher's exact test was used to determine whether the frequency of cytoplasmic NR4A1 was associated with any clinical parameter. Furthermore, Spearman correlation was applied to estimate the correlation of Caspase 3 and cNR4A1.

7.2 Part II

7.2.1 Mouse Models

C57/Bl6, B6.Cg-Tg(IghMyc)22Bri/J (*EμMyc*) and *Nr4a1*-/- mice for analyses of survival and tumor formation were bought from the Jackson Lab (Bar Harbor, ME, USA). Breeding and housing was performed under specific pathogen-free (SPF) conditions. To explore the role of *Nr4a1* in oncogene-driven B cell lymphoma development, mice deficient for *Nr4a1* were crossed with *EμMyc* transgenic mice and C57/Bl6 (wt) controls. Mice were monitored every other day until sings of hunched posture, ruffled fur, enlarged lymph nodes and other signs of overt disease. Upon tumor formation, mice were sacrificed under deep isoflurane anesthesia (#B 506, AbbVie Ltd., Berkshire, United Kingdom) by cervical dislocation. All animal work was done in accordance with a protocol approved by the Institutional Animal Care and Use Committee at the Medical University of Graz.

For transplantation of tumor cells, 4 weeks old male mice were used. 40 C57/Bl6 animals were bought from Janvier Labs (Le Genest-Saint-Isle, France) and 30 immunodeficient Fox Chase Scid Beige mice from Charles River (Sulzfeld, Germany). The Fox Chase Scid beige mouse model is characterized by both, autosomal recessive mutations in SCID (*Prkdcscid*) and beige (*Lystbg*). While the SCID mutation results in severe combined immunodeficiency affecting B- and T lymphocytes, the beige mutation results in defective natural killer cells (300). All animals were housed under SPF conditions. After acclimation of one week, mice were injected intravenously with $1x10^6$ tumor cells resuspended in 100µl sterile phosphate-buffered saline (PBS) (#10010056, Gibco, Thermo Fisher Scientific, Waltham, MA, USA). Mice were monitored on a daily base until onset of overt disease and sacrificed as described above.

7.2.2 Preparation of Single Cell Suspensions

Single cell suspensions were prepared for flow cytometric analysis and freezing of tumor tissue, respectively. For isolation of bone marrow, the tibia and femur of mice were cleaned from residual tissue and the bones were pounded in a mortar using Hank's balanced salt solution (HBSS) (#24020133, Gibco, Thermo Fisher Scientific, Waltham, MA, USA). To remove residual bones, the suspension was passed through a 70µM cell strainer (#352350, BD Biosciences, San Jose, CA, USA). For obtaining single cell

suspensions of spleen and tumor, the tissue was mashed using a 70µM cell strainer and HBSS. All single cell suspension were washed in HBSS and cells were pelleted at 500xg, 5min, RT. Supernatant was aspirated and the pellet was resuspended in complete Roswell Park Memorial Institute medium (RPMI 1640 medium) (#11875093, Gibco, Thermo Fisher Scientific, Waltham, MA, USA) containing 20% fetal bovine serum (FBS) (#10500064, Gibco, Thermo Fisher Scientific, Waltham, MA, USA) and 1% Antibiotic-Antimycotic (#15240062, Gibco, Thermo Fisher Scientific, Waltham, MA, USA). For flow cytometric analysis, cells were stained as described under points 7.2.3 – 7.2.5 and 7.2.9. Tumor cells were frozen in 90% complete RPMI 1640 medium containing 20% FBS and 10% CryoSure Dimethyl Sulfoxide (DMSO) (#WAK-DMSO-10, WAK-Chemie Medical GmbH, Steinbach, Germany) and stored at -80°C.

7.2.3 Apoptotic Assays

For detection of apoptosis by AnnexinV/ 7-aminoactinomycin D (7-AAD) staining, single cell suspensions were counted automatically using a CASY® Cell Counter and Analyzer (OLS OMNI Life Science, Bremen, Germany). 100µl single cell suspensions from tumor, bone marrow and spleen containing $1x10^6$ cells were blocked for 10 minutes at 4°C with 50µl RPMI 1640 medium containing 1.5µl TruStain fcX™ (anti-mouse CD16/32) antibody (#101320, Biolegend, San Diego, CA, USA). Subsequently, cells were stained with antibodies against IgM-eF450 (clone II/41, #48-9998, eBioscience, Thermo Fisher Scientific, Waltham, MA, USA), IgD-BV605 (clone 11-26c.2a, #563003, BD Biosciences, San Jose, CA, USA), CD19-BV510 (clone 1D3, #562956, BD Biosciences, San Jose, CA, USA) and CD43-APC (clone S7, #560663, BD Biosciences, San Jose, CA, USA), respectively. Cells and antibodies were mixed by vortexing. Following 30 minutes incubation at 4°C in the dark, cells were washed once with 100µl HBSS at 500xg, 5min, RT. Pellet was resuspended 100µl Annexin V Binding Buffer (#422201, Biolegend, San Diego, CA, USA) and 5µL Annexin V-APC (#640919, Biolegend, San Diego, CA, USA) were added. Cells were mixed by vortexing and incubated 15min at RT in the dark. Cells were diluted in 400µl Annexin V Binding Buffer and 5µL 7-AAD (#420403, Biolegend, San Diego, CA, USA) were added.

Cells were analyzed on an LSR II cytometer (BD Biosciences, San Jose, CA, USA) using BD FACSDIVA™ Software (BD Biosciences, San Jose, CA, USA).
Raw data were analyzed using FlowJo V10 software (FlowJo LLC, Ashland, OR, USA).
For detection of cleaved caspase 3, $1x10^6$ cells were blocked and stained with antibodies as described above. For cleaved caspase 3 staining, cell pellet was resuspended in 25µl 4% paraformaldehyde (#403052731, Gatt-Koller, Absam, Austria) for fixation. After incubation for 15min at RT, cells were washed with excess of 1x PBS at 500xg, 5min, RT. Permeabilization of cells was performed by adding slowly 300µl of ice-cold 90% methanol (#1.06007.2500 Merck, Darmstadt, Germany) under constant vortexing, followed by 30 minutes incubation on ice. Subsequently, cells were washed with excess of 1x PBS at 500xg, 5min, RT. Pellet was resuspended by pipetting in 100µl incubation buffer containing 0.5% bovine serum albumin (BSA) (# A9418, Sigma-Aldrich, Thermo Fisher Scientific, Waltham, MA, USA) in 1x PBS. 5µL anti-cleaved caspase 3 antibody (Asp175) (#9602, Cell Signaling, Leiden, The Netherlands) was added and cells were mixed well. Cells were incubated for 1h at RT protected from light. After washing with an excess of incubation buffer for 500xg, 5min, RT, pellet was resuspended by pipetting in 100µl incubation buffer. Cells were analyzed on an LSR II cytometer using BD FACSDIVA™ Software. Raw data were analyzed using FlowJo V10 software.

7.2.4 Determination of B Cell Subpopulations by Flow Cytometric Analysis

Single cell suspensions of bone marrow and spleen were counted automatically using a CASY® Cell Counter and Analyzer. 100µl single cell suspensions from tumor, bone marrow and spleen containing $1x10^5$ cells were blocked for 10 minutes at 4°C with 50µl RPMI 1640 medium containing 1.5µl TruStain fcX™ (anti-mouse CD16/32) antibody. Subsequently, cells were stained with antibodies against IgM-eF450 (clone II/41, #48-9998, eBioscience, Thermo Fisher Scientific, Waltham, MA, USA), IgD-BV605 (clone 11-26c.2a, #563003, BD Biosciences, San Jose, CA, USA), CD19-BV510 (clone 1D3, #562956, BD Biosciences, San Jose, CA, USA), CD43-APC (clone S7, #560663, BD Biosciences, San Jose, CA, USA), CD21-APC (clone 7G6, #558658, BD Biosciences, San Jose, CA, USA) and CD23-PECy7 (clone B3B4, # 25-0232-82, eBioscience, Thermo Fisher Scientific, Waltham, MA, USA), respectively. Cells and antibodies were mixed by vortexing.

Following 30 minutes incubation at 4°C in the dark, cells were washed once with 100µl HBSS. After centrifugation at 500xg, 5min, RT, supernatant was removed and the pellet was resuspended in 100µl HBSS. Prior to measurement, 3µl 7-AAD were added to each sample. Acquisition was performed on an LSR II cytometer using BD FACSDIVA™ Software. Raw data were analyzed using FlowJo V10 software.

7.2.5 Flow Cytometric Analysis of Tumor, Bone Marrow and Spleen

Blocking of single cells from tumor, bone marrow and spleen was done as described above. Subsequently, cells were stained with antibodies against IgM-eF450 (clone II/41, #48-9998, eBioscience, Thermo Fisher Scientific, Waltham, MA, USA), CD19-BV510 (clone 1D3, #562956, BD Biosciences, San Jose, CA, USA), B220-APC (clone RA3-6B2, #103211, Biolegend, San Diego, CA, USA) and TCR-FITC (clone H57-597, #11-5961-82, eBioscience, Thermo Fisher Scientific, Waltham, MA, USA), respectively. Staining, acquisition, and data analysis was performed as described above.

7.2.6 RNASeq

For RNASeq fresh frozen tumor material derived from *EµMyc Nr4a1*+/+, *EµMyc Nr4a1*-/- and wt mice (n=5 per group and genotype) as used. Total RNA was isolated from the tumors and RNA quality was determined on the Bioanalyzer. For barcoded library preparation a total of 500 ng RNA was used according to the Lexogen 3'QuantSeg manual. Sequencing reaction was performed on the Ion Proton with Hi-Q chemistry.

For bioinformatics analysis of the sequencing process, first the bases with bad quality scores were removed by processing the fastq reads through a quality control pipeline consisting of 3'adapter removal with Cutadapt (301) and quality trimming with Trimmomatic (302), whereby all reads shorter than 22 nucleotides were removed. These reads were then further used to be aligned to the *Mus musculus* mm10 genome using STAR in the first (303) and Bowtie in the second step (304). From the reads mapping to multiple locations in the genome, only the primary alignment was retained. In order to count the number of reads mapping to each gene, HTSeq-count (305) was applied and DEseq2 (306) was used to test for differential expression of the genes. In order to determine the differentially expressed genes, *EµMyc Nr4a1*+/+ vs. wt mice, *EµMyc*

Nr4a1-/- vs. *EμMyc Nr4a*+/+ and *EμMyc Nr4a1*-/- vs. wt mice, respectively were compared. The results were corrected for multiple testing using the incorporated Benjamini-Hochberg method (297). GO analyses were performed to determine the significantly up- and downregulated genes according to an adjusted p-value (<0.1) using BiNGO (307) in Cytoscape (308) and subsequent hypergeometrical testing gave a p-value if the enrichment terms associated with the genes. The resulting p-value was further corrected with the Benjamini-Hochberg method (297) with a significance threshold of p<0.1. Only the biological processes were investigated using the *Mus musculus* annotation as reference. As in BiNGO, a certain gene annotated with a GO term is included in all the parental terms, the resulting redundancy was removed by applying ClueGO (309), a Cytoscape (308) plug-in integrating GO terms and KEGG/ Reactome/ Wiki pathways. Hence, non-redundant biological terms could be visualized into a functionally grouped network. Up- and downregulated genes were both used together as an input for GO and Pathway analysis. Using kappa statistics calculation, the biological terms were grouped together based in their shared genes.

Finally, Genesis gave a z-score heatmap of the log transformed normalized counts of the intersect of the differentially regulated genes between the three distinct comparisons including 393 genes. Hierarchical clustering of both the samples and the genes using Euclidean distance revealed five clusters. Therefore finally, k-means clustering with k=5 using Eucledian distance was performed.

7.2.7 RNA Isolation and Preparation of cDNA

Total RNA extraction from primary and transplanted *EμMyc Nr4a1*-/- and *EμMyc Nr4a1*+/+ tumors was performed using the Qiagen RNeasy Mini Kit (Qiagen, Hilden, Germany) according to the manufacturer's protocol. Removal of genomic DNA from RNA preparations was done with the RNase-free DNase set (Thermo Fisher Scientific, Waltham, MA, USA) according to the manufacturer's instructions. Total RNA was transcribed into cDNA by using the RevertAid RT Reverse Transcription Kit (Thermo Fisher Scientific, Waltham, MA, USA) according to the manufacturer's instructions.

7.2.8 Semi-Quantitative Real Time PCR

RQ-PCR was performed with the QuantiNova SYBR Green PCR Kit (Qiagen, Hilden, Germany) using a Bio-Rad CFX96 Touch™ Real-Time PCR Detection System (Bio-Rad, Hercules, CA, USA). All samples were assayed in duplicates. *TATA-Box Binding Protein* (*Tbp*), *Hprt1*, *Ppia*, and *ßActin* (*Actb*) served as housekeeping genes. Results are expressed as fold changes based on calculation $2^{-\Delta\Delta CT}$ and normalized to the geometric mean of the housekeeping genes. QuantiTect Primer Assays for validation of deregulated genes are listed in Table 4 and 5 and were bought from Qiagen (Qiagen, Hilden, Germany).

Table 4: QuantiTect Primer Assays for validation of RNASeq.

Genes determined for validation of RNASeq. *Tbp*, *Hprt*, *Actb* and *Ppia* were used as housekeeping genes.

Gene	Alternative Name	Assay Name	Reference
Tbp	TATA-Box Binding Protein	Mm_Tbp_1_SG	#QT00198443
Hprt	Hypoxanthine Phosphoribosyltransferase 1	Mm_Hprt_1_SG	#QT00166768
Ppia	Peptidylprolyl Isomerase A	Mm_Ppia_1_SG	#QT00247709
Actb	β-Actin	Mm_Actb_1_SG	#QT00095242
Bcl2a1a	B cell leukemia/lymphoma 2 related protein A1a	Mm_Bcl2a1a_1_SG	#QT00142016
Bcl2a1d	B cell leukemia/lymphoma 2 related protein A1d	Mm_Bcl2a1d_1_SG	#QT00136465
Tnfsf11	Tumor Necrosis Factor Superfamily Member 11	Mm_Tnfsf11_1_SG	#QT00147385
S1pr5	Sphingosine-1-Phosphate Receptor 5	Mm_S1pr5_1_SG	#QT00282744
Cd226	CD226 Antigen	Mm_Cd226_1_SG	#QT01062187
Tnfrsf8	Tumor Necrosis Factor Receptor Superfamily Member 8	Mm_Tnfrsf8_1_SG	#QT00116599
Dll1	Delta-Like 1 (Drosophila)	Mm_Dll1_1_SG	#QT00113239
Gata3	GATA binding protein 3	Mm_Gata3_1_SG	#QT00170828
Ccl22	C-C Motif Chemokine Ligand 22	Mm_Ccl22_1_SG	#QT00108031
Il12b	Interleukin 12B	Mm_Il12b_1_SG	#QT00153643
Ptgs2	prostaglandin-endoperoxide synthase 2 (COX2)	Mm_Ptgs2_1_SG	#QT00165347

Gene	Alternative Name	Assay Name	Reference
Tnfaip3	Tumor Necrosis Factor, Alpha-Induced Protein 3	Mm_Tnfaip3_1_SG	#QT00134064
cFlip/ Cflar	CASP8 And FADD Like Apoptosis Regulator	Mm_Cflar_1_SG	#QT00171738
Bcl2	B cell CLL/Lymphoma 2	Mm_Bcl2_1_SG	#QT00156282
Ccnd1	Cyclin D1	Mm_Ccnd1_1_SG	#QT00154595
Irf4	Interferon Regulatory Factor 4	Mm_IRF-4_1_SG	#QT00109984
Ccr7	C-C Motif Chemokine Receptor 7	Mm_Ccr7_1_SG	#QT00240975
Cd96	CD96 Molecule	Mm_Cd96_1_SG	#QT00112959
Aicda	Activation Induced Cytidine Deaminase	Mm_Aicda_1_SG	#QT00123676
Ccl20	C-C Motif Chemokine Ligand 20	Mm_Icos_1_SG	#QT00261898
Icos	Inducible T cell Costimulator	Mm_Icos_1_SG	#QT00131579
Cd27	CD27 Molecule	Mm_Cd27_1_SG	#QT01077608
Havcr2	Hepatitis A Virus Cellular Receptor 2	Mm_Havcr2_1_SG	#QT00112427
Il7	Interleukin 7	Mm_Il7_1_SG	#QT00101318
Gcsam	Germinal Center Associated Signaling And Motility	Mm_Gcsam_1_SG	#QT00113225
Pdcd1	Programmed Cell Death 1	Mm_Pdcd1_1_SG	#QT00111111
Pdcd1lg2	Programmed Cell Death 1 Ligand 2	Mm_Pdcd1lg2_1_SG	#QT00136640

Table 5: QuantiTect Primer Assays for deregulated genes in primary and transplanted tumors.

Genes determined for deregulated genes in primary and transplanted tumors. *Hprt*, *Actb* and *Ppia* were used as housekeeping genes.

Gene	Alternative Name	Assay Name	Reference
Hprt	Hypoxanthine Phosphoribosyltransferase 1	Mm_Hprt_1_SG	#QT00166768
Ppia	Peptidylprolyl Isomerase A	Mm_Ppia_1_SG	#QT00247709
Actb	β-Actin	Mm_Actb_1_SG	#QT00095242
Cd80	CD80 Molecule	Mm_Cd80_1_SG	#QT00129787
Cd86	CD86 Molecule	Mm_Cd86_1_SG	#QT01055250
Lag3	Lymphocyte Activating 3	Mm_Lag3_1_SG	#QT00113197
Lgals9	Galectin 9	Mm_Lgals9_1_SG	#QT00173236
Hvem/ Tnfrsf14	TNF Receptor Superfamily Member 14	Mm_Tnfrsf14_1_SG	#QT00142184
Btla	B And T Lymphocyte Associated	Mm_Btla_1_SG	#QT00117635

Gene	Alternative Name	Assay Name	Reference
Cd155/ Pvr	Poliovirus Receptor	Mm_D7Ertd458e_1_SG	#QT00174034
Cd112/ Nectin2	Nectin Cell Adhesion Molecule 2	Mm_Pvrl2_1_SG	#QT00098280
Irak4	Interleukin 1 Receptor Associated Kinase 4	Mm_Irak4_1_SG	#QT00166453
Il2	Interleukin 2	Mm_Il2_1_SG	#QT00112315
Il21	Interleukin 21	Mm_Il21_1_SG	#QT00134358
Il27	Interleukin 27	Mm_Il27_1_SG	#QT00143017
Il10	Interleukin 10	Mm_Il10_1_SG	#QT00106169
Il16	Interleukin 16	Mm_Il16_1_SG	#QT00116550
Il17a	Interleukin 17a	Mm_Il17a_1_SG	#QT00103278
Cd25/ Il2ra	Interleukin 2 Receptor Subunit Alpha	Mm_Il2ra_1_SG	#QT00101108
Il12a	Interleukin 12a	Mm_Il12a_1_SG	#QT01048334
Il23a	Interleukin 23a	Mm_Il23a_2_SG	# QT01663613
Ifng	Interferon gamma	Mm_Ifng_1_SG	#QT01038821
Foxp3	Forkhead Box P3	Mm_Foxp3_1_SG	#QT00138369
Cd28	CD28 Molecule	Mm_Cd28_1_SG	#QT01058316
Icos	Inducible T cell Costimulator	Mm_Icos_1_SG	#QT00131579
Icosl	Inducible T Cell Costimulator Ligand	Mm_Icosl_1_SG	#QT00105805
Cd96	CD96 Molecule	Mm_Cd96_1_SG	#QT00112959
Cd226	CD226 Molecule	Mm_Cd226_2_SG	#QT01165738
Cd160	CD160 Molecule	Mm_Cd160_1_SG	#QT00125342
Tigit	T Cell Immunoreceptor With Ig And ITIM Domains	Mm_Tigit_2_S	#QT02372314
Tim3/ Havcr2	Hepatitis A Virus Cellular Receptor 2	Mm_Havcr2_1_SG	#QT00112427
Pd1/ Pdcd1	Programmed Cell Death 1	Mm_Pdcd1_1_SG	#QT00148617
Pdcd1lg1	Programmed Cell Death 1 Ligand 1	Mm_ Pdcd1lg1_1_SG	#QT00112427
Pdcd1lg2	Programmed Cell Death 1 Ligand 2	Mm_Pdcd1lg2_1_SG	#QT00136640
Ctla4	Cytotoxic T-Lymphocyte Associated Protein 4	Mm_Ctla4_1_SG	#QT00103929

The non-parametric Mann-Whitney U-test was used to identify statistical differences between gene expression levels using the IBM SPSS Statistics 23.0 (IBM, Vienna, Austria).

7.2.9 Flow Cytometric Analysis for Immune Cell Infiltrates of Tumor Cells

Specific immune cell infiltrates were analyzed on tumor cells derived from transplanted C57/Bl56 mice. Single cell suspensions were prepared and cells were subjected to cell surface and intracellular staining protocols. Marker molecules used for extra- and intracellular stainings are listed in Table 6.

Table 6: Markers used for flow cytometric analysis of tumor cells.

Marker	Clone	Reference	Company
CD45-AF700	30-F11	#103128	Biolegend
CD3e-BUV395	145-2C11	#563565	BD Biosciences
CD4-APC	RM4-5	#100516	Biolegend
CD8-PerCP/Cy5.5	53-6.7	#100734	Biolegend
γδTCR-PE-CF594	GL3	#563532	BD Biosciences
NKp46-BV510	29A1.4	#137623	Biolegend
CD19-PECy7	6D5	#115520	Biolegend
CD44-FITC	IM7	#103005	Biolegend
CD19-BV510	1D3	#562956	BD Bioscience
CD62L-BV605	MEL-14	#104438	Biolegend
PD1-BV421	29F.1A12	#135221	Biolegend
Tim3-PE	B8.2C12	#134003	Biolegend
FoxP3-PE	FJK-16s	#12-5773-82	eBisocience
RORγT-BV421	Q31-378	#562894	BD Biosciences

7.2.9.1 Cell Surface Staining

Single cell suspensions containing $5x10^6$ cells were prepared in PBS. Cells were centrifuged at 500xg, 5min, 4°C. Pellet was resuspended in 100µl PBS and mixed with 100µl Fixable Viability Dye-eFluor780 (#65-0865, eBioscience, Thermo Fisher Scientific, Waltham, MA, USA) (1:1000 diluted in PBS). Cells were pipetted to mix and incubated 30 minutes at 4°C in the dark. Afterwards cells were washed twice at 500xg, 5min, 4°C with 200µl staining buffer (PBS+2% FBS) and pellet was resuspended in 100µl IC Fixation Buffer (#00-8222-49, eBioscience, Thermo Fisher Scientific, Waltham, MA, USA). After an incubation step of 10 minutes at 4°C, 100µl staining buffer was added and cells were centrifuged twice at 500xg, 5min, 4°C. For antibody staining, cells were resuspended in 48.5µl staining buffer containing 1.5µl TruStain fcX™ (anti-mouse CD16/32) antibody

and blocked for 10 minutes at 4°C. Afterwards a total of 50µl staining buffer containing the respective antibodies was added and cell incubated for 30 minutes at 4°C in the dark. Cells were washed twice with 200µl staining buffer. For flow cytometric analysis, cells were resuspended in 50-100µl staining buffer.

7.2.9.2 Intracellular Staining

Single cell suspensions containing $5x10^6$ cells were prepared in PBS. Cells were centrifuged at 500xg, 5min, 4°C. Pellet was resuspended in 100µl PBS and mixed with 100µl Fixable Viability Dye-eFluor780. Cells were pipetted to mix and incubated 30 minutes at 4°C in the dark. Afterwards cells were washed twice at 500xg, 5min, 4°C with 200µl staining buffer (PBS+2% FBS) and pellet was resuspended in 100µl 1x TF Fix/Perm Buffer (#562725, BDBiosciences, San Jose, CA, USA) prepared according to the manufacturers' protocol. Cells were incubated for 40 minutes at 4°C in the dark and washed once with 100µl staining buffer. Afterwards 100µl 1x Perm/Wash buffer (#562725, BDBiosciences, San Jose, CA, USA) prepared according to the protocol were added to the pellet and cells were washed twice at 500xg, 5min, 4°C. For antibody staining, cells were resuspended in 48.5µl 1x Perm/Wash buffer containing 1.5µl TruStain fcX™ (anti-mouse CD16/32) antibody and blocked for 10 minutes at 4°C. Afterwards a total of 50µl 1x Perm/Wash buffer containing the respective antibodies was added and cells incubated for 30 minutes at 4°C in the dark. Cells were washed twice with 200µl 1x Perm/Wash buffer and subsequently once with 200µl staining buffer. For flow cytometric analysis, cells were resuspended in 50-100µl staining buffer.

7.2.10 Preparation of Tumor Cells for Injection

Tumor single cell suspensions were thawed rapidly in a 37°C water bath and washed once in 10ml RPMI 1640 medium containing 10% FBS and 1% Antibiotic-Antimycotic. Cells were centrifuged at 500xg, 5min, RT. Supernatant was removed and cells were resuspended in 1ml RPMI 1640 medium containing 10% FBS and 1% Antibiotic-Antimycotic. Cells were counted using a CASY® Cell Counter and Analyzer and $1x10^5$ cells were stained with 3µl 7-AAD to determine the percentage of dead cells. Flow cytometric analysis was performed was described above. The volume of cells corresponding to $1x10^6$ cells was centrifuged at 500xg, 5min, RT. The pellet was resuspended in 100µl PBS and cells were stored at 4°C until injection.

8 Results

8.1 Part I: Cytoplasmic NR4A1 in Diffuse Large B Cell Lymphomas (reproduced from Fechter K. *et al.* (286) with permission of Scientific Reports

8.1.1 Higher Cytoplasmic NR4A1 Correlates with the GCB-DLBCL Subtype and Increased Survival

In order to better understand the contribution of cytoplasmic NR4A1 location to survival and subtype in DLBCL, first a histologic examination of patient specimens in our cohort of DLBCL (n=60) was performed. With respect to the patients' characteristics, the genders in our cohort were almost equally distributed. (52% male vs 48% female patients). The cohort included more patients aged over 65, and more male patients were present in the patient cohort being under 65. Regarding the clinical parameters, there were more patients with elevated clinical stages according to the Ann Arbor classification. 35% showed involvement on both sides of the diaphragm (Ann Arbor stage III) and 23.3% showed involvement of extranodal sites (Ann Arbor stage IV). Moreover, four patient samples could not be classified due treatment in another center. Using the international prognostic index (IPI) - encompassing the age, Ann Arbor stage III to IV, serum LDH levels, ECOG performance status ≥2 and involvement of more than 1 extranodal site for tumor staging - more than half of the patients revealed an IPI of 1 or 2. 36.67 % of patients could be classified to the NGCB-DLBCL, having a worse prognosis, compared to 20% of patients being classified as *de novo* GCB-DLBCL (pGCB-DLBCL). Importantly, 38.33% of patients exhibited follicular lymphomas, which were due to transformation into the GCB-DLBCL (tGCB-DLBCL) further on characterized as such, while three patient samples (5%) could not be characterized to any subtype due to lacking histologic material (Table 7)

Table 7: Clinico-pathologic characteristics of patients included in the study.

Reproduced with modifications from Fechter K. *et al*. (286) with permission of Scientific Reports.

Clinico-pathologic parameters	Patients (n=60)	Proportion
Gender		
Male	31	52%
Female	29	48%
Age at diagnosis		
<65	27	45%
Male	15	55.6%
Female	12	44.4%
>65	33	55%
Male	16	48.5%
Female	17	51.5%
Ann Arbor Stage		
1	10	16.7%
2	11	18.3%
3	21	35%
4	14	23.3%
Unclassified	4	6.7%
IPI (International Prognostic Index)		
1	19	31.7%
2	14	23.3%
3	12	20%
4	11	18.3%
Unclassified	4	6.7%
Immunophenotype (Hans algorithm)		
NGCB-DLBCL	22	36.67%
pGCB-DLBCL	12	20%
tGCB-DLBCL	23	38.33%
Unclassified	3	5%

As we previously reported, *NR4A1* expression was significantly reduced in the NGCB-DLBCL subtype (284). As shown in Figure 3 a-d, a varying percentage of aggressive lymphoma cells (5-80%) exhibited cytoplasmic NR4A1 in stark contrast to their normal controls - germinal center B cells - in which no cytoplasmatic NR4A1 was found (on average 27.1% for NGCB- and 48.5% for GCB-DLBCL, $p<0.0048$, Figure 3a-d). Furthermore, we could not detect any significant differences in cytoplasmic NR4A1 abundance in *de novo* GCB-DLCBL compared to the transformed subtype (on average 41.7% vs. 52.4%, $p=0.19$, Figure 3d). For association of the cytoplasmic NR4A1 staining pattern with survival in our cohort of diffuse large B cell lymphomas, the patients were stratified using the median percentage of lymphoma cells (median=40%) exhibiting cytoplasmic NR4A. Results of the Kaplan Meier survival analysis showed that there was a significant association between high cytoplasmic NR4A1 levels and favorable cancer-specific survival ($n=60$, $p=0.016$, log-rank test, Figure 3e).

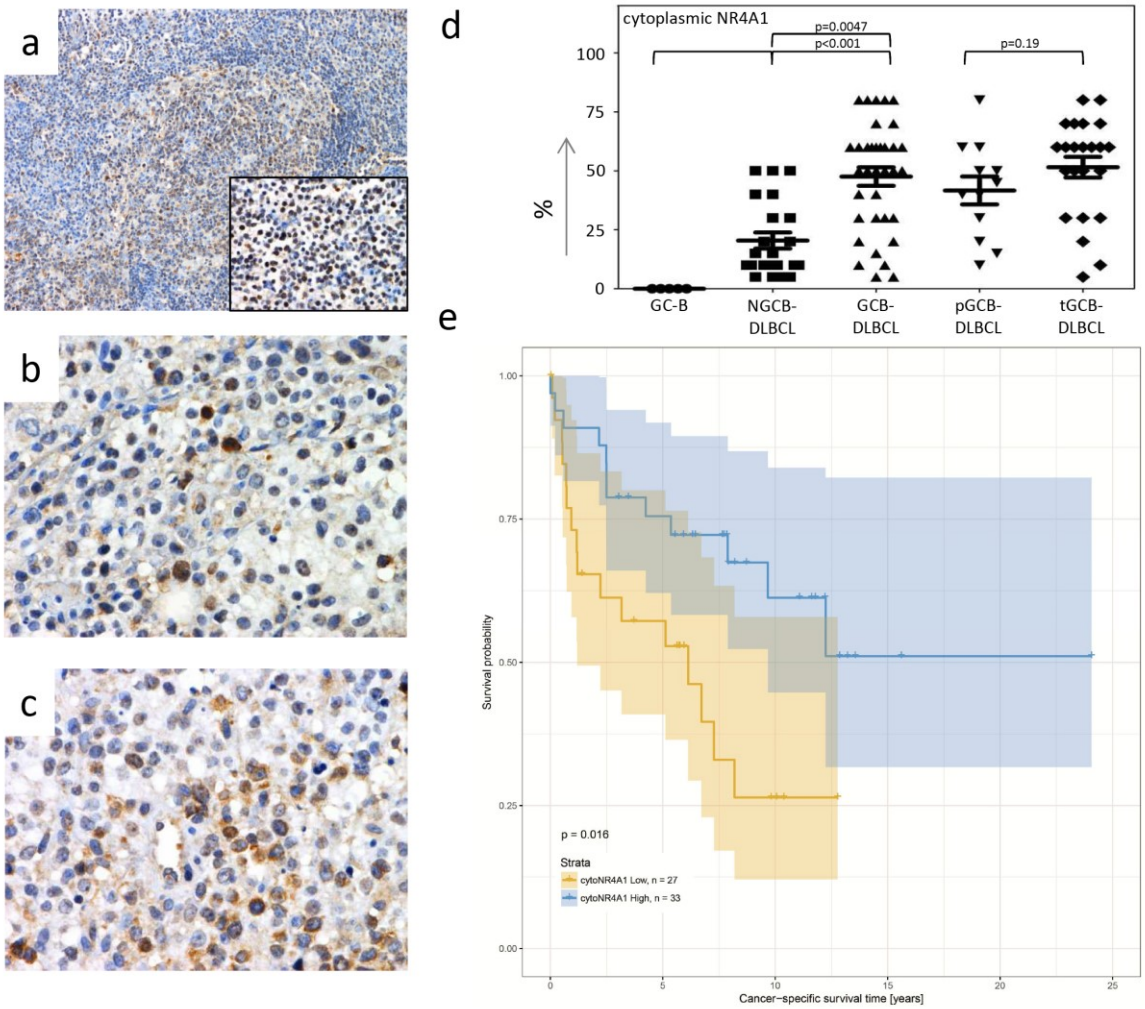

Figure 3: Immunohistochemical NR4A1 analysis and overall survival.

(a-c) NR4A1 expression in (a) non-neoplastic lymph nodes (magnification x100 for the overview and magnification x400 for the big picture), (b) NGCB-DLCBL (magnification x400) and (c) GCB-DLBCL (magnification x400) (35) determined by immunohistochemical analysis. All images were captured by using an Olympus BX51 microscope and an Olympus E-330 camera. (d) Distribution of the cytoplasmic levels of NR4A1 in GC-B (n=5), NGCB- (n=22)- and GCB-DLBCL (n=35) consisting of GCB-DLBCL (pGCB-DLBCL, n=12) and transformed (tGCB-DLBCL, n=23) GCB-DLBCL as two different subtypes of GCB-DLBCL. Each bar represents the mean values of cytoplasmic NR4A1 levels of each group ± standard error of the mean (SEM). (e) Kaplan Meyer graphical illustration of the cancer-specific survival classified by levels of cytoplasmic NR4A1 of all lymphoma patients. Patients with high cytoplasmic NR4A1 expression are shown in blue and with low cytoplasmic expression in yellow. Reproduced from Fechter K. *et al*. (286) with permission of Scientific Reports.

Applying the Fisher's exact test for significance testing, the more frequent high cytoplasmic NR4A1 expression in GCB-DLBCL compared to the NGCB-subtype could be confirmed (71.4% vs. 31.8%, p=0.0057, Table 8).

Table 8: Cytoplasmic NR4A1 expression in DLBCL.

The frequency of cytoplasmic NR4A1 expression was stratified by the median percentage of lymphoma cells exhibiting cytoplasmic NR4A1 expression (40%). Statistical calculation was performed using the Fisher's exact test. Reproduced from Fechter K. *et al*. (286) with permission of Scientific Reports.

	Low (<40%)	High (>40%)	p-value
NGCB-DLBCL	15	7	0.0057
GCB-DLBCL	10	25	

Furthermore, we used uni- and multivariate analysis for calculation of the Cox proportional hazards ratio. For the calculation, we omitted three cases, where we were not able to determine the specific lymphoma subtype (see Table 7). In either case, we detected subtype, age, cytoplasmic NR4A1 levels and tumor stage as independent prognostic factors, having a significant association with survival ($p<0.05$). However, advanced tumor stage (3 or 4), the NGCB subtype, increasing age and low cytoplasmic NR4A1 levels were corroborated to be of poor prognostic value.

Table 9: Cox Proportional Hazards Regression Analysis. Univariate and multivariate Cox proportional hazard ratio calculation.

Hazard ratios (HR) are stated for the 2nd group relative to the 1st group. Reproduced from Fechter K. *et al*. (286) with permission of Scientific Reports.

Univariate

	1st group, Ref	2nd group	HR	Lower 95% CI	Upper 95% CI	P-value	
Age	continuous		1.070	1.031	1.110	**0.0004**	***
Sex	male, n = 32	female, n = 25	0.641	0.296	1.388	0.2590	
Stage	1-2, n = 22	3-4, n = 35	1.520	0.682	3.388	0.3060	
cytoNR4A1	low, n = 25	high, n = 32	0.385	0.175	0.847	**0.0176**	*
Subtype	GCB, n = 35	NGCB, n = 22	9.556	3.743	24.390	**<0.0001**	***

Multivariate

	1st group, Ref	2nd group	HR	Lower 95% CI	Upper 95% CI	P-value	
Age	continuous		1.066	1.011	1.123	**0.0173**	*
Sex	male, n = 32	female, n = 25	0.533	0.189	1.503	0.2342	
Stage	1-2, n = 22	3-4, n = 35	2.735	1.006	7.439	**0.0487**	*
cytoNR4A1	low, n = 25	high, n = 32	0.378	0.148	0.966	**0.0422**	*
Subtype	GCB, n = 35	NGCB, n = 22	4.790	1.538	14.922	**0.0069**	**

This indicates that cytoplasmic location of NR4A1 influences survival of DLBCL patients and that this can be related to its higher expression in the clinically less aggressive GCB-DLBCL subtype.

8.1.2 Transformed DLBCL Cases Have No Influence on the Correlation of Survival with the GCB-DLBCL Subtype, while *NR4A1* Expression Does

As 38.33% of patients exhibited transformed follicular lymphomas, we repeated the survival analysis omitting the tGCB-DLBCL cases. By stratifying this *de novo* DLBCL patient cohort - consisting of 21 cases with low and 16 cases with high cytoplasmic NR4A1- according to the median percentage of lymphoma cells exhibiting cytoplasmic NR4A1 (median=40%), we could again see a significant association between high cytoplasmic NR4A1 staining and favorable cancer-specific survival (n=37, p=0.036, log-rank test, Figure 4).

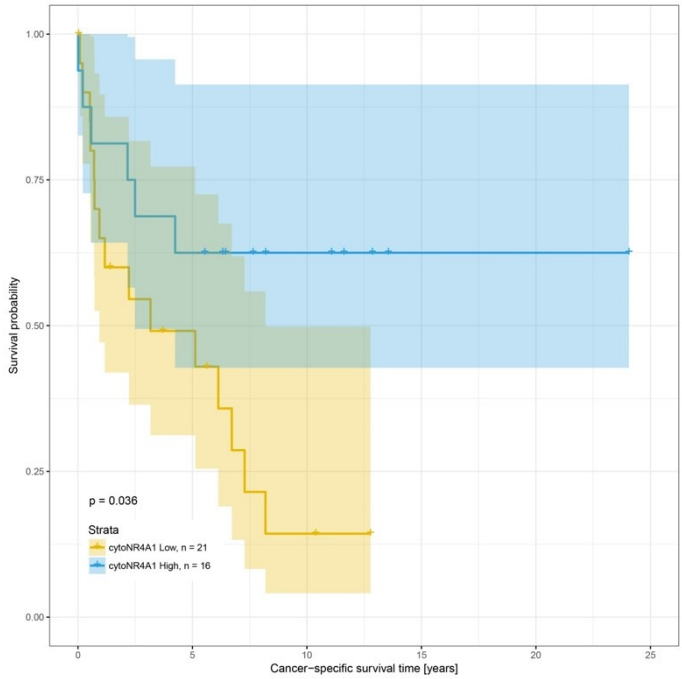

Figure 4: Kaplan-Meier graphical illustration of the cancer-specific survival of *de novo* DLBCL patients.

Kaplan Meyer graphical illustration of the cancer-specific survival classified by levels of cytoplasmic NR4A1 of *de novo* DLBCL patients. Patients with high levels of cytoplasmic NR4A1 are depicted in blue and with low levels in yellow. Reproduced from Fechter K. *et al.* (286) with permission of Scientific Reports.

To investigate whether cytoplasmic NR4A1 is caused by high *NR4A1* expression, we further analyzed expression and protein content in the entire DLBCL cohort: In 30% (18/60) of all DLBCL cases and 35.1% (13/37) of *de novo* DLBCL cases, the *NR4A1* gene expression status (high vs. low) did not correspond to cytoplasmic NR4A1 expression (high vs. low). Survival analysis based on cytoplasmic NR4A1 abundance was statistically more significant than that based on *NR4A1* gene expression levels (p=0.016, compared to p=0.032, Figure 5a). Noteworthy, we could not observe any significant differences in survival when excluding the tGCB-DLCBL cases and stratifying based on *NR4A1* expression (n=37, p=0.108, log-rank test, Figure 5b).

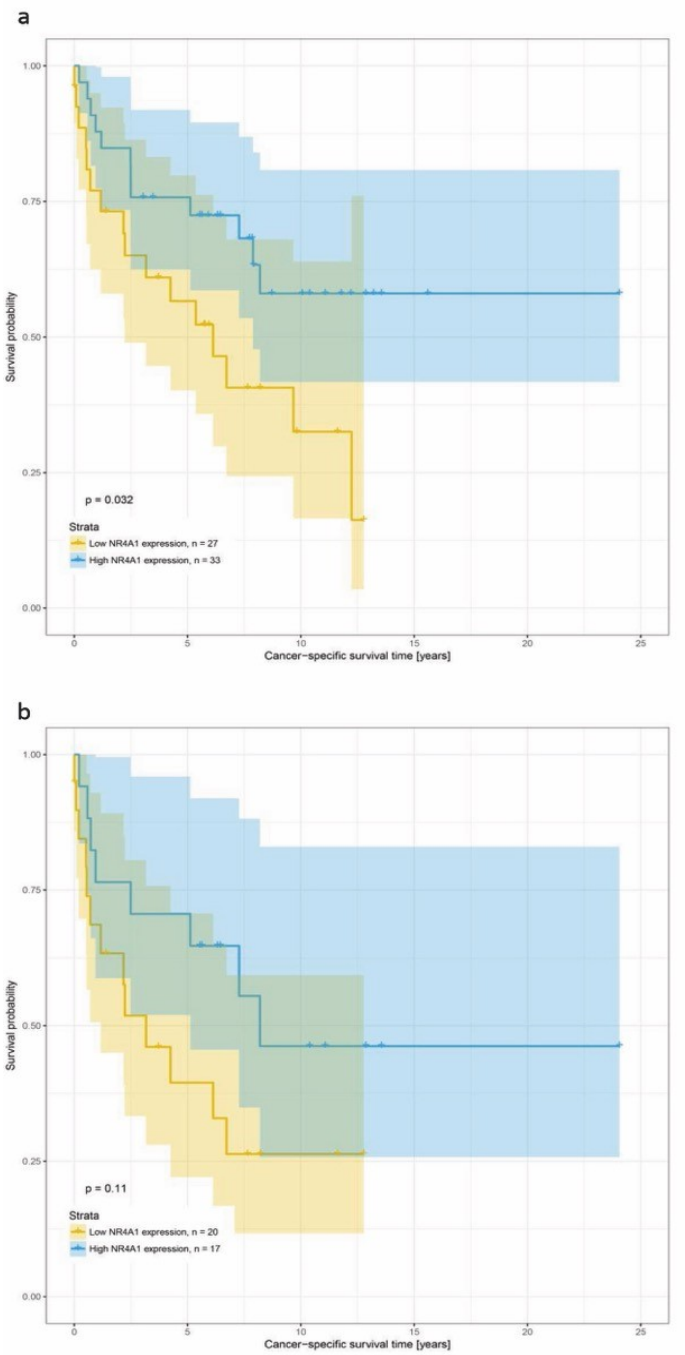

Figure 5: Kaplan-Meier graphical illustration of the cancer-specific survival classified by *NR4A1* expression of lymphoma patients.

(a) Kaplan-Meier graphical illustration of all DLBCL patients. High *NR4A1* expression correlates with better survival (p=0.032). (b) Kaplan-Meier graphical illustration of the *de novo* DLBCL patients. We have updated the figure to incorporate the extended follow-up time (p=0.11). Patients with high *NR4A1* expression are shown in blue and with low expression in yellow. Reproduced from Fechter K. *et al.* (286) with permission of Scientific Reports.

Taken together, these data suggest that high cytoplasmic NR4A1 levels might not be caused by high *NR4A1* expression levels and consequently other mechanisms influence higher protein abundance of NR4A1 in the cytoplasm.

8.1.3 Cytoplasmic NR4A1 Is Associated with Higher Occurrence of Apoptotic Lymphoma Cells

In several publications, the role of cytoplasmic NR4A1 in the induction of apoptosis has been investigated (263, 267). Therefore, we decided to further examine this pro-apoptotic function in our cohort of aggressive lymphomas and performed an immunohistochemical analysis of cleaved caspase 3. We found a significant correlation of cells showing cytoplasmic NR4A1 and cleavage of caspase 3 (spearman's rho=0.741, $p<0.001$). As shown in a representative IHC stain in Figure 6a, we were able to prove cleaved caspase 3 expression in both, the NGCB- and GCB-DLBCL subtypes. Further analysis comparing the number of positive cells/ mm^2 demonstrated a clear association with the GCB-DLBCL subtype. While there was no detectable cleaved caspase 3 expression in non-neoplastic control GC-B cells compared to GCB-DLBCL specimens ($p<0.001$), we detected a 3.3 fold higher expression of cleaved caspase 3 in GCB-DLBCL samples opposed to the NGCB-DLBCL subtype ($p=0.0041$, Figure 6b). A more detailed analysis of the distinct GCB-DLBCL types, either *de novo* or transformed, revealed no significant differences in the number of positive cells/ mm^2 exhibiting cleaved caspase 3 expression (pGCB- and tGCB-DLBCL, $p=0.506$, Figure 6b).

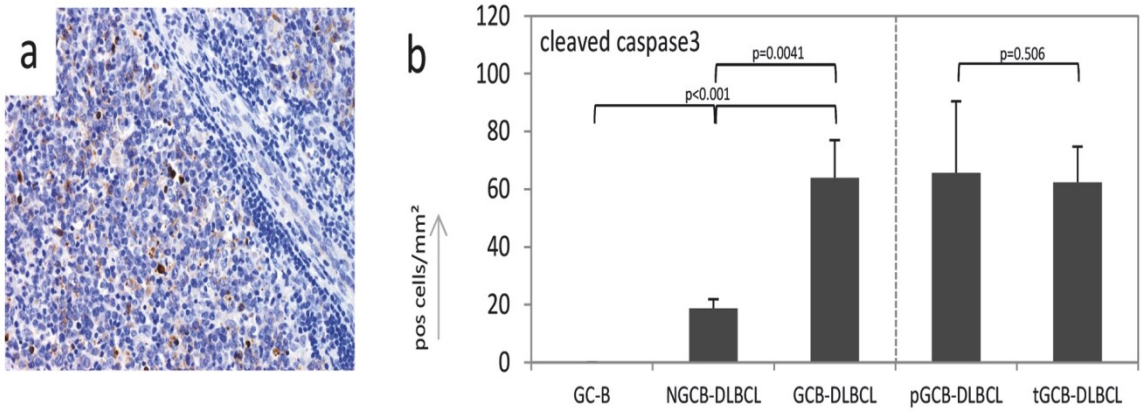

Figure 6: Immunohistochemical analysis of cleaved caspase 3.

(a) Immunohistochemical stain for cleaved caspase 3 in a representative GCB-DLBCL sample. (b) Number of cells exhibiting a cleaved caspase 3 depicted in cells/mm^2 in non-neoplastic GC-B (n=4), NGCB-DLBCL (n=19) and GCB-DLBCL (n=33) samples and samples of the two different GCB subtype namely primary GCB- (n=12) and transformed GCB-DLBCL (n=21). Each bar represents the mean values of each group ± standard error of the mean (SEM). Reproduced from Fechter K. *et al.* (286) with permission of Scientific Reports.

These data suggest that cytoplasmic NR4A1 is able to induce apoptosis and that this is in turn associated to the GCB-DLBCL subtype irrespective of its origin.

8.1.4 Exportin 1 Is Not Responsible for the Translocation of NR4A1 to the Cytoplasm

Exportin 1 (XPO1) is a crucial transporter of NR4A1, leading to its translocation to the cytoplasm (310). In order to find a possible relation of XPO1 and cytoplasmic NR4A1, we determined relative *XPO1* expression levels by means of semiquantitative RQ-PCR in relation to cytoplasmic NR4A1 abundance. Both, the GCB-DLBCL and NGCB-DLBCL subtype showed a significant higher expression of *XPO1* compared to GC-B cell controls (22.4 fold, $p<0.001$ for GCB-DLBCL, 19.8 fold $p<0.001$ for NGCB-DLBCL, Figure 7a). Nevertheless, we could not see any significant differences when comparing the NGCB-DLBCL with the GCB-DLBCL subtype ($p=0.611$, Figure 7a). Likewise, differentiation between the pGCB-DLCBL and tGCB-DLCBL subtype revealed no differences ($p=0.632$, Figure 7a). In addition, *XPO1* expression was comparable in lymphoma specimens with high and low cytoplasmic NR4A1 expression ($p=0.601$, Figure 7b).

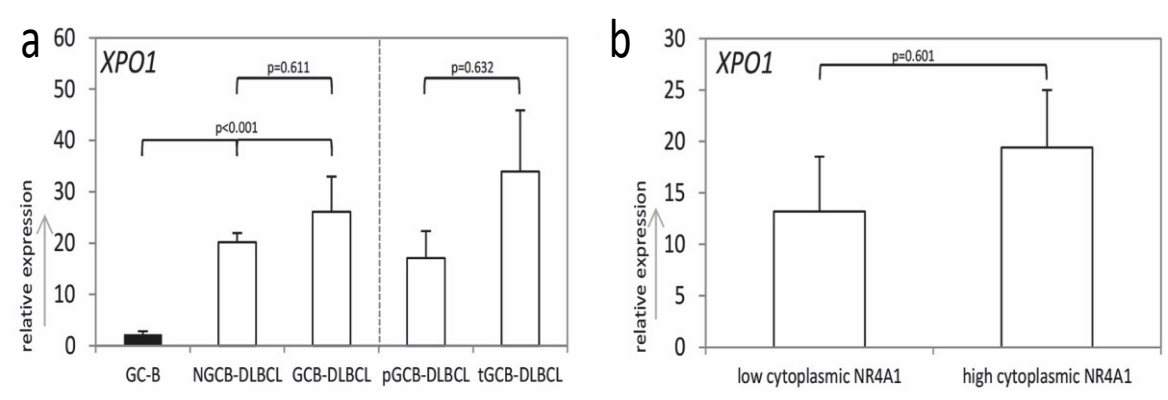

Figure 7: Expression levels of XPO1.

(a) Relative *XPO1* expression levels in non-neoplastic lymph nodes (GC-B) (n=4), NGCB-DLBCL (n=19), GCB-DLBCL (n=33) and the two different GCB subtype namely *de novo* GCB- (pGCB-DLBCL, n=12) and transformed GCB-DLBCL (tGCB-DLBCL, n=21) as determined by RQ-PCR. Each bar represents the mean values of expression levels ± standard error of the mean (SEM) (b) Relative *XPO1* expression levels as determined by RQ-PCR set of low (n=26) and high (n=26) cytoplasmic NR4A1 expression DLCBL. Reproduced from Fechter K. *et al*. (286) with permission of Scientific Reports.

Taken together, these results show that overexpression of *XPO1* is not the sole reason for the cytoplasmic localization of NR4A1 in aggressive lymphomas.

8.1.5 High Cytoplasmic NR4A1 Is Associated with Prominent Kinase Pathways in Aggressive Lymphomas

Based on the association of cytoplasmic NR4A1 expression levels with GCB-DLBCL (71.4% in GCB vs. 31.8% in NGCB, p=0.0057, Fisher's exact test, Table 8), we determined differentially expressed genes to identify the molecular mechansism causing cytoplasmic NR4A1. Therefore, we compared GCB- and NGCB-DLCBL cases in the publicly available dataset of Lenz *et al.* (119), containing samples from 200 R-CHOP-treated patients. A total of 959 genes were found to be differentially expressed based on an adjusted p-value <0.05 and abs(log2FC) > log2(1.5). For complementary functional profiling, a GO analysis was used together with gene set enrichment analysis of Reactome pathways. GO analysis led to 308 significantly enriched GO terms (p-value <= 0.01), with many of the terms being associated with immune response. Especially these terms were associated with immune response of B cells, being the result of differences in cellular

origin of the two DLCBL subtypes (GCB vs. NGCB). In agreement with the results of cleaved caspase 3, eleven out of 308 GO terms were related to apoptosis, suggesting a distinct regulation of apoptotic pathways in the two lymphoma subtypes. Besides, we found 15 GO terms to be associated with kinase activity and/or protein phosphorylation. A more detailed analysis of these kinase pathways revealed that four GO terms were associated with the extracellular signal-regulated kinase 1/2 (ERK1/2) or the MAPK cascade, and two GO terms with PKB/AKT signaling. Analysis of Reactome pathways gave 110 significantly enriched pathways (q-value <= 0.05). In this analysis, the PI3K/AKT activation', 'phosphatidylinositol (3,4,5) triphosphate (PI3P) activates AKT signaling', 'PI3K/AKT Signaling in Cancer', and 'Constitutive Signaling by aberrant PI3K in Cancer' pathways showed a significant different regulation in GCB- and NGCB-DLBCL. The enrichment map (Figure 8) shows these and other related pathways e.g. pathways associated with receptors that signal through AKT.

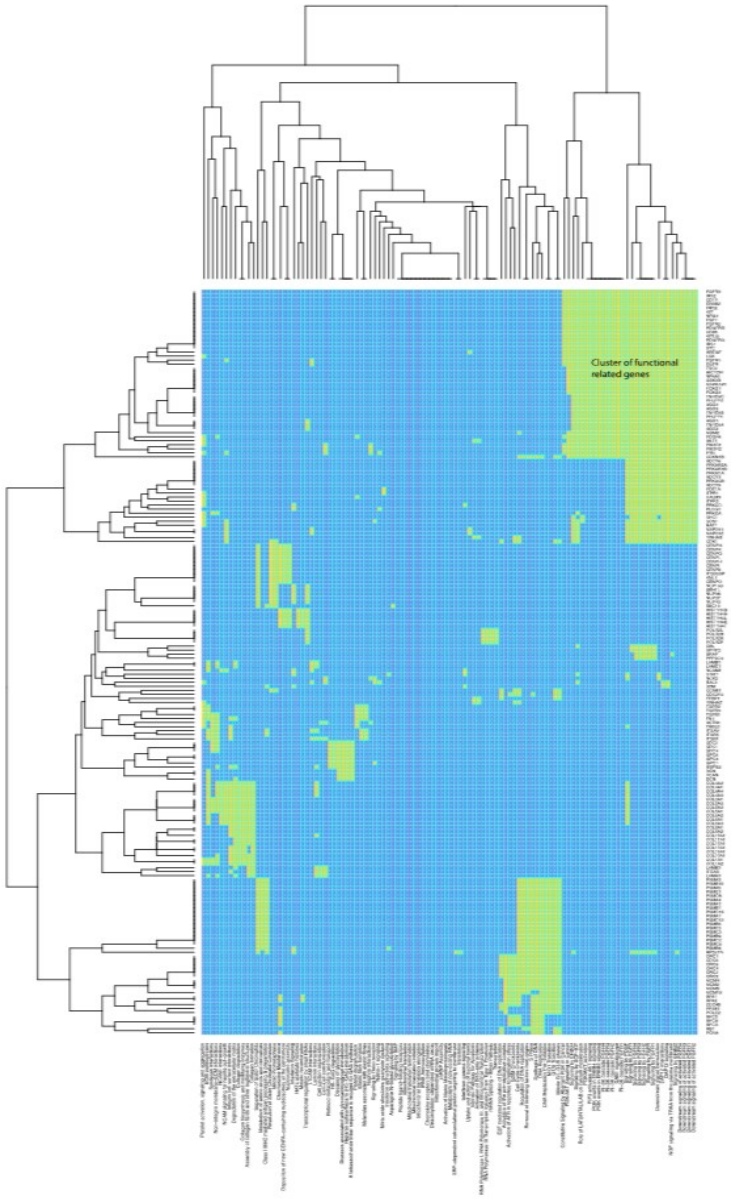

Figure 8: Hierarchical clustering of enriched pathways and associated genes, visualized as a heatmap

A functional related group is denoted in the figure. Genes associated with a given pathway are presented in yellow. Genes not associated with a given pathway are shown in blue. Reproduced from Fechter K. *et al*. (286) with permission of Scientific Reports.

This indicates that there is a hyperactivation of specific kinase pathways in GCB-DLBCL samples as opposed to NGCB-DLBCL and therefore potentially also in cytoplasmic high vs. cytoplasmic low DLBCL.

8.1.6 Higher Expression of ERK1/2 Target Genes Is Related to High Cytoplasmic NR4A1 Expression in Aggressive Lymphomas

JNK, ERK 1/2, AKT, and RSK all are known to post-translationally phosphorylate NR4A1, resulting in cytoplasmic localization of NR4A1 (258, 275). Thus, we thought to assess hyperactivation of these pathways in cytoplasmic NR4A1 high compared to cytoplasmic NR4A1 low DLCBL samples. First, we used selected cases with extremely low (below 20%, n=9 consisting of 6 NGCB- and 3 GCB-DLBCL) or high (above 80%, n=8 consisting of 2 NGCB- and 6 GCB-DLBCL) cytoplasmic NR4A1 expression to perform an explorative gene expression analysis. In total, four different pathways were analyzed. Two pathways were found to be differentially regulated by GO analysis. Hence, *cyclin dependent kinase inhibitor 1B* (*CDKN1B*), *cyclin dependent kinase inhibitor 1A* (*CDKN1A*), *growth arrest and DNA damage inducible alpha* (*GADD45*), BCL-6, *cyclin G2* (*CCNG2*), *cyclin B1* (*CCNB1*), *catalase* (*CAT*), *superoxide dismutase 2* (*SOD2*), and *polo like kinase 1* (*PLK1*) - regulated by AKT (311-313) - and *early growth response 3* (*EGR3*), *cFOS*, *BUB1 mitotic checkpoint serine/threonine kinase* (*BUB1*), *MAX dimerization protein 1* (*MXD1*), *JUNB*, *cJUN*, *ETS variant 5* (*ETV5*) and *dual specificity phosphatase 1* (*DUSP1*) - regulated by ERK1/2 (314)- were used to detect hyperactivated pathways in GCB- and NGCB-DLBCL samples. Moreover, we decided to analyze the JNK (315, 316) and mammalian target of rapamycin (mTOR) pathway (317-319), representing two other pathways contributing to lymphoma development. Hence, expression levels of *C-C motif chemokine ligand 22* (*CCL22*), *C-C motif chemokine receptor 7* (*CCR7*), *CD44*, *IL10*, *matrix metallopeptidase 2* (*MMP2*), *fibronectin 1* (*FN1*), *collagen Type I alpha 1 chain* (*COL1A*), *CASP8 and FADD like apoptosis regulator* (*CFLAR*) and *double-stranded RNA-specific editase B2* (*ADARB*), known to be regulated by JNK (based on the Ingenuity Pathway Analysis (IPA) tool), and *eukaryotic translation initiation factor 4E* (*EIF4E*) and *EIF4E binding protein 1* (*EIF4EBP1*) for mTOR pathway analysis (320) were determined. For five of the eight ERK target genes investigated, we detected an increased expression in DLBCL samples with high cytoplasmic NR4A1. Expression levels of *cFOS* (5.1 fold, p=0.03), *JUNB* (1.9 fold, p=0.03), *cJUN* (2.6 fold, p=0.04), *MXD1* (7.6 fold, p=0.07), and *DUPS1* (21.1 fold, p=0.06), were significantly higher (Figure 9b, p=0.071), while we found no significant differences in the other pathways examined (Figure 9a, c & d).

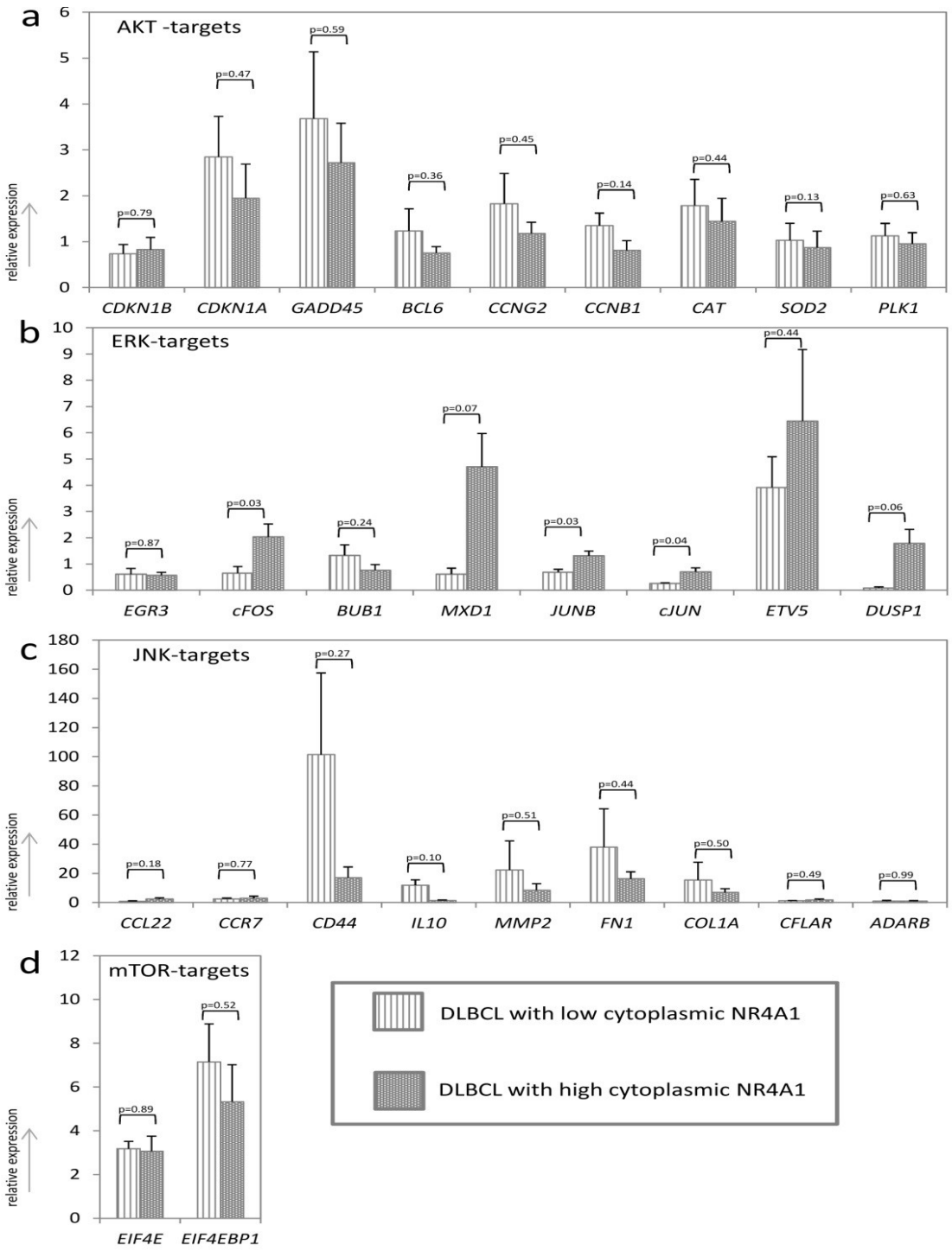

Figure 9: Expression analysis of AKT-, ERK1/2-, JNK- and mTOR- target genes (based on literature) in low (n=9) and high (n=8) cytoplasmic expressing aggressive lymphoma specimens determined by RQ-PCR.

(a) Relative expression levels of (a) AKT (b) ERK1/2 (c) JNK and (d) mTOR target genes. Each bar represents the mean values of expression levels ± standard error of the mean (SEM). Reproduced from Fechter K. *et al*. (286) with permission of Scientific Reports.

In order to rule out that the higher expression of *cFOS*, *JUNB*, *cJUN*, *MXD1* and *DUPS1* in cytoplasmic NR4A1 expressing DLBCL was due the stringent conditions applied (below 20% and above 80%), the number of lymphoma cases in our patient cohort was increased to n=34 consisting of 12 low and 22 high cytoplasmic NR4A1 expressing DLBCL (51 in total). For this stratification we used the stratification according to lymphoma samples exhibiting a lower or higher cytoplasmic NR4A1 expression than the median of 40% of lymphoma cells positive for cytoplasmic NR4A1. Likewise, expression of *cFOS* (3.7 fold, p=0.035), *JUNB* (3.1 fold, p=0.006), *cJUN* (3.4 fold, p=0.023), *MXD1* (7.1 fold, p=0.005) and *DUSP1* (9.1 fold, p=0.018) was significantly higher in lymphomas with high cytoplasmic NR4A1 expression ($p<0.036$, Figure 10a). Additionally, we performed a separate analysis for these factors in the GCB- and NGCB-DLBCL subtype, respectively. As shown in Figure 10b, *cFOS* (2.1 fold, p=0.08), *JUNB* (1.5 fold, p=0.06), *cJUN* (6.3 fold, p=0.03) and *MXD1* (2.1 fold, p=0.013) were significantly higher expressed in GCB-DLCBL compared to NGCB-DLBCL (*MXD1* and *cJUN*, p=0.03, tendency in *cFOS* and *JUNB*, p=0.081).

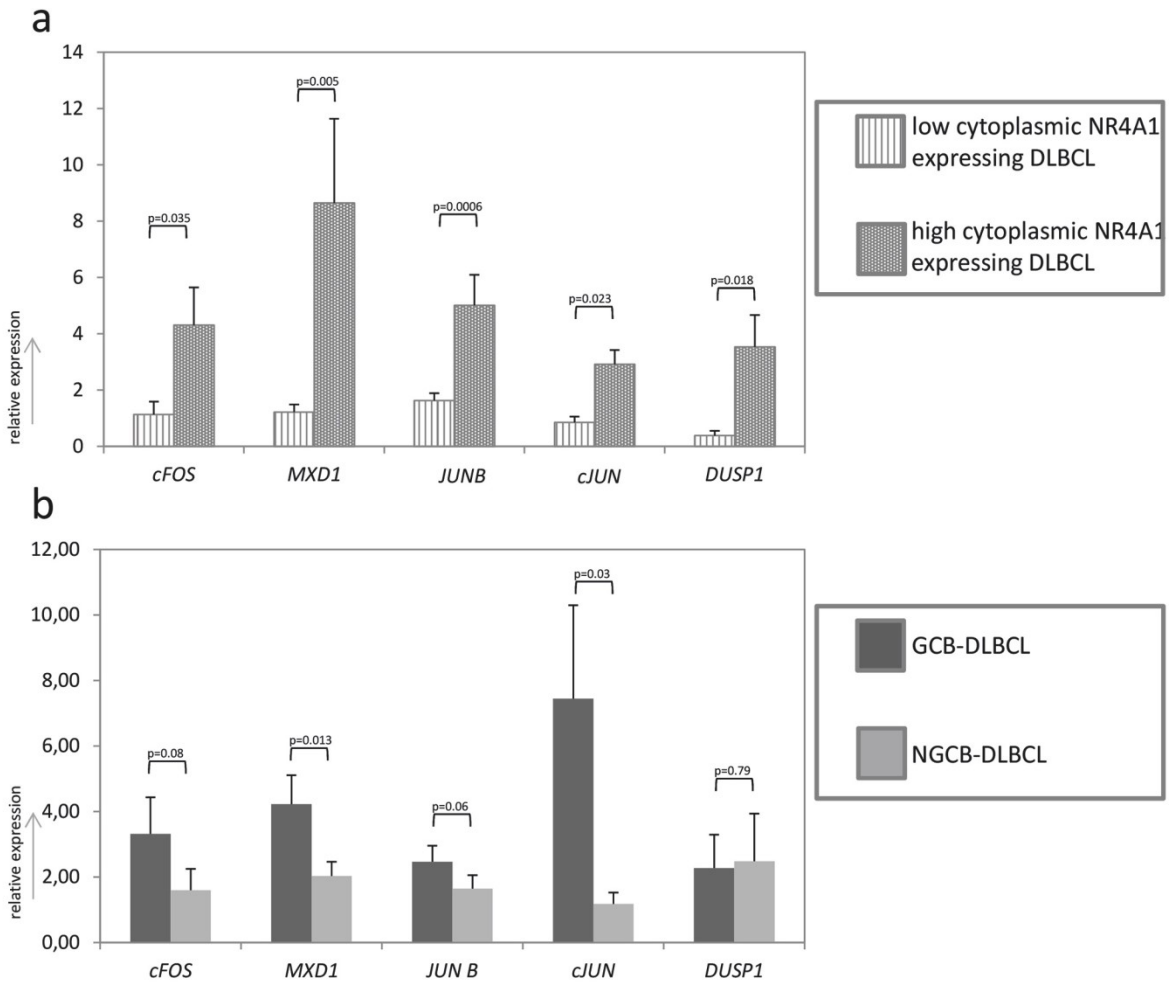

Figure 10: Expression analysis of ERK1/2 target genes.

(a) Relative expression levels of ERK1/2 target genes in low (n=21) and high (n=30) cytoplasmic expressing DLBCL determined by RQ-PCR. (b) Relative expression levels of ERK1/2 target genes in GCB- (n=29) and NGCB- (n=22) DLBCL determined by RQ-PCR. Each bar represents the mean values of expression levels ± standard error of the mean (SEM). Reproduced from Fechter K. *et al*. (286) with permission of Scientific Reports.

Last, we investigated expression levels in pGCB-DLBCL and tGCB-DLCBL, respectively. None of the respective genes exhibiting a higher expression in lymphomas with high cytoplasmic NR4A1 content, either under stringent or less stringent conditions, or in the GCB-DLBCL subtype genes was found to be differentially expressed (p=0.17, Figure 11).

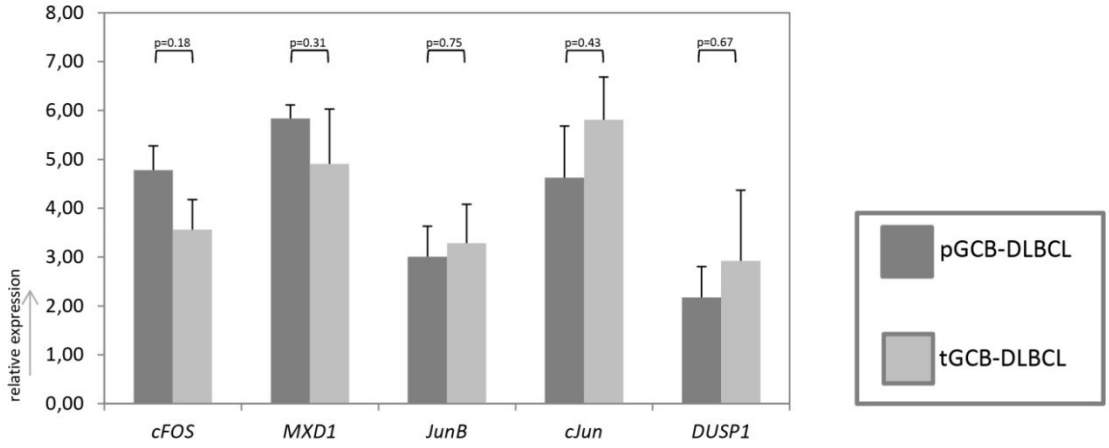

Figure 11: Expression analysis of ERK1/2 target genes in GCB-DLBCL subtypes.

(a) Relative expression levels in *de novo* (pGCB-DLBCL, n=9) and transformed (tGCB-DLCL, n=20) GCB-DLBCL determined by RQ-PCR. Each bar represents the mean values of expression levels ± standard error of the mean (SEM). Reproduced from Fechter K. *et al*. (286) with permission of Scientific Reports.

Collectively, these data suggest that the ERK1/2 pathway activation might be implicated in NR4A1 nuclear export in DLBCL, as already shown in lung cancer cells as well as human primary T cells and kidney cells (321-323).

8.2 Part II: The Role of the Nuclear Receptor *Nr4a1* in *Myc*-Driven Lymphomagenesis

8.2.1 *Nr4a1* Loss Accelerates *Myc*-Driven B Cell Lymphomagenesis

In order to investigate *in vivo* the tumor suppressive function of *Nr4a1* on B cell lymphoma development, mice lacking *Nr4a1* were crossed with *EμMyc* mice. Hence in this setting, proto-oncogene-driven lymphoma development could be monitored concomitantly with *Nr4a1* loss with respect to tumor formation and survival. A cohort of *EμMyc Nr4a1*+/+ (n=134), *EμMyc Nr4a1*-/- (n=84) and mice with a heterozygous *Nr4a1* loss (*EμMyc Nr4a1* +/-; n=59) was generated and mice were monitored until onset of disease. With respect to tumor formation, *EμMyc Nr4a1*-/- developed tumors significantly faster than *EμMyc* mice without *Nr4a1* loss. In detail, the median tumor formation was 45 days for *EμMyc Nr4a1*-/- compared to 107 days for *EμMyc Nr4a1*+/+ mice ($p < 0.001$). Likewise, *EμMyc Nr4a1*-/- showed a reduced survival with a median of 92 days compared to *EμMc Nr4a1*+/+ mice with a median survival of 123 days ($p<0.037$). In either case, *EμMyc Nr4a1*+/- mice gave intermediate results with a median tumor formation of 66 days ($p<0.001$) and a median survival of 102 days ($p<0.037$) (Figure 12).

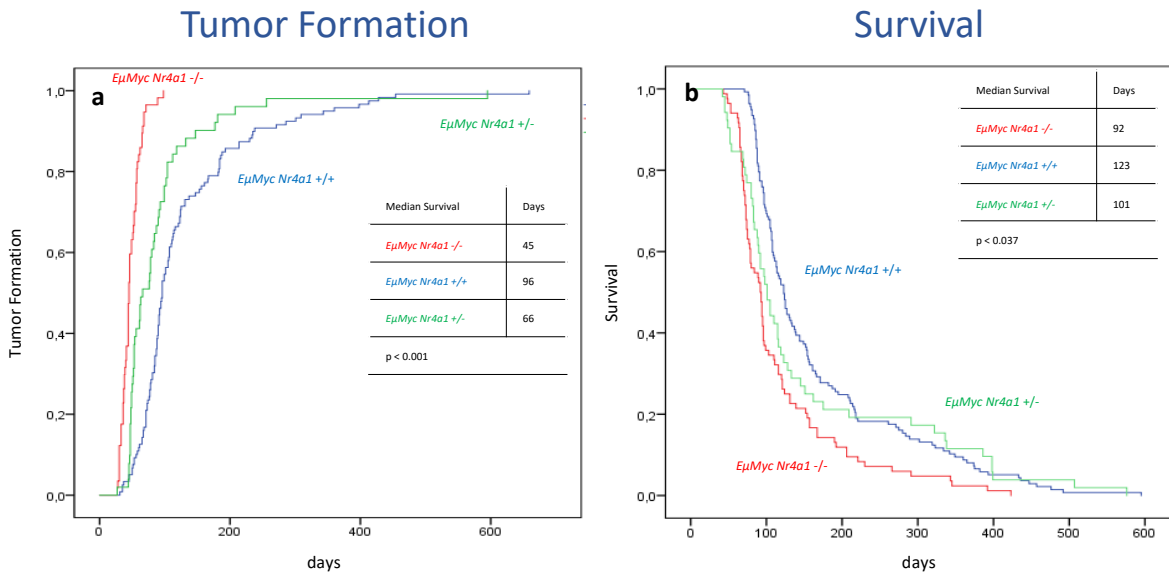

Figure 12: Tumor formation and survival in *EμMyc Nr4a1*+/+, *EμMyc Nr4a1*-/- and *EμMyc Nr4a1*+/- mice.

(a) Tumor formation in *EμMyc Nr4a1*+/+ (blue, n=134), *EμMyc Nr4a1*-/- (red, n=84), and *EμMyc Nr4a1*+/- (green, n=59) mice ($p<0.001$). (b) Survial of *EμMyc Nr4a1*+/+ (blue, n=134), *EμMyc Nr4a1*-/- (red, n=84), and *EμMyc Nr4a1*+/- (green, n=59) mice ($p<0.037$).

In summary, these results demonstrate that *Nr4a1* exerts a tumor suppressive function in *Myc*-driven lymphomagenesis by impacting survival and tumor formation.

8.2.2 Nr4a1 Is Essential to Mediate the Pro-Apoptotic Function of *c-Myc* at the Premalignant Stage

Despite the rapid tumor formation in the *EμMyc* mouse model due to enhanced proliferation of B cells, this model needs a second hit for tumor formation. This is characterized by counteracting the pro-apoptotic function of *c-Myc* through inhibition of the Mdm2-p19Arf-p53 pathway and/ or overexpression of the anti-apoptotic genes *Bcl-2* and *Bcl-xL* (129, 324, 325). Furthermore, caused by *c-Myc*-driven proliferation, premalignant *EμMyc* mice display an expanded population of pre-B cells and immature IgM+ transitional B (T1) cells. This leads to accumulation of these cells in secondary lymphoid organs concomitantly with a reduced number of mature B cells. Nevertheless, expansion of these premalignant cells is time-limited by the pro-apoptotic function of *c-Myc* (126). Therefore, the rate of B cell apoptosis in bone marrow and spleen of wt and *Nr4a1*-/- mice as well as *EμMyc Nr4a1*-/- and *EμMyc Nr4a1*+/+ mice at an age of 5 weeks, representing the premalignant stage of *EμMyc Nr4a1*-/- and *EμMyc Nr4a1*+/+ mice, was quantified (n=5 per genotype) by using flow cytometric analysis for cleaved caspase 3 and Annexin V/ 7AAD staining in combination with antibodies directed against Cd19, Cd43, IgM and IgD expressed on B cells.

In the bone marrow, Annexin V levels were 13.3% for *EμMyc Nr4a1*+/+ B cells compared to 3.4% for *EμMyc Nr4a1*-/- B cells. Furthermore, we observed higher levels of cleaved caspase 3 comparing B cells from *EμMyc Nr4a1*+/+ to *EμMyc Nr4a1*-/- mice (15.6% vs 3.33%, respectively) ($p<0.009$). In spleen, the apoptotic potential in more immature Cd19+IgM- pre-B cells was similar to the trend observed in bone marrow. We detected 15.0% Annexin V positive splenic B cells from *EμMyc Nr4a1*+/+ mice opposed to 1.5% in *EμMyc Nr4a1*-/- mice. Likewise, cleaved caspase 3 levels were 17.4% for B cells from *EμMyc Nr4a1*+/+ mice vs 0.8% for those from *EμMyc Nr4a1*-/- mice ($p<0.007$). With respect to more mature CD19+IgM+ B cells, we again found higher levels of Annexin V (15.6% vs 1.1%, respectively) and higher levels of cleaved caspase 3 (19.4% vs 3.3%, respectively) in *EμMyc Nr4a1*+/+ derived B cells in contrast to *EμMyc Nr4a1*-/- dervived B cells ($p<0.03$).

Apoptosis rate was comparable in *EμMyc Nr4a1*-/-, wt mice and mice with *Nr4a1 loss* in all B cell populations examined in bone marrow and spleen (Figure 13).

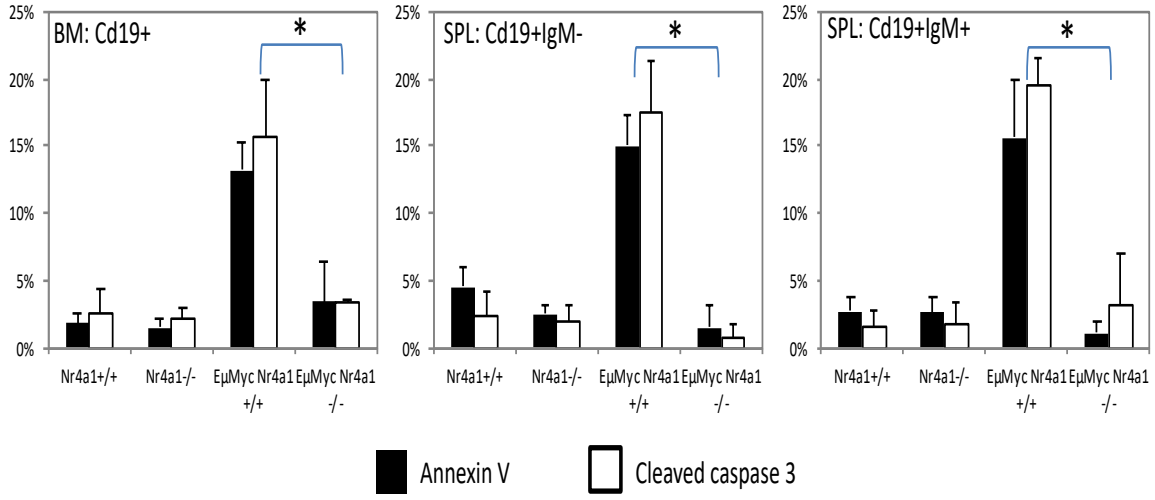

Figure 13: Loss of Nr4a1 enhances survival of premalignant *EμMyc* B cells.

Annexin V and cleaved caspase 3 staining of B cells (Cd19+) isolated from bone marrow and pre-B cells (Cd19+IgM-) and B cells (Cd19 IgM+) isolated from spleen. Data represent means of positive cells ± SD from at least 4 independent experiments for each genotype. "*" indicates $p<0.05$ compared to *EμMyc Nr4a1*+/+.

With respect to the number of the different B cell subpopulations, results were similar, indicating an enhanced survival of B cells upon the loss of *Nr4a1* in the *c-Myc* induced model of lymphomagenesis. A combination of total cell count with different fluorophore-labeled antibodies for flow cytometric analysis showed that the number of several B cell populations was increased in *EμMyc Nr4a1*-/- mice at the premalignant stage. While the numbers of B cells (Cd19+), pro/pre B cells (Cd19+, IgM-, Cd43-), T1 B cells (IgM^{high} Cd21+) and T2 B cells (IgM^{high} Cd21+ Cd23+) were similar in the compared cohorts of wt, *Nr4a1*-/-, *EμMyc Nr4a1*+/+ and *EμMyc Nr4a1*-/- mice, respectively, results demonstrated an increased number of T3 and mature B cells (IgM+ and IgD+) in bone marrow (4 fold, $p<0.03$) and spleen 3 fold, $p<0.03$) of *EμMyc Nr4a1*-/- mice compared to the other mouse cohorts (Figure 14a & b).

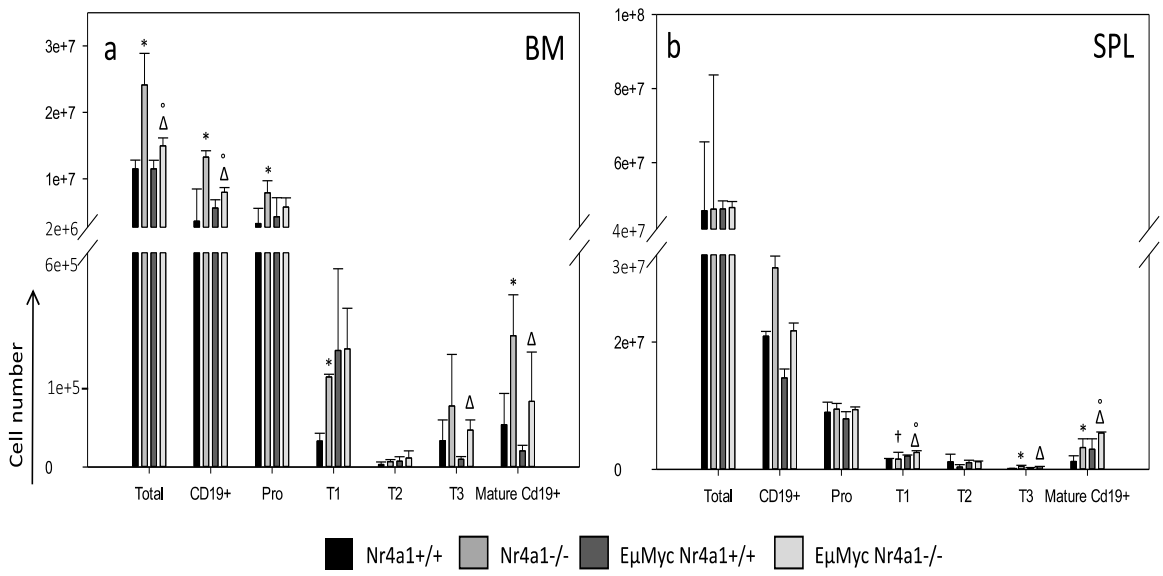

Figure 14: Loss of *Nr4a1* alters B cell subpopulations at the premalignant stage.

Cell number and B cell subset composition determined by cell counting and flow cytometric analysis of (a)bone marrow (2 femora) and (b) spleen of 5-week-old mice of the indicated genotypes (n=5). "*" indicates $p<0.05$ compared to *Nr4a1*+/+, "Δ" indicates $p<0.05$ compared to *EμMyc Nr4a1*+/+, "°"$p<0.05$ compared to *Nr4a1*-/- mice.

Considering that B cells developing in the bone marrow and different B cell populations in the spleen show a defect in the apoptotic potential and that the numbers of T3 transitional and mature B cells in the bone marrow and spleen are significantly increased, these results indicate that *Nr4a1* loss facilitates survival of B cell upon oncogenic stress conditions and consequently lymphoma development.

8.2.3 *Nr4a1* Loss Leads to a Higher Percentage of B Cells in the Bone Marrow but Not in Spleen

In order to determine base line values of B cells in the bone marrow and spleen of *EμMyc Nr4a1*+/+ (n=15) and *EμMyc Nr4a*1-/- mice (n=18), we isolated single cells from the two respective organs and stained them with antibodies against Cd19 and B220. In spleen, the percentage of B cells was comparable in both mouse cohorts (61.03% in *EμMyc Nr4a1*+/+ vs 66.28% in *EμMyc Nr4a1*-/- mice, p=0.759, Figure 15a). In contrast we found increased percentages of B cells in the bone marrow of *EμMyc Nr4a1*-/- mice (50.30%) compared to the bone marrow of mice without *Nr4a1* loss (33.78%, p=0.065, Figure 15b).

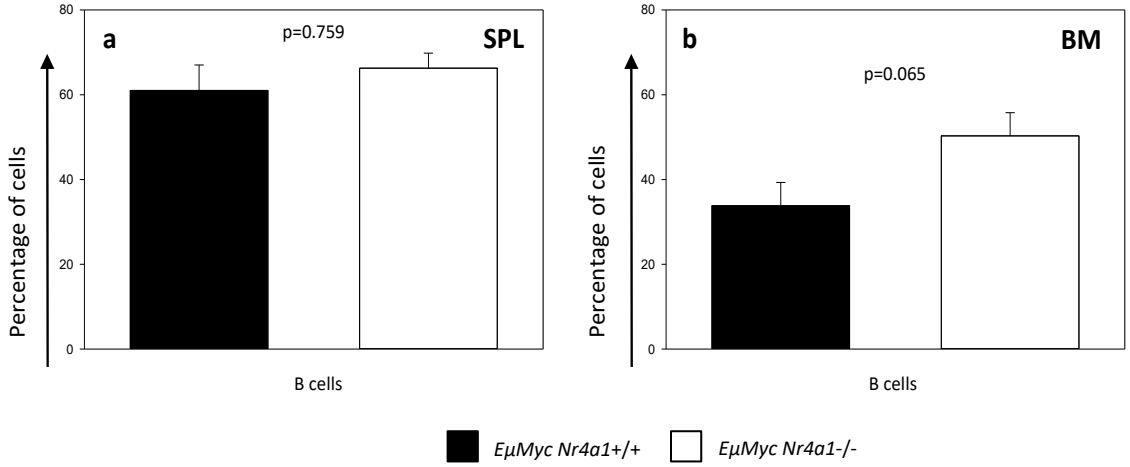

Figure 15: Percentages of B cells in spleen and bone marrow after transplantation of *EμMyc Nr4a1*+/+ and *EμMyc Nr4a1*-/- derived tumors.

(a) Spleenic B cells from *EμMyc Nr4a1*+/+ (black, n=15) or *EμMyc Nr4a1*-/- (white, n=18) were stained with antibodies against Cd19 and B220 (p=0.759). (b) B cells from bone marrow of *EμMyc Nr4a1*+/+ (black, n=15) or *EμMyc Nr4a1*-/- (white, n=18) were stained with antibodies against Cd19 and B220 (p=0.065). Each bar represents the mean values of expression levels ± standard error of the mean (SEM). p-values are depicted in the respective graphs.

These data demonstrate that upon loss of *Nr4a1*, B cells preferably infiltrate the bone marrow as opposed to the spleen and that *Nr4a1* is obviously implicated in tumor cell dissemination and regulation of infiltrating immune cells.

8.2.4 Genes Involved in Immunoregulation and the NfKb Pathway Are Upregulated upon Loss of *Nr4a1*

RNASeq enables the determination of differentially transcribed genes of the whole genome at a given time. As survival analysis as well as B cell development and apoptotic potential at the premalignant stage revealed differences in *EμMyc Nr4a1*-/- and *EμMyc Nr4a1*+/+ mice, we decided to determine RNA expression in a total of ten tumors comprising of *EμMyc Nr4a1*+/+ (Lexogen 01-05) and *EμMyc Nr4a1*-/- mice (Lexogen 06-10), respectively (n=5 per group and genotype). Filtered reads were mapped to the *Mus Musculus* mm 10 genome and results corrected for multiple testing with the Benjamini Hochberg method (297) (Figure 16).

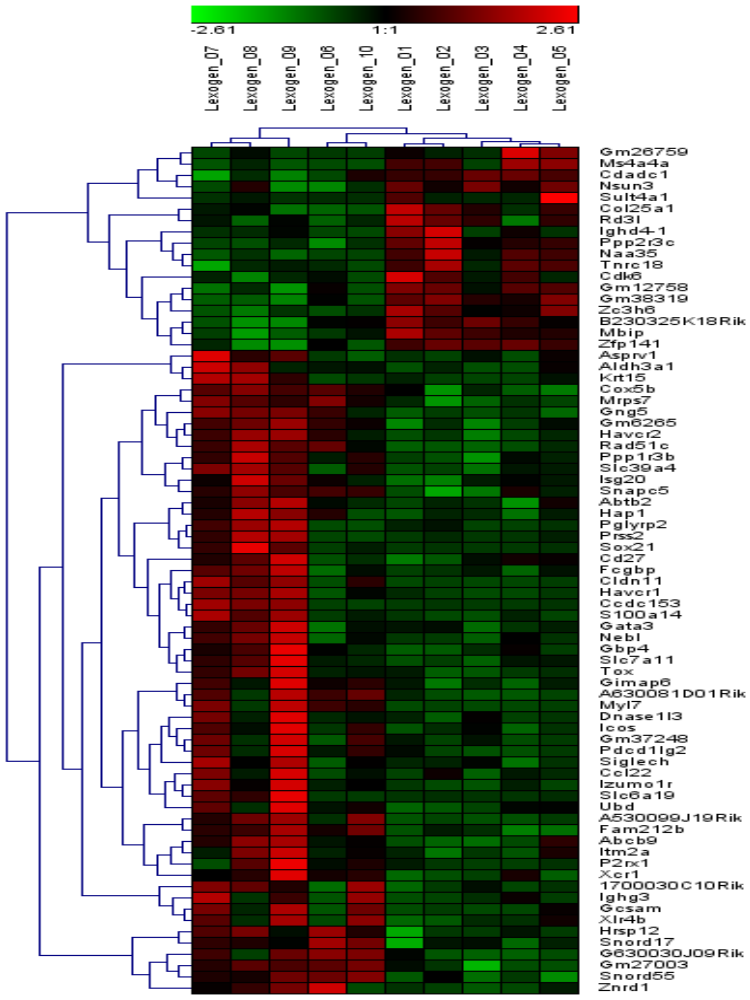

Figure 16: Heat map of the results of RNASeq.

Green represents reduced expression and red enhanced expression of genes. Lexogen 06-10 are *EμMc Nr4a1*-/- tumors and Lexogen 01-05 are *EμMc Nr4a1*+/+ tumors.

Using a corrected p-value below <0.1 we could detect 57 genes which were significantly up- and 18 which were significantly downregulated when comparing the *EμMyc Nr4a1*-/- with the *EμMyc Nr4a1*+/+ mouse. Moreover, applying a log fold change of logFC <1.5 or logFC >1.5 this number could be decreased to 48 up- and nine genes downregulated (Table 10).

Table 10: Differentially expressed genes in *EμMyc Nr4a1*-/- and *EμMyc Nr4a1*+/+ mice.

Red color denotes upregulated and green color denotes downregulated genes.

Comparison	#Genes (FDR p-value < 0.10)	#Genes (uncorrected p-value < 0.05)	#Genes (FDR p-value < 0.10; logFC>1.5 or logFC<-1.5)	#Genes (uncorrected p-value < 0.05; logFC>1.5 or logFC<-1.5)
***EμMyc Nr4a1*-/- vs *EμMyc Nr4a1*+/+**	57↑+18↓	800↑+412↓	48↑+9↓	410↑+128↓

The gene list of differentially expressed genes was used to perform gene ontology and Ingenuity Pathway analysis in order to determine whether these genes clustered in distinct pathways and/ or cellular functions. Results revealed that mainly genes involved in immunological processes and the Nf-kB pathway were overexpressed in the *EμMyc Nr4a1*-/- mouse compared to *EμMyc* mice without *Nr4a1* loss. Among the most prominent pathways being differentially regulated were negative regulation of T cell proliferation, negative regulation of response to biotic stimuli, negative regulation of immune response, lymphocyte migration, chemokine receptors bind chemokines and acute phase response, respectively (Figure 17).

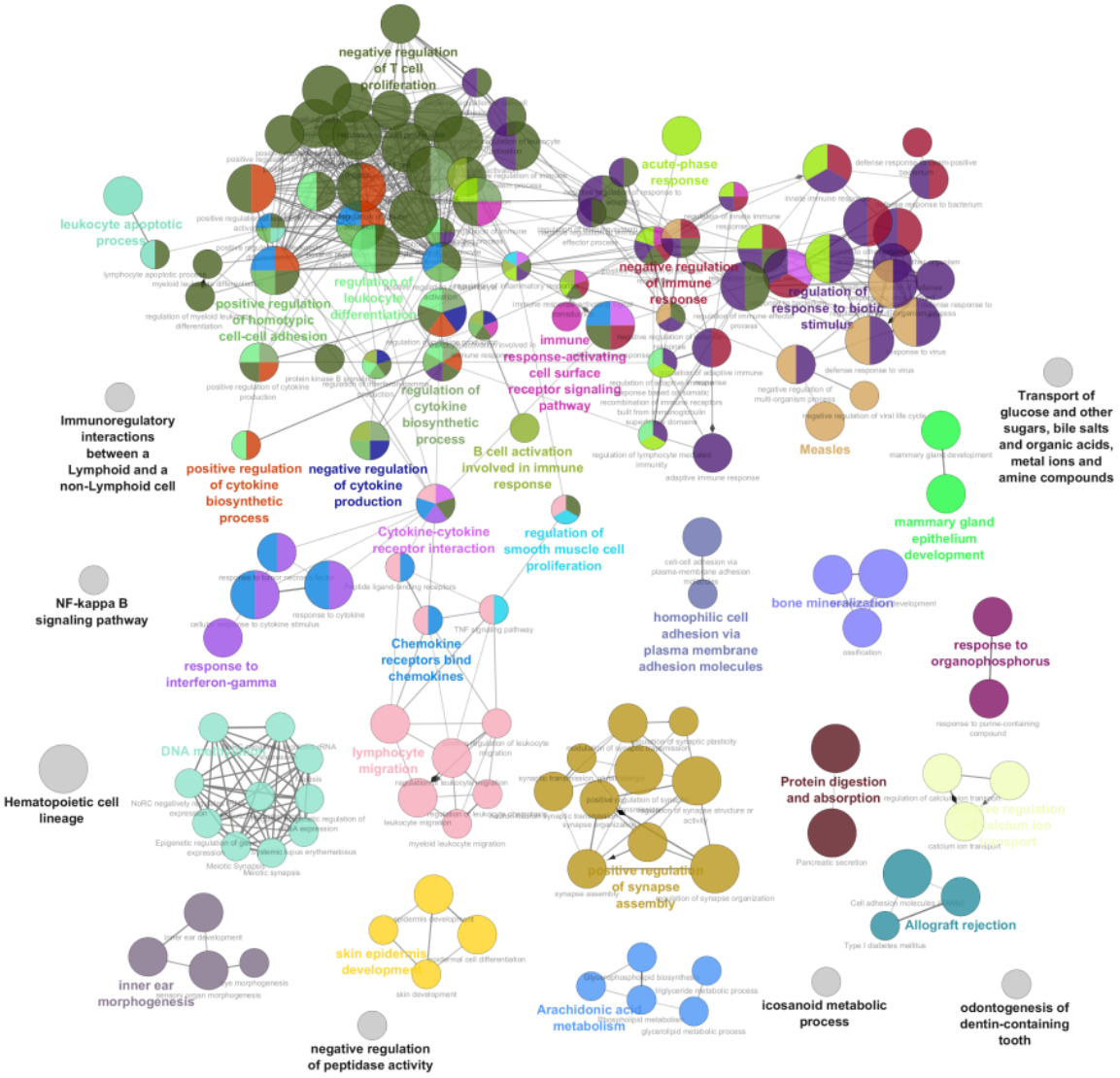

Figure 17: Results from the ClueGO analysis.

Clusters show a network from ClueGO produced using the list of up and downregulated genes for *EμMyc Nr4a1*-/- vs *EμMyc Nr4a1*+/+ with log2FC<-1.5 or log2FC>1.5, uncorrected p-value <0.05. The network represents the enriched terms as nodes that are linked based on the similarity of their shared genes (the size of the node reflects the enrichment significance of the terms). The functional groups are represented and visualized by their most significant term. The light gray are the ones that didn't group. The analyses were done using medium GO levels (levels 3-8).

Validation of the differentially expressed genes was performed by means of semi-quantitative RQ-PCR. Therefore, RNA was isolated from in total 19 fresh- frozen tumors specimens derived from 19 *EμMyc Nr4a1*-/- mice (n= 10 IgM- and n= 9 IgM+ tumors) and 21 *EμMyc Nr4a1*+/+ mice (n=13 IgM- and n=8 IgM+ tumors) including those tumors used for RNASeq. Genes evaluated encompassed those involved in positive and negative regulation of immune responses of B and T cells, immune checkpoint inhibitors, Nf-kB target genes as well as proteins regulating cell cycle, respectively. Figure 18 represents the results for genes involved in B cell immunology (Figure 18a-c) and T cell immunology-related genes (Figure 19a-c). *Germinal center associated signaling and motility* (*Gcsam*) – a protein specific for the germinal center in lymphoid follicles (326, 327), *Ccl20* – ligand for the chemokine receptor CCR6 and important for T_H17 and Treg cell responses (328), *GATA binding protein 3* (*Gata 3*) – a transcription factor involved especially in T_H2 cell differentiation (329) and *Icos* – belonging to a group of cell surface molecules important for T cell stimulation and proper immune function (330), were significantly upregulated in *EμMyc Nr4a1*-/- mice compared to *EμMyc Nr4a1*+/+ mice (Figure 18a & 19a). In detail, *Gcsam* was 7.4 fold (p=0.014), *Ccl20* 3.7 fold (p=0.015), *Gata3* 7.7 fold (p=0.040) and *Icos* 7.6 fold (p=0.007) higher expressed in *EμMyc Nr4a1*-/- mice. Moreover, *Bcl-2-related protein A1* (*Bcl2a1a*) (3.7fold, p=0.064) and *Bcl-2-related protein D1* (*Bcl2a1d*) (4.6 fold, p=0.088), being both Bcl-2-related proteins (331), were also upegulated in *EμMyc Nr4a1*-/- mice (Figure 18a). As the *EμMyc* tumor model is known to produce pre-B, immature B, or mixed pre-B/immature B immunophenotypes and that these distinct types of lymphomas feature different gene expression patterns as well as oncogenic pathways, we decided to dissect the role of early (IgM-) and late onset lymphomas (IgM+) in our mouse cohort (126, 332). Interestingly, when dissecting IgM negative and IgM positive tumors within the two respective groups of *EμMyc Nr4a1*-/- and *EμMyc Nr4a1*+/+ mice, respectively, we found even more genes being significantly differentially expressed in the IgM- subgroup (Figure 18b & 19b), while this was not the case in the more mature IgM+ tumor specimens (Figure 18c & 19c).

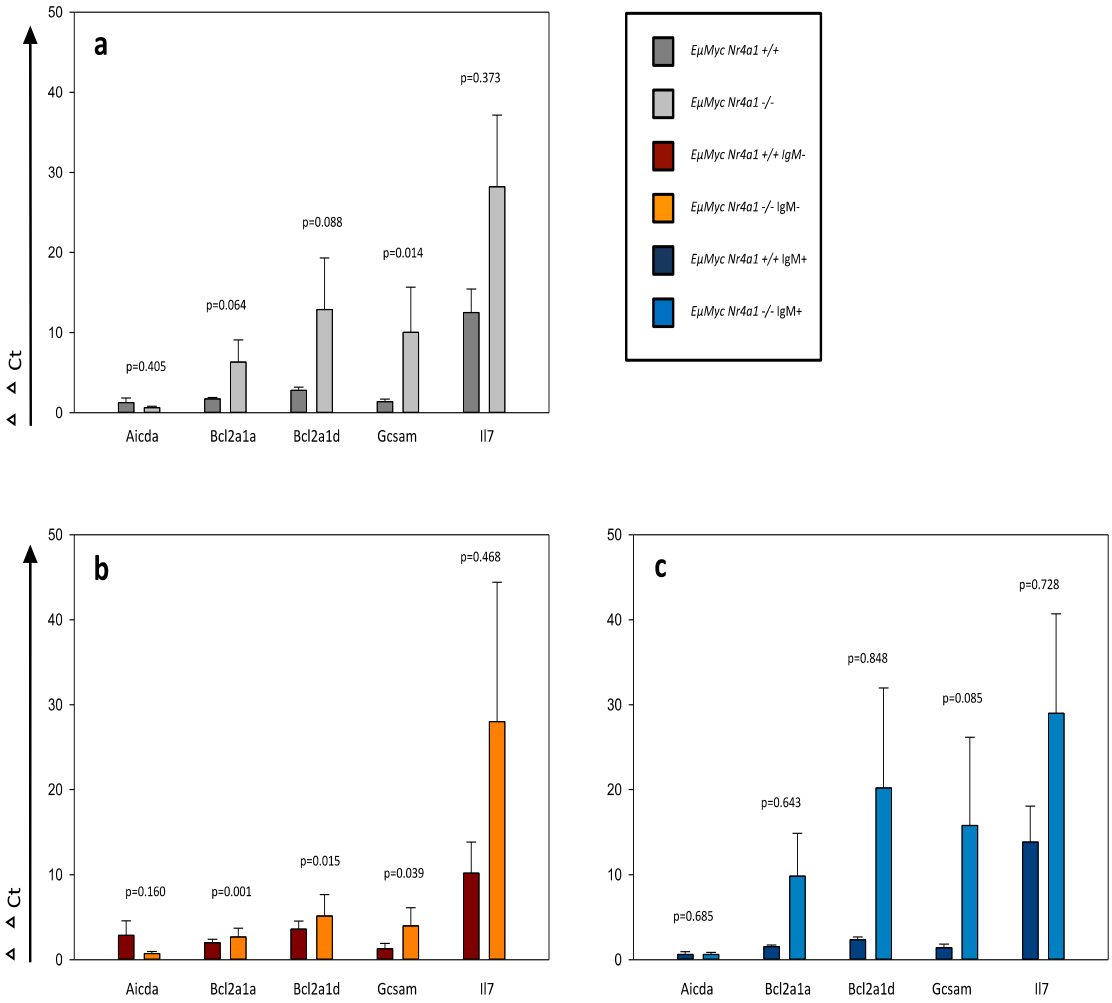

Figure 18: Semi-quantitative RQ-PCR for genes involved in B cell immunology.

(a) Relative expression values of *EμMyc Nr4a1*+/+ (n=21) and *EμMyc Nr4a1*-/- (n=19) mice (Figure 18a, grey bars). (b) Relative expression levels of IgM- tumors of *EμMyc Nr4a1*+/+ (n=13) and *EμMyc Nr4a1*-/- (n=10) mice (Figure 18b, orange bars). (c) Relative expression values of and IgM+ tumors of *EμMyc Nr4a1*+/+ (n=8) and *EμMyc Nr4a1*-/- (n=9) mice (Figure 18c, blue bars). Each bar represents the mean values of expression levels ± standard error of the mean (SEM). p-values are depicted in the respective graphs.

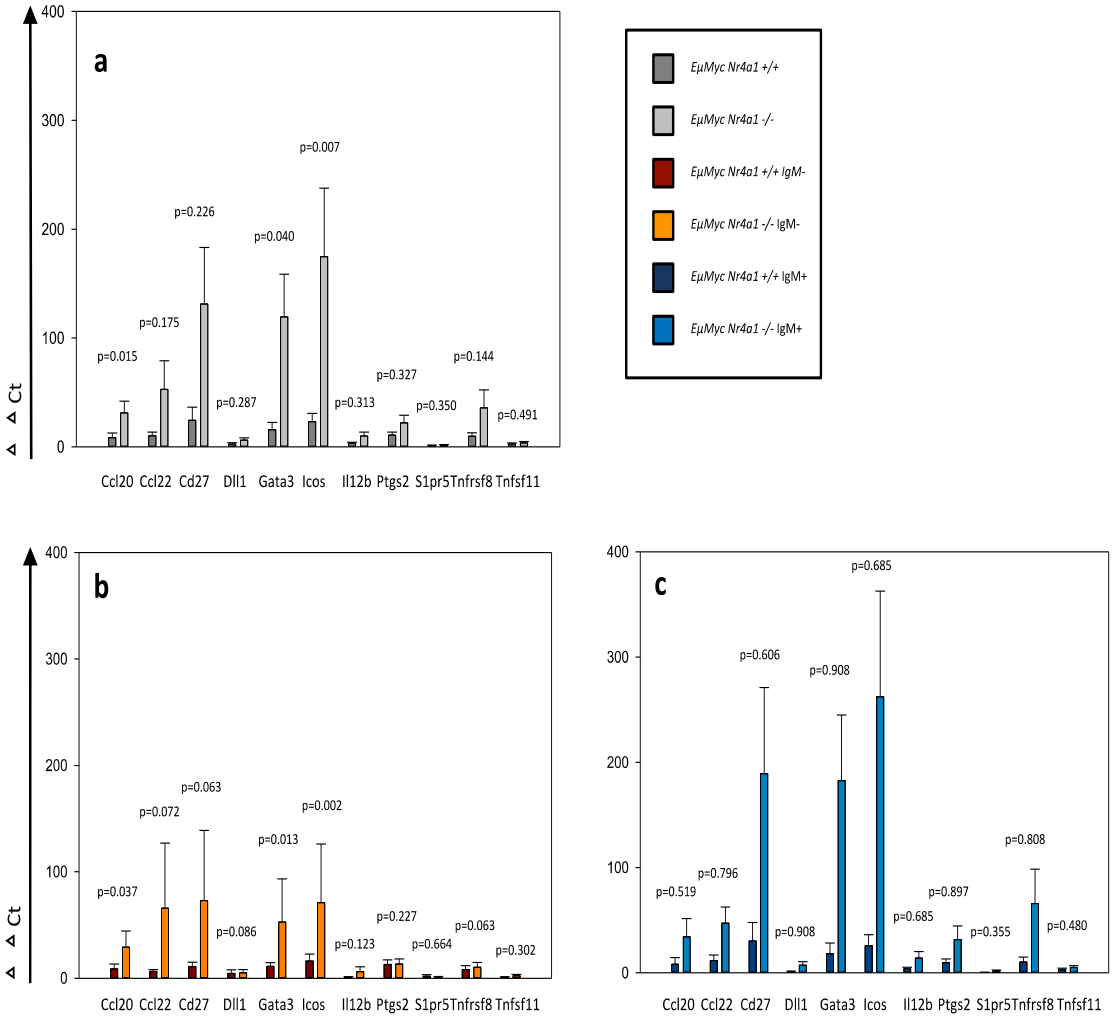

Figure 19: Semi-quantitative RQ-PCR for genes involved in T cell immunology.

(a) Relative expression values of *EμMyc Nr4a1*+/+ (n=21) and *EμMyc Nr4a1*-/- (n=19) mice (Figure 19a, grey bars). (b) Relative expression levels of IgM- tumors of *EμMyc Nr4a1*+/+ (n=13) and *EμMyc Nr4a1*-/- (n=10) mice (Figure 19b, orange bars). (c) Relative expression values of and IgM+ tumors of *EμMyc Nr4a1*+/+ (n=8) and *EμMyc Nr4a1*-/- (n=9) mice (Figure 19c, blue bars). Each bar represents the mean values of expression levels ± standard error of the mean (SEM). p-values are depicted in the respective graphs.

Furthermore, we could detect a significant overexpression of genes involved in the Nf-kB pathway. *Bcl-2* - an anti-apoptotic protein, whose translocation to the IgH locus or over-expression is an important clinical predictive parameter in indolent and aggressive lymphomas (333) - was 2.8 fold (p=0.001), and *cFlip* and *Ccnd1* (*Cyclin D1*) - involved in apoptosis and cell cycle control (334-336) - were 2.1 fold (p=0.040) and 1.2 fold (p=0.034) higher expressed in tumors derived from *EμMyc Nr4a1*-/- mice (Figure 20a). Additionally, we found a 1.3 fold (p=0.018) increased expression of *Ccr7* – important for B and T cell homing to secondary lymphoid organs and B cell homing to T cell-rich zones (337) - and a 2.8 fold (p=0.004) increased expression *Tnfaip3* - a negative feedback regulator of the Nf-kB pathway (338) - in IgM- tumors of *EμMyc Nr4a1*-/- mice (Figure 20b). Except for *Bcl-2*, there were no markedly distinct RNA expression levels in IgM+ positive tumors from either of the two mouse cohorts ($p < 0.05$, Figure 20c).

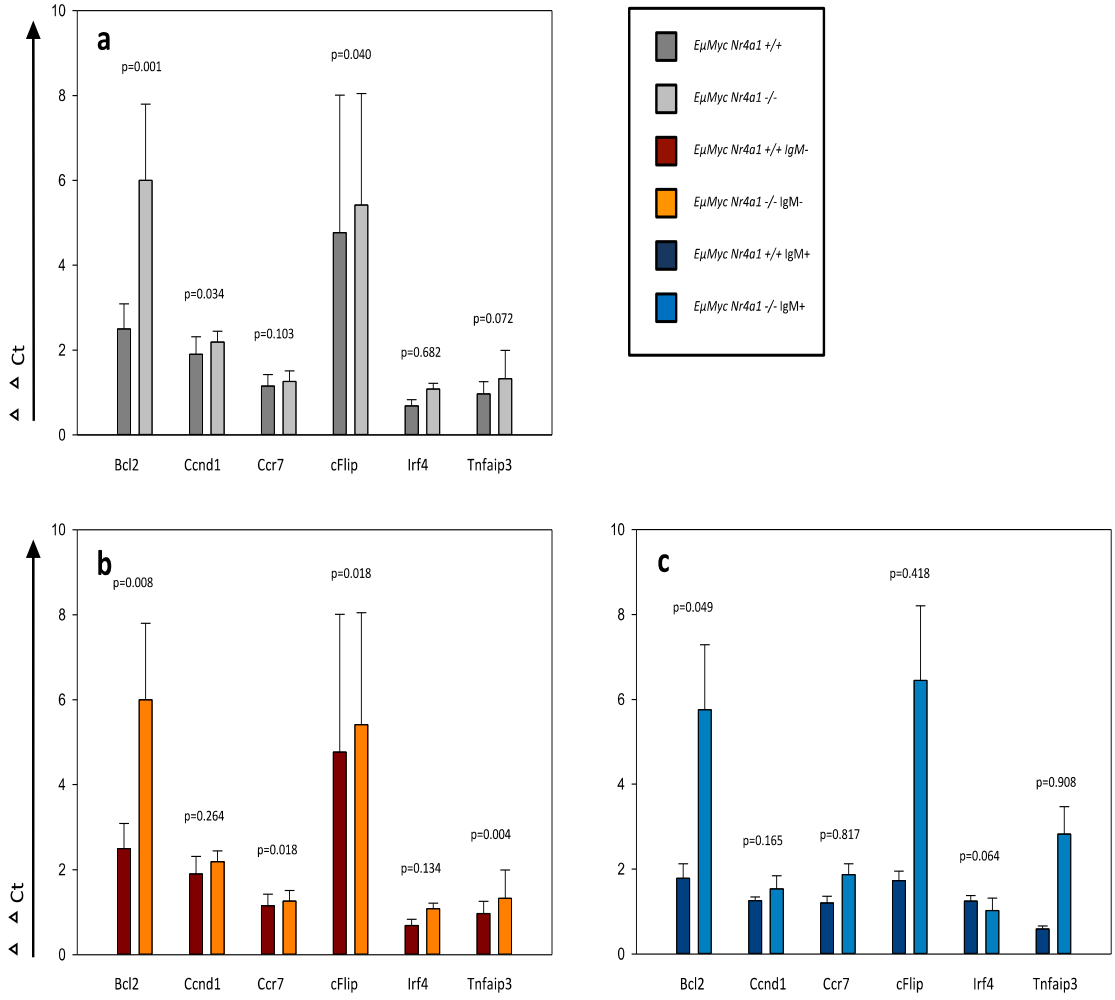

Figure 20: Semi-quantitative RQ-PCR for Nf-kB target genes.

(a) Relative expression values of *EμMyc Nr4a1*+/+ (n=21) and *EμMyc Nr4a1*-/- (n=19) mice (Figure 20a, grey bars). (b) Relative expression levels of IgM- tumors of *EμMyc Nr4a1*+/+ (n=13) and *EμMyc Nr4a1*-/- (n=10) mice (Figure 20b, orange bars). (c) Relative expression values of and IgM+ tumors of *EμMyc Nr4a1*+/+ (n=8) and *EμMyc Nr4a1*-/- (n=9) mice (Figure 20c, blue bars). Each bar represents the mean values of expression levels ± standard error of the mean (SEM). p-values are depicted in the respective graphs.

Last, results showed that when comparing either tumors derived from *EμMyc Nr4a1*-/- mice to those derived from *EμMyc Nr4a1*+/+ mice or just IgM- tumors within the two mouse cohorts, there was a trend of higher expression of immunoregulatory markers on *EμMyc Nr4a1*-/- derived tumors. *Havcr2* (*Tim3*) was 4.7 fold (p=0.038) overexpressed in *EμMyc* mice lacking *Nr4a1*, while *Pdcd1lg2* (*Pdl2*) showed a significant 15.8 fold

(p=0.019) higher expression only in IgM- tumors (Figure 21a&b). For other immunosuppressive molecules like *Cd96* and *Cd226* a trend was visible in *EμMyc Nr4a1*-/- mice and IgM- tumors of the latter, while there were no significant differences detectable in IgM+ tumors (Figure 21a-c) (234).

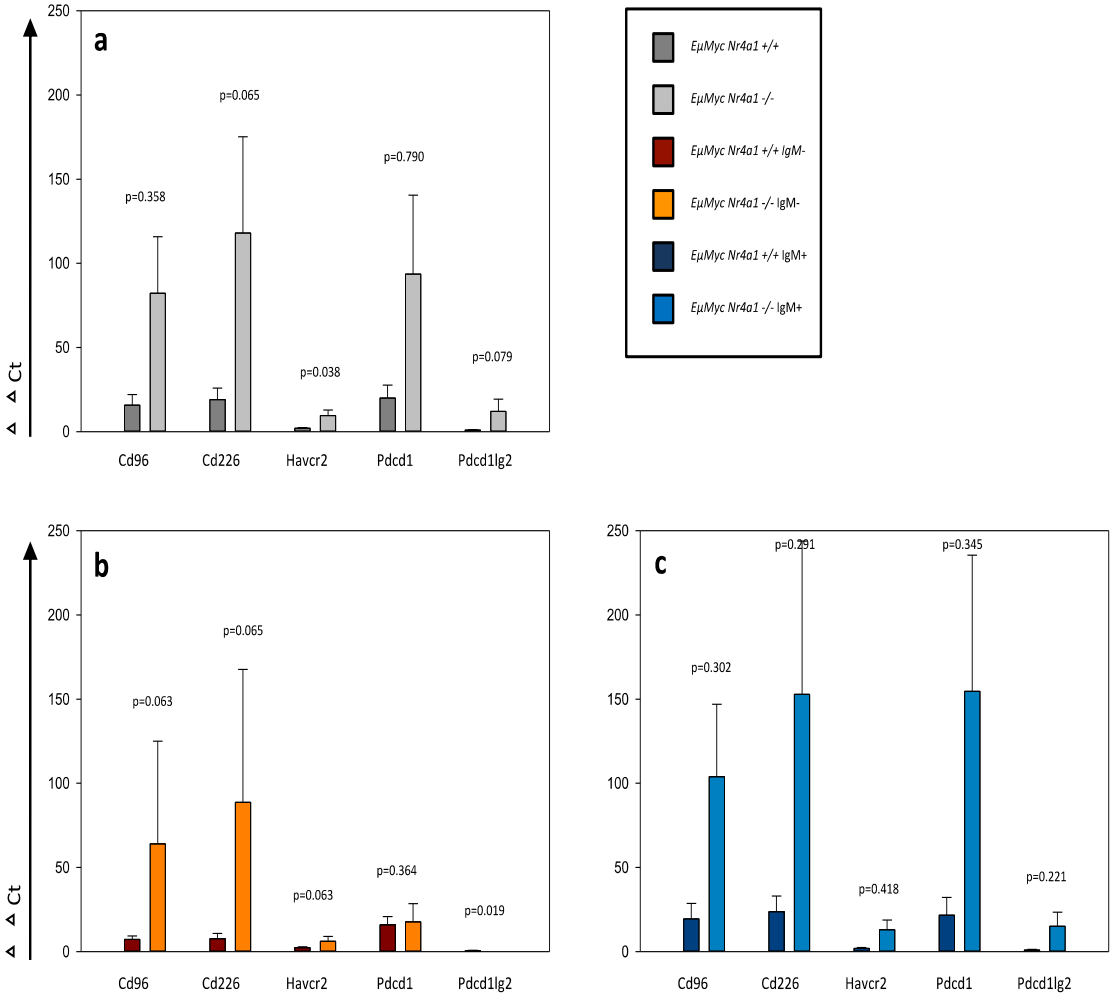

Figure 21: Semi-quantitative RQ-PCR for immunoregulatory molecules.

(a) Relative expression values of *EμMyc Nr4a1*+/+ (n=21) and *EμMyc Nr4a1*-/- (n=19) mice (Figure 21a, grey bars). (b) Relative expression levels of IgM- tumors of *EμMyc Nr4a1*+/+ (n=13) and *EμMyc Nr4a1*-/- (n=10) mice (Figure 21b, orange bars). (c) Relative expression values of and IgM+ tumors of *EμMyc Nr4a1*+/+ (n=8) and *EμMyc Nr4a1*-/- (n=9) mice (Figure 21c, blue bars). Each bar represents the mean values of expression levels ± standard error of the mean (SEM). p-values are depicted in the respective graphs.

Altogether, semi-quantitative RQ-PCR could validate the results obtained by RNASeq and underpin the role of Nr4a1 loss not only by acceleration of lymphoma formation in the *Myc* mouse model, but furthermore by skewing gene expression towards a profile favoring lymphoma development.

8.2.5 Immunoregulatory Molecules Are Upregulated in Tumors from *EμMyc Nr4a1*-/- Mice

As results of the RNASeq validation showed that many molecules implicated in immunological processes were differentially expressed in tumors derived from *EμMyc Nr4a1*-/- and *EμMyc Nr4a1*+/+ mice, we decided to evaluate the RNA expression levels of a set of marker molecules known to be important for activation, induction of tolerogenic processes, and a set of cytokines involved in immunoregulatory processes. Therefore, the markers tested, were subdivided into three distinct groups, including molecules having an immunosuppressive effect, costimulatory molecules, and a set of cytokines and transcription factors.

RNA was isolated from frozen tumor samples derived from *EμMyc Nr4a1*-/- and *EμMyc Nr4a1*+/+ mice (n=20 per genotype). *Tpb*, *Hprt*, *Actb* and *Ppia* served as housekeeping genes.

With respect to immunoinhibitory molecules, the majority of molecules tested was higher expressed in tumors from *EμMyc* mice with *Nr4a1* loss. As shown in Figure 22, *Pd1* and both of its ligands *Pdl1* and *Pdl2*, were all overexpressed upon loss of *Nr4a1*. In detail we detected a 19.7 fold higher expression of *Pd1* (p=0.000), a 3.7 fold higher expression of *Pdl1* (p=0.101) and a 5.8 fold higher expression of *Pdl2* (p=0.013) in tumors from *EμMyc Nr4a1*-/-. Furthermore, *Lag3* (5.4 fold, p=0.002), *Tim3* (2.3 fold, p=0.144), as well as its ligand *Gal9* (2.2 fold, p=0.002) were also higher expressed in *EμMyc* derived tumors with *Nr4a1* loss (Figure 22).

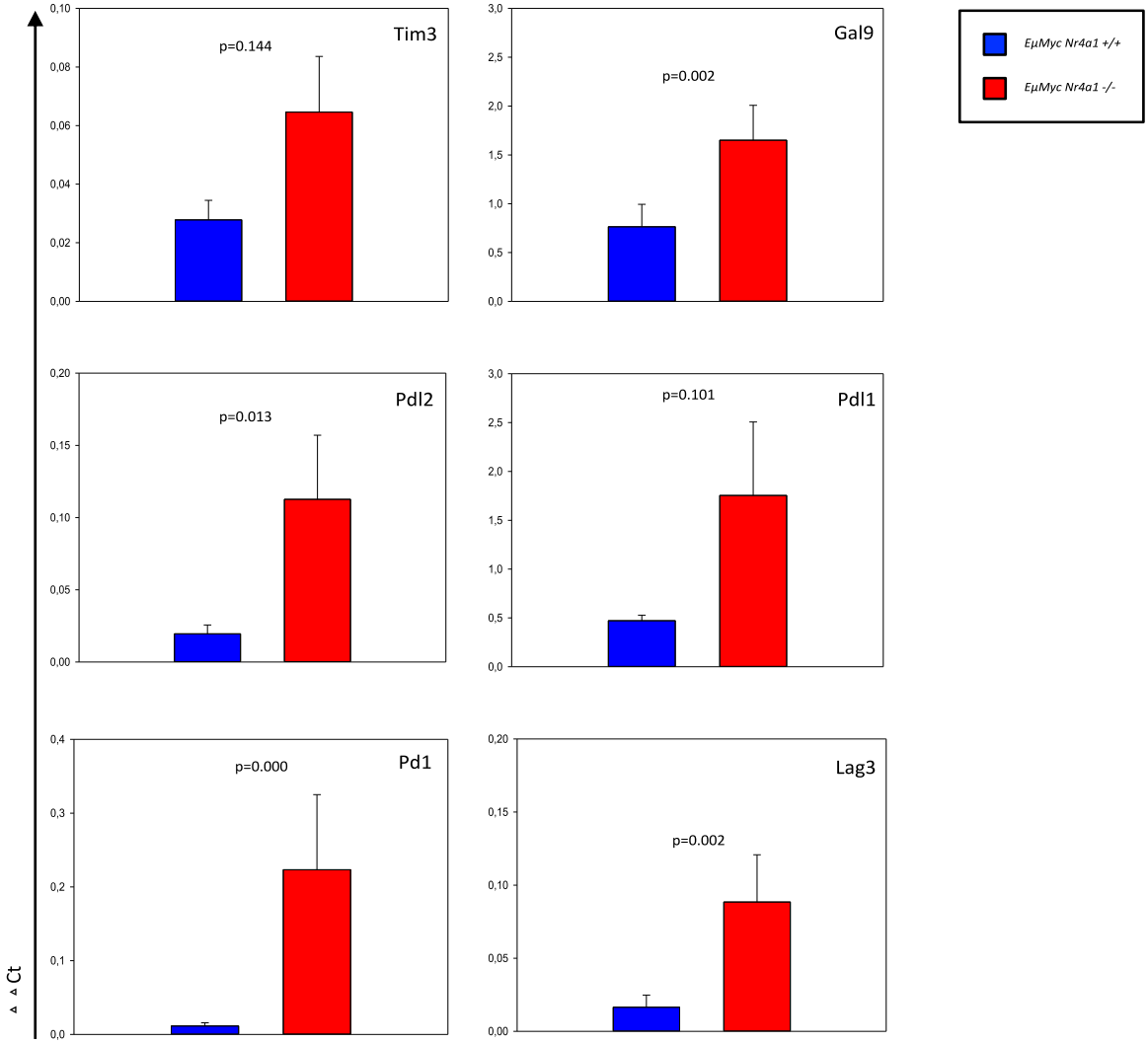

Figure 22: Semi-quantitative RQ-PCR for immunoinhibitory genes in primary tumors.

Relative expression values of *EμMyc Nr4a1*+/+ (n=20, blue bars) and *EμMyc Nr4a1*-/- mice (n=20, red bars). Each bar represents the mean values of expression levels ± standard error of the mean (SEM). p-values are depicted in the respective graphs.

Likewise, several other - more or less well-known - immunoinhibitory molecules were overexpressed in primary tumors derived from *EμMyc Nr4a1*-/- compared to tumors derived from *EμMyc Nr4a1*+/+ mice. We found an overexpression of the inhibitory molecules *Cd96* (11.5 fold, p=0.028) and its ligands *Cd112* (4.1 fold, p=0.001) and *Cd155* (3.2 fold, p=0.007) in tumors from *EμMyc Nr4a1*-/- mice. Furthermore, *Btla* (2 fold, p=0.009), *Hvem* (2.3 fold, p=0.002) and *Cd160* (7.9 fold, p=0.009) were all higher expressed in tumors from *EμMyc Nr4a1*-/- mice compared to tumors from *EμMyc Nr4a1*+/+ mice. In contrast the expression levels of *Tigit* and *Ctla4* were similar in both mouse cohorts evaluated, with a rather slightly higher expression in tumors derived from *EμMyc Nr4a1*+/+ mice. Results showed a 1.1 fold higher expression of *Tigit* (p=0.880) and 1.2 fold higher expression levels of *Ctla4* (p=0.832) in tumors without *Nr4a1* loss. (Figure 23).

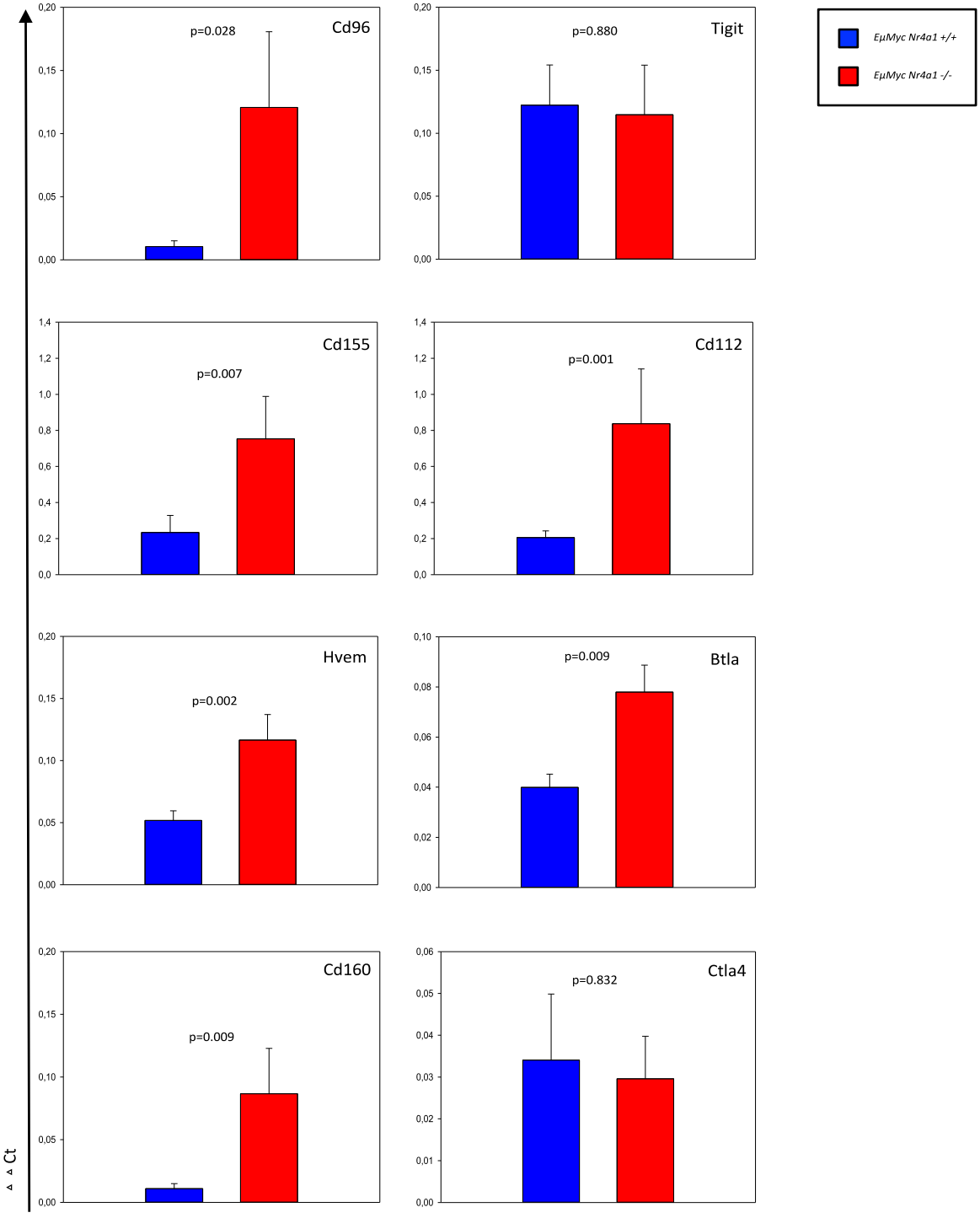

Figure 23: Semi-quantitative RQ-PCR for immunoinhibitory genes in primary tumors (cont.)

Relative expression values of *EμMyc Nr4a1*+/+ (n=20, blue bars) and *EμMyc Nr4a1*-/- mice (n=20, red bars). Each bar represents the mean values of expression levels ± standard error of the mean (SEM). p-values are depicted in the respective graphs.

Interestingly, many molecules with an immunostimulatory function were also overexpressed in tumors from of *EμMyc Nr4a1*-/- mice (Figure 24). In primary tumors, we found higher expression levels of members of the Cd80/Cd86–Cd28/Ctla4 IgG superfamily. In tumors of *EμMyc* mice with *Nr4a1* loss, *Cd28* was 13.3 fold higher (p=0.001), *Cd80* 8.3 fold higher (p=0.000), and *Cd86* 1.7 fold higher (p=0.003) expressed. Moreover, the co-stimulatory molecules *Icos* and its ligand *IcosL* were 5.2 fold (p=0.002) and 1.5 fold (p=0.304) higher expressed, respectively. *Irak4*, another immunostimulatory molecule, was also 2.2 fold (p=0.001) overexpressed in *EμMyc Nr4a1*-/- tumors. Last, *Cd25* and *Cd226* showed quite a high overexpression in *EμMyc* tumors with *Nr4a1* loss. *Cd25* was 7.7 fold (p=0.025) and *Cd226* was 9.4 fold (p=0.004) higher expressed on these tumor cells.

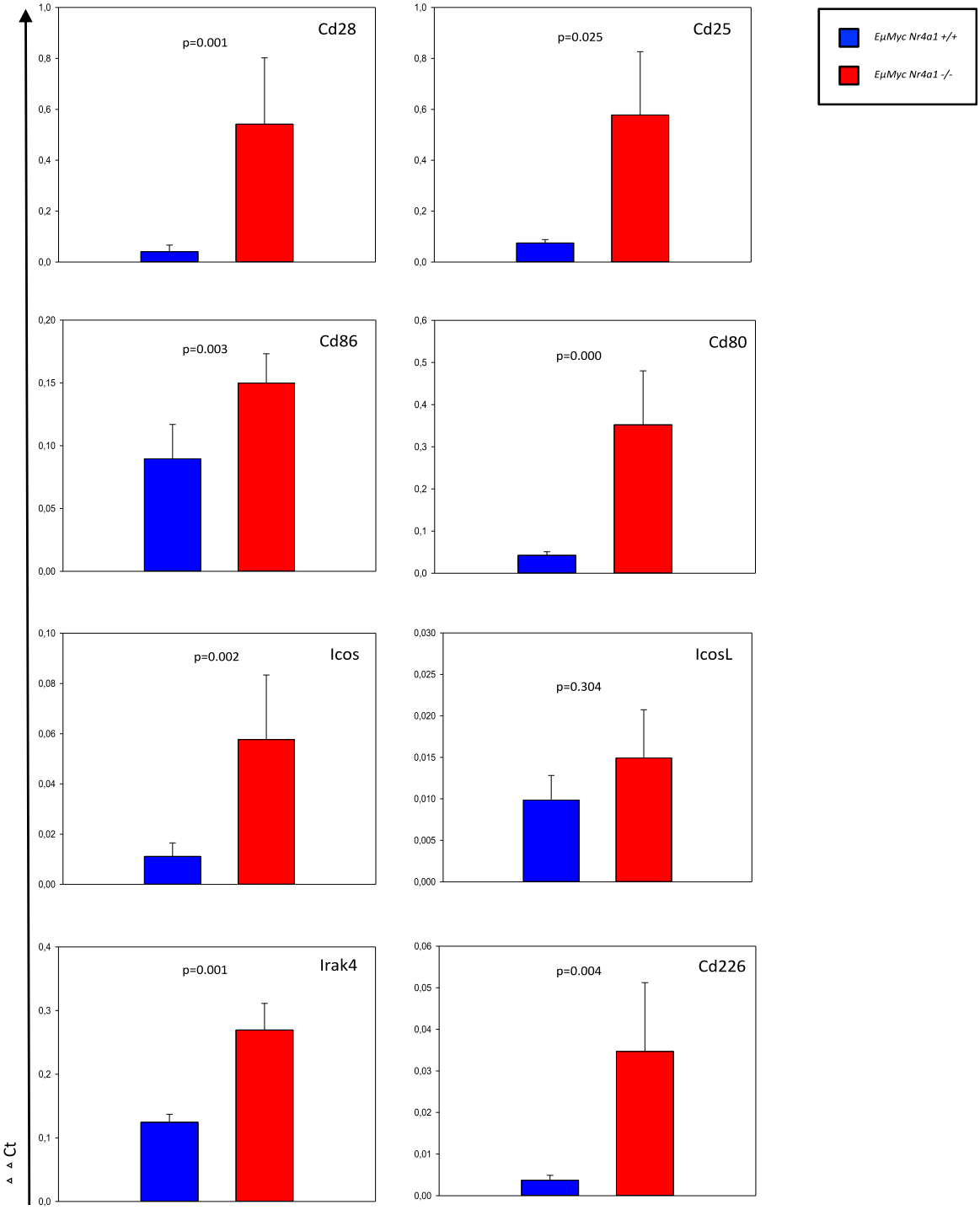

Figure 24: Semi-quantitative RQ-PCR for immunostimulatory genes in primary tumors.

Relative expression values of *EμMyc Nr4a1*+/+ (n=20, blue bars) and *EμMyc Nr4a1*-/- mice (n=20, red bars). Each bar represents the mean values of expression levels ± standard error of the mean (SEM). p-values are depicted in the respective graphs.

Regarding cytokine and transcription factor expression profiles, we determined expression levels of several pro- and anti-inflammatory cytokines and expression of Foxp3. Expression of the anti-inflammatory *interleukin 10* was slightly higher in *EμMyc Nr4a1*+/+ derived tumors (1.2 fold, p=0.074). The immunoinhibitory transcription factor *Foxp3* was 5.2 fold higher expressed in *EμMyc Nr4a1*-/- tumors (p=0.007). Similarly, we found a 2.9 fold overexpression of *Il2* in the same tumor specimens (p=0.565). Members of the Il12 family of cytokines showed all an enhanced expression in *EμMyc Nr4a1*-/- tumors as opposed to *EμMyc Nr4a1*+/+ tumors. *Il12* was 9.7 fold (p=0.003), *Il23* 5.1 fold (p=0.002), and *Il27* 2.1 fold (p=0.101) higher expressed. *Il17* was found to be 3.8 fold overexpressed in *EμMyc* Nr4a1+/+ tumors compared to *EμMyc* Nr4a1-/- tumors (p=0.836), while *Il21* was 1.3 fold higher (p=0.199) and *Il16* 2.9 fold higher (p=0.000) expressed in *EμMyc* tumors with Nr4a1 loss. Interestingly, we detected a 3 fold overexpression of *IFNγ* in tumors without Nr4a1 loss (p=0.001) (Figure 25).

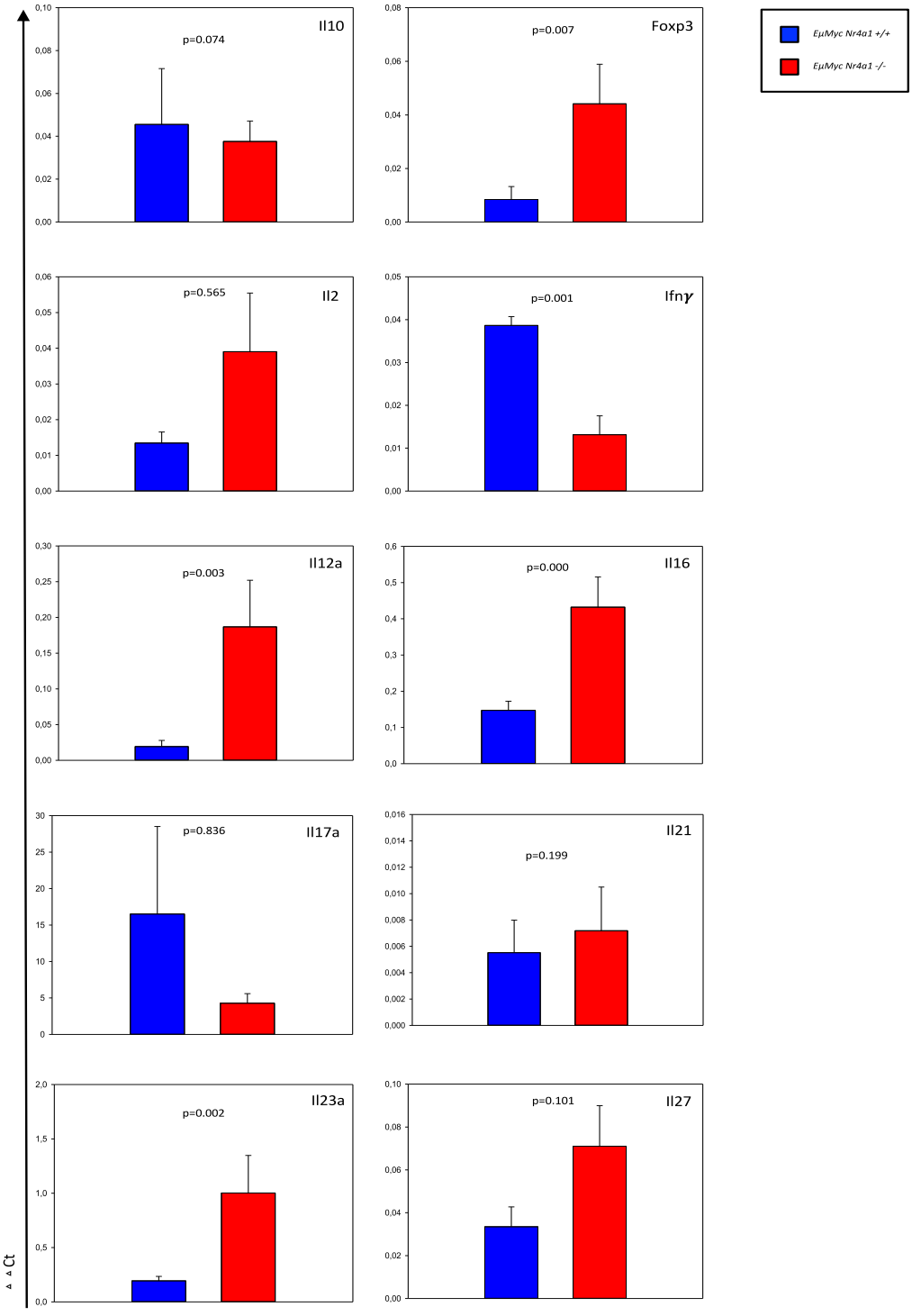

Figure 25: Semi-quantitative RQ-PCR for cytokines and transcription factors in primary tumors.

Relative expression values of *EμMyc Nr4a1*+/+ (n=20, blue bars) and *EμMyc Nr4a1*-/- mice (n=20, red bars). Each bar represents the mean values of expression levels ± standard error of the mean (SEM). p-values are depicted in the respective graphs.

Taken together, the expression data of tumors of both mouse cohorts demonstrate that the loss of *Nr4a1* leads to an upregulation of many immunoregulatory molecules. Importantly, many of them have immunoinhibiting functions on diverse immune cells. This indicates a role of *Nr4a1* in immunomodulation.

8.2.6 *Nr4a1* Loss Leads to Decreased Survival upon Transplantation of Tumors into wt but Not into Immunodeficient Mice

Based on the fact that the *Nr4a1*-/- mouse has an immunological phenotype and, on our observation, that *Nr4a1* loss resulted in higher expression of genes being implicated in immunoregulation, we decided to decipher this effect by transplantation of tumor cells into wt and immunodeficient mice. It has been described that *Nr4a1*-/- mice lack $Ly6C^-$ monocytes subpopulations, and harbour changes in macrophage tolerance and phagocytosis, clonal deletion, Treg cell differentiation and increased numbers of Cd8 T cells (339-341).Therefore, we transplanted single cell suspensions derived from tumors of *EμMyc Nr4a1*-/- and *EμMyc Nr4a1*+/+ into C57/Bl6 wt recipients (n=20 per genotype) as an immunocompetent model and Fox Scid Beidge mice (n=15 per genotype) as an immunodeficient model to investigate the lymphoma cell intrinsic function and the immune regulatory function of *Nr4a1* loss in *Myc*-driven lymphomagenesis.

Fourteen wt mice transplanted with *EμMyc Nr4a1*-/- tumor cells and thirteen mice transplanted with *EμMyc Nr4a* +/+ tumor cells developed visible tumors. In five Fox Scid Beidge mice we could not detect any engraftment of either tumor cells derived from *EμMyc Nr4a1*-/- or *EμMyc Nr4a1* mice, respectively.

In both experiments, mice were monitored on a daily base until onset of overt disease, ruffled fur and signs of poor general condition. As shown in Figure 26a, the median survival of mice transplanted with *EμMyc Nr4a1*-/- tumor cells (red line) was 23 days compared to 28 days for mice transplanted with *EμMyc*-derived tumors without *Nr4a1* loss (blue line) (p= 0.003; Figure 26a). In contrast, we did not observe any differences in survival upon transplantation of tumor cells derived from either *EμMyc Nr4a1*-/- (red line) or *EμMyc Nr4a1*+/+ (blue line) mice into immunodeficient Fox Chase SCID Beige mice (median survival 24 days for *EμMyc Nr4a1*-/- derived tumors and 23 days for *EμMyc Nr4a1*+/+ derived tumors; p=0.552, Figure 26b).

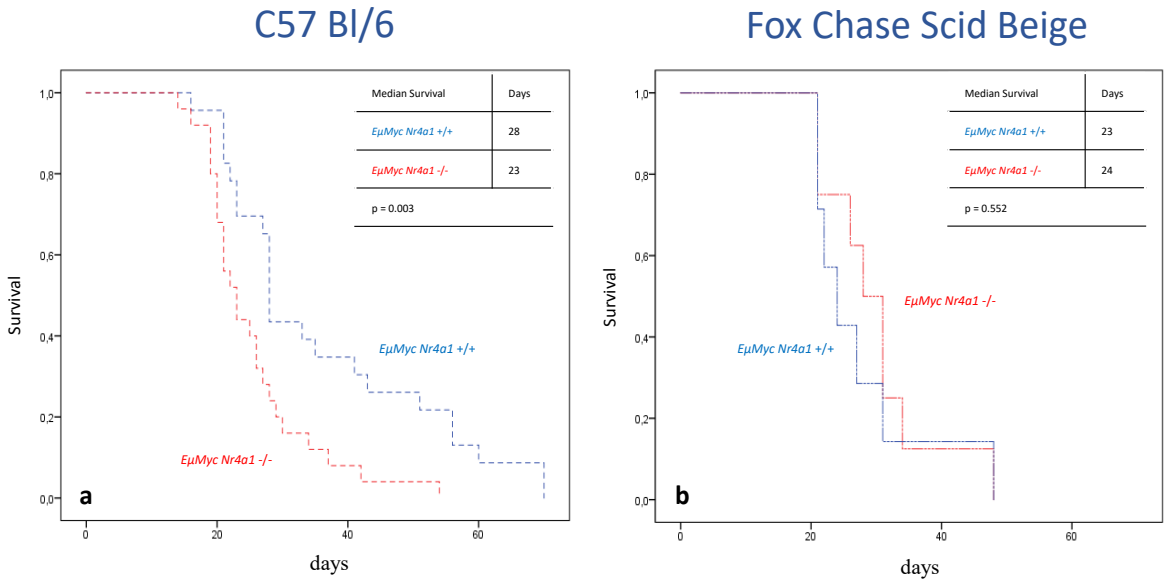

Figure 26: Kaplan Meyer analysis of wt C57/Bl6 and immunodeficient Fox Chase SCID Beige recipients after transplantation with tumor cells.

(a) C57/Bl6 mice were injected i.v. with tumors derived from *EμMyc Nr4a1*+/+ mice (n=13, blue line) or *EμMyc Nr4a1*-/- mice (n=14, red line) and survival was monitored (p=0.003). (b) Fox Chase SCID Beige mice were injected i.v. with tumors derived from *EμMyc Nr4a1*+/+ mice (n=10, blue line) or *EμMyc Nr4a1*-/- mice (n=10, red line) and survival was monitored (p=0.552).

These data indicate that the tumor microenvironment plays a role in *Nr4a1*-mediated lymphomagenesis.

8.2.7 *Nr4a1* Loss Is Linked to a Higher Dissemination Potential of Tumor Cells into Bone Marrow of wt but Not Immunodeficient Mice

Dissemination of lymphoid neoplasms is, like metastasis in solid tumors, a hallmark of these diseases. It is guided by adhesion molecules as well as chemokines and their receptors, and is therefore linked to specific tissues for distinct lymphoma entities and influenced by the interaction of malignant cells with immune cells (342, 343). With this respect, we investigated dissemination of tumor cells from *EμMyc Nr4a1*+/+ and *EμMyc Nr4a1*-/- tumors into bone marrow and spleen and compared data of C57/Bl6 and Fox Chase Scid Beige mice. Therefore, tumor single cell suspensions were stained with antibodies against Cd19 and B220, and expression levels of B cells were detected by flow cytometric analysis. After transplantation of tumors cell into C57/Bl6 wt mice we observed

a similar percentage of B cells in the spleen while we found increased percentages of B cells in the bone marrow. In detail, we found 28.1% vs 31.2% Cd19+ B220+ cells in the spleen of wt mice after transplantation of *EμMyc Nr4a1*+/+ and *EμMyc Nr4a1*-/- tumors, respectively (Figure 27a, p=0.778). In contrast, the percentage of B cells in the bone marrow of wt mice was 42.0% after transplantation of *EμMyc Nr4a1*+/+ tumors and 62.5% after transplantation of tumors with *Nr4a1* loss (Figure 27b, p=0.065). Importantly, differences in dissemination into spleen and bone marrow were negligible in Fox Chase Scid Beige mice. In the spleen of immunodeficient mice we detected 48.3% vs 37.9% when comparing transplantation of *EμMyc Nr4a1*-/- to *EμMyc Nr4a1*+/+ tumors (Figure 27c, p=0.673). Furthermore, there was no difference regarding dissemination into the bone marrow with similar percentages of B cells upon transplantation of both tumor genotypes (44.9% vs 41.1% for *EμMyc Nr4a1*-/- and *EμMyc Nr4a1*+/+ tumors, respectively, Figure 27d, p=1.000).

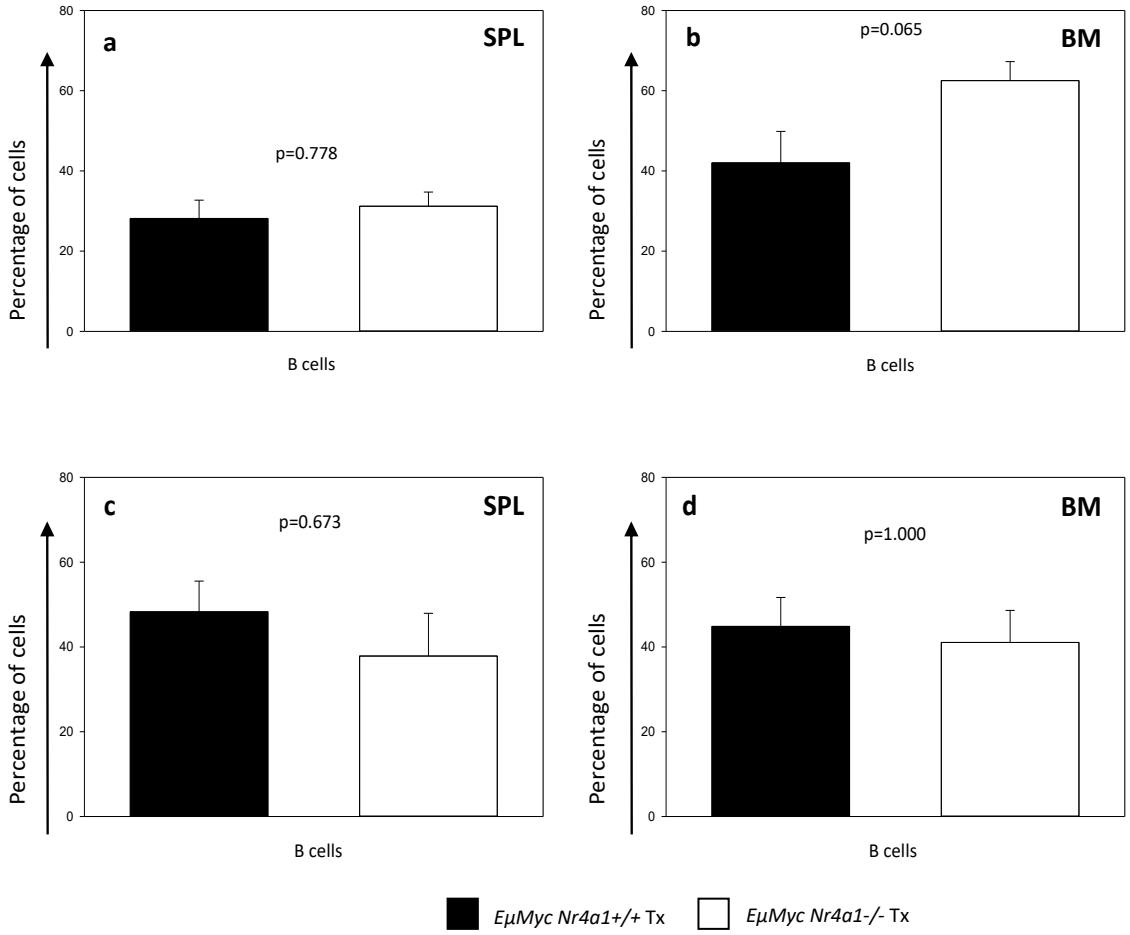

Figure 27: Percentages of B cells in spleen and bone marrow after transplantation of C57/Bl6 and Fox Chase Scid Beige mice with *EμMyc Nr4a1*+/+ or *EμMyc Nr4a1*-/- derived tumors.

(a) Single cell suspensions of spleen cells derived from wt mice transplanted with tumors from *EμMyc Nr4a1*+/+ (n=13 black bar) or *EμMyc Nr4a1*-/- (n=14, white bar) mice were stained with antibodies against Cd19 and B220. (b) Single cell suspensions of bone marrow cells derived from wt mice transplanted with tumors from *EμMyc Nr4a1*+/+ (n=13 black bar) or *EμMyc Nr4a1*-/- (n=14, white bar) mice were stained with antibodies against Cd19 and B220. (c) Single cell suspensions of spleen cells derived from immunodeficient mice transplanted with tumors from *EμMyc Nr4a1*+/+ (n=10 black bar) or *EμMyc Nr4a1*-/- (n=10, white bar) mice were stained with antibodies against Cd19 and B220. (d) Single cell suspensions of bone marrow cells derived from immunodeficient mice transplanted with tumors from *EμMyc Nr4a1*+/+ (n=10 black bar) or *EμMyc Nr4a1*-/- (n=10, white bar) mice were stained with antibodies against Cd19 and B220. Each bar represents the mean values of expression levels ± standard error of the mean (SEM). p-values are depicted in the respective graphs.

These results show that spreading of tumor cells exhibiting *Nr4a1* loss - especially into the bone marrow - is higher in immunocompetent mice. Lack of tumor microenvironment in immunodeficient mice diminishes dissemination and thus underpins the role of immunoregulatory mechanisms in *Nr4a1*-based tumor development.

8.2.8 Transplantation of Tumors into C57/Bl6 Mice Further Enhances the Immunomodulatory Effect of Nr4a1 Loss

In order to compare expression levels of those immunoregulatory molecules examined in primary tumors, tumor tissue of transplanted C57/Bl6 mice (n=13 for *EμMyc Nr4a1*+/+ and n=14 for *EμMyc Nr4a1*-/- mice) was frozen and further analyzed by RQ-PCR. In accordance with the higher expression levels of immunosuppressive molecules detected on tumor cells of primary tumors, we could confirm these results in transplanted tumors. *Pd1* was 5.9 fold overexpressed in transplanted tumors from *EμMyc Nr4a1*-/- mice (p=0.027), while its ligands *Pdl1* and *Pdl2* were 7.9 fold (p=0.038) and 9.04 fold (p=0.007) overexpressed. Expression levels of the other molecules were 3.5 fold higher in the tumors derived from transplantation of tumors with *Nr4a1* loss for *Tim3* (p=0.293), 3.2 fold higher for *Gal9* (p=0.027), and 5.2 fold higher for *Lag3* (p=0.013) (Figure 28).

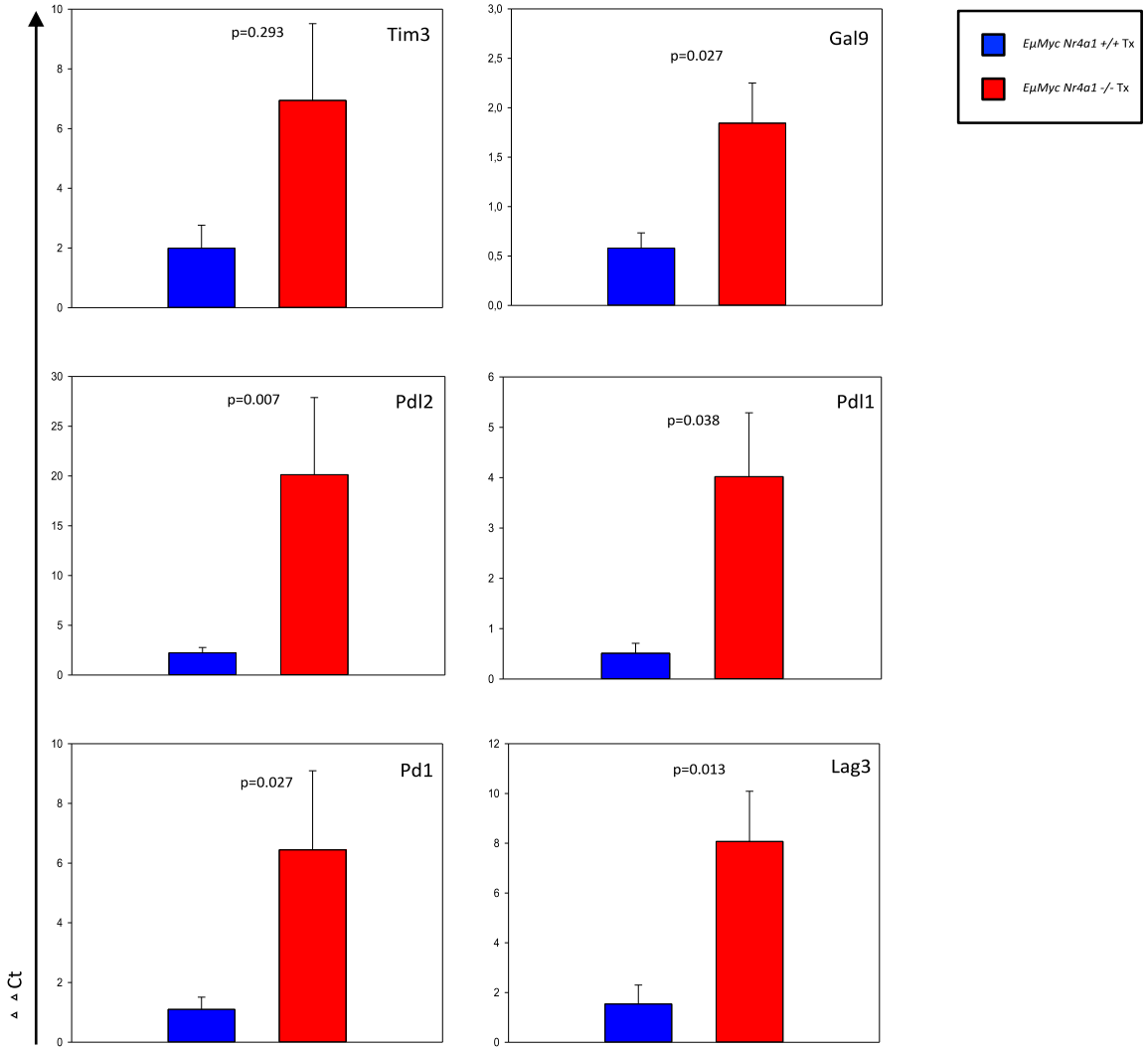

Figure 28: Semi-quantitative RQ-PCR for immunoinhibitory genes in tumors from transplantation of C57/Bl6 mice.

Relative expression values of *EμMyc Nr4a1*+/+ (n=13, blue bars) and *EμMyc Nr4a1*-/- mice (n=14, red bars). Each bar represents the mean values of expression levels ± standard error of the mean (SEM). p-values are depicted in the respective graphs.

With respect to expression levels of other immunoinhibitory molecules, the levels ranged from a 1.4 fold overexpression for *Tigit* (p=0.421) to a 55.6 fold overexpression for *Ctla4* (p=0.006) in *EμMyc Nr4a1*-/- derived transplanted tumors, which is in contrast to primary tumors. Moreover, we detected a 3.6 fold higher expression of *Cd96* (p=0.003) and a 5.2 fold and 3.6 fold higher expression of its ligands *Cd155* (p=0.021) and *Cd112* (p=0.218), respectively, in *EμMyc Nr4a1*-/- derived transplanted tumors. Likewise, *Hvem* was 3.9 fold (p=0.042), *Btla* 2.4 fold (p=0.003), and *Cd160* 2.8 fold (p=0.108) overexpressed upon transplantation of tumors with *Nr4a1* loss (Figure 29).

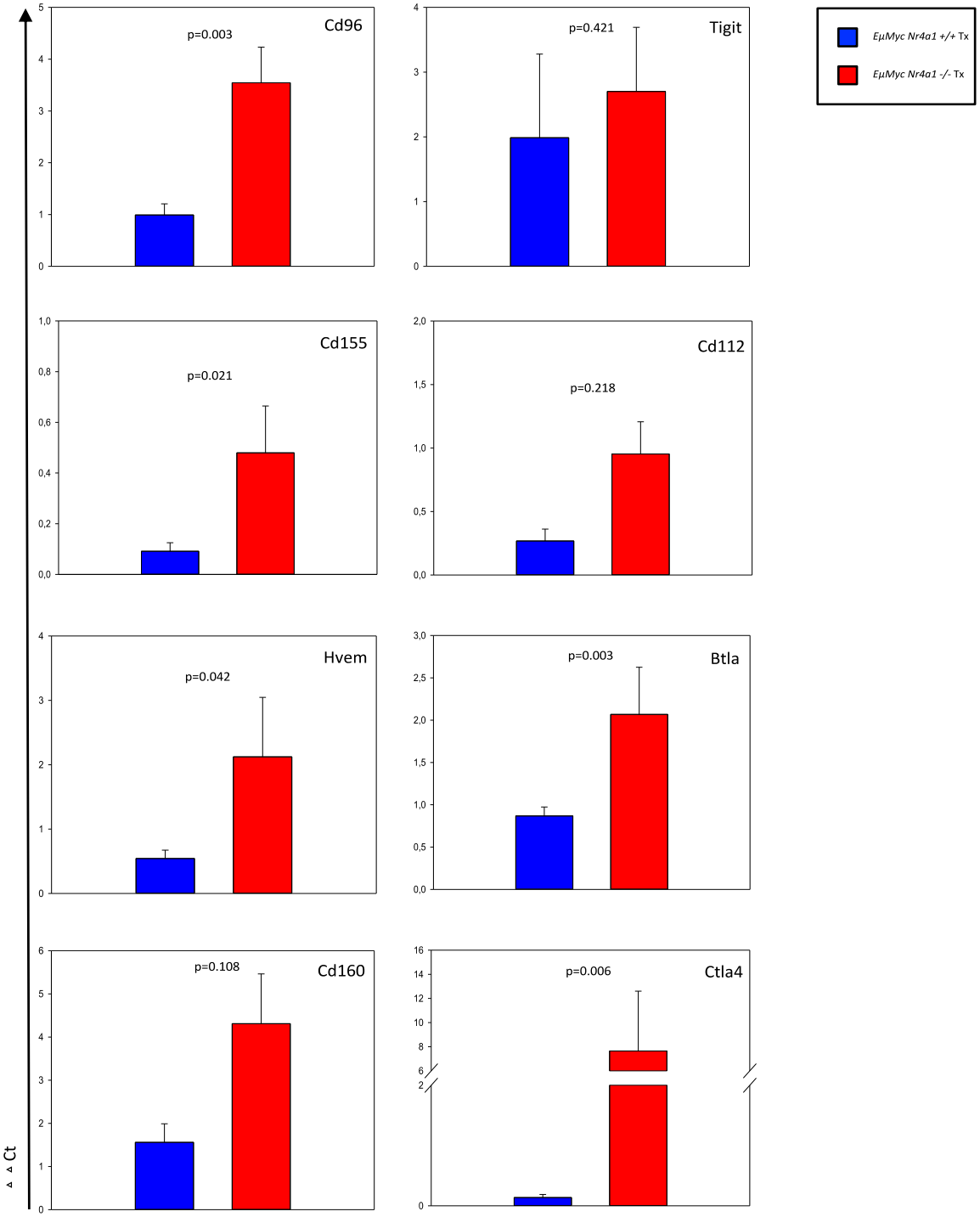

Figure 29: Semi-quantitative RQ-PCR for immunoinhibitory genes in tumors from transplantation of C57/Bl6 mice (cont).

Relative expression values of *EμMyc Nr4a1*+/+ (n=13, blue bars) and *EμMyc Nr4a1*-/- mice (n=14, red bars). Each bar represents the mean values of expression levels ± standard error of the mean (SEM). p-values are depicted in the respective graphs.

As shown in Figure 30, the expression levels of immunostimulatory molecules was changed for some genes tested when comparing primary to transplanted tumors. Expression levels of *Cd25* (p=0.602), *Cd80* (p=0.955) and *Irak4* (p=0.941) were similar in both groups. All other genes examined, were higher expressed in tumors derived from mice transplanted with *EμMyc Nr4a1*-/- tumors opposed to mice transplanted with tumors without *Nr4a1* loss. In particular, *Cd28* was 3.6 fold higher (p=0.128), *Cd86* 1.5 fold higher (p=0.186), *Cd226* 4 fold higher (p=0.027), and *Icos* and *IcosL* 4.6 fold (p=0.104) and 3.7 fold (p=0.026) higher expressed.

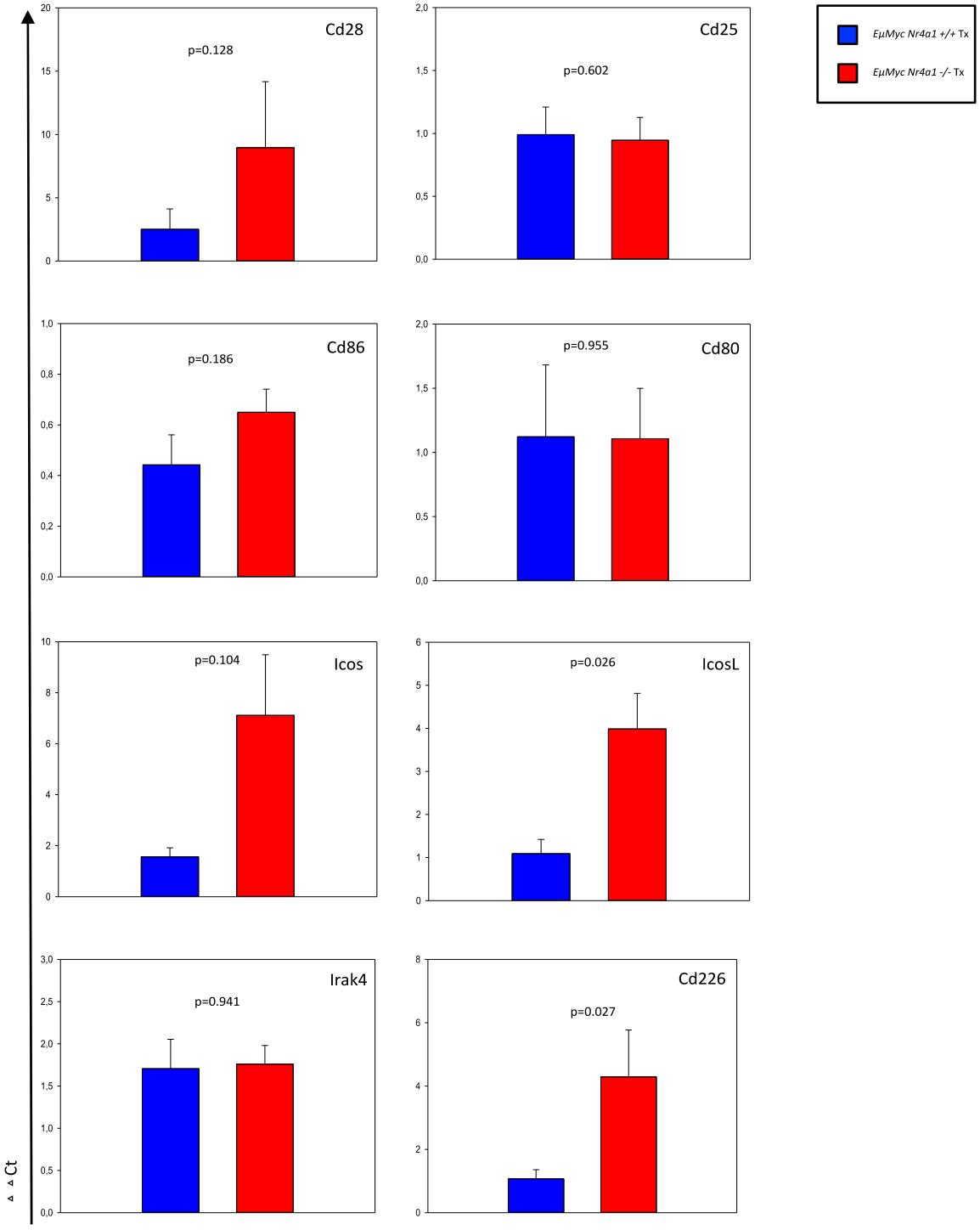

Figure 30: Semi-quantitative RQ-PCR for immunostimulatory genes in tumors from transplantation of C57/Bl6 mice.

Relative expression values of *EμMyc Nr4a1*+/+ (n=13, blue bars) and *EμMyc Nr4a1*-/- mice (n=14, red bars). Each bar represents the mean values of expression levels ± standard error of the mean (SEM). p-values are depicted in the respective graphs.

Furthermore, we examined again RNA expression levels of several cytokines and *Foxp3* (Figure 31). Intriguingly, expression levels of the proinflammatory cytokine *Ifnγ* were drastically diminished in *EμMyc Nr4a1*-/- derived tumors (7.9 fold lower expression compared to tumors derived from transplantations without *Nr4a1* loss, p=0.020), while expression levels of the anti-inflammatory cytokine *Il10* were 6.9 fold increased in the same tumors (p=0.09). Moreover, we found an 81 fold overexpression of *Il2* in tumors with *Nr4a1* loss (p=0.034), while *Foxp3* expression was almost the same in both groups (p=0.738). Several other cytokines were higher expressed in tumors derived from transplantations of *EμMyc Nr4a1*-/- tumors. Among them *Il12* (2 fold, p=0.298), *Il17a* (2.6 fold, p=0.688), *Il21* (13.4 fold; p=0.870), and *Il27* (7.4 fold, p=0.01). Interestingly, *Il23*, forming a heterodimeric protein with the Il-12p40 subunit was 1.9 fold lower expressed in *EμMyc Nr4a1*-/- derived tumors as opposed to *Il12* (p=0.499). For *Il16* we could not detect any differences in the expression levels similar to the expression of Foxp3 (p=0.765).

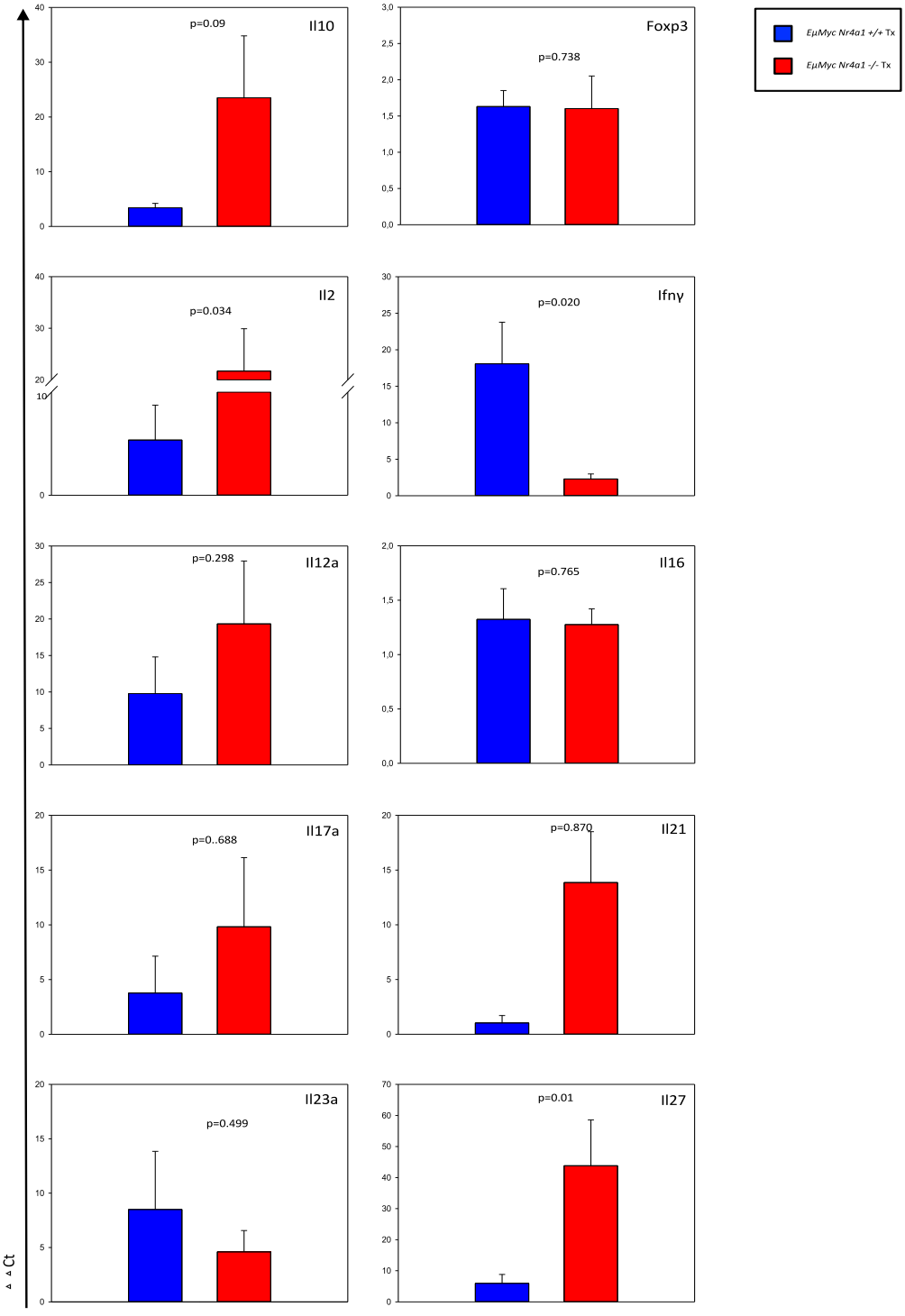

Figure 31: Semi-quantitative RQ-PCR for cytokines and transcription factors in tumors from transplantation of C57/Bl6 mice.

Relative expression values of *EμMyc Nr4a1*+/+ (n=13, blue bars) and *EμMyc Nr4a1*-/- mice (n=14, red bars). Each bar represents the mean values of expression levels ± standard error of the mean (SEM). p-values are depicted in the respective graphs.

Collectively, these data underpin the immunomodulatory role of the orphan receptor *Nr4a1* and shows its tumor suppressive function by transcriptionally regulating genes involved in immunoregulation.

8.2.9 Transplantation of Tumor Cells Exhibiting *Nr4a1* Loss Leads to an Altered Immune Cell Infiltrate of Tumors in wt Mice

Fox Chase SCID Beige mice have non-functional T- and B cell compartments was well as missing NK cells. This indicates that these cells might contribute to immunosurveillance mechanisms owing to loss of *Nr4a1*. Therefore, tumors of C57/Bl6 wt recipients transplanted with tumor cells from *EμMyc Nr4a1*-/- (n=12) or *EμMyc Nr4a1*+/+ (n=12) mice were isolated upon tumor formation. Single cell suspensions of these tumors were stained with antibodies against Cd19, B220 and TCRß, respectively, and cells were subjected to flow cytometric analysis. Interestingly, we detected more reactive B (B220+Cd19+) cells, corresponding to the hosts' own B cells, and T cell (Tcrß+) infiltrates in tumors of wt mice transplanted with tumor cells derived from *EμMyc Nr4a1*-/- mice. Determination of the percentages of B- and T cells in developing tumors gave 1.4% vs 3.1% reactive B cells and 4.9% vs 12.2% T cells in transplanted tumors from *EμMyc Nr4a1*+/+ mice compared to those from *EμMyc Nr4a1*-/- mice (Figure 32).

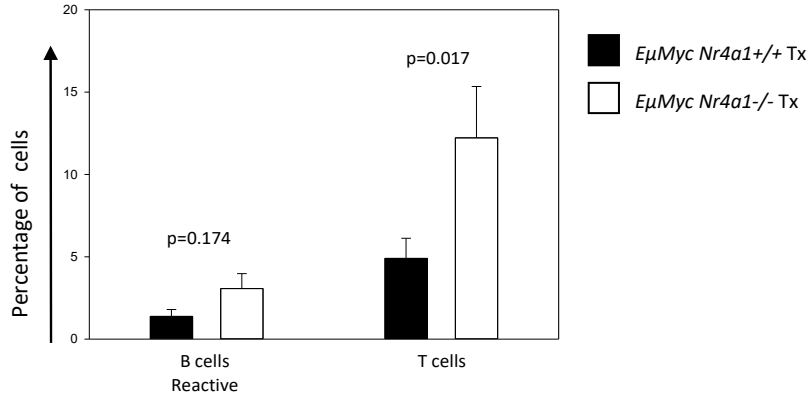

Figure 32: Percentages of reactive B cells and T cells in tumors after transplantation of C57/Bl6 mice with *EμMyc Nr4a1*+/+ or *EμMyc Nr4a1*-/- derived tumors.

Single cell suspensions of tumor cells derived from transplantation of wt mice with tumors from *EμMyc Nr4a1*+/+ (n=12, black bars) or *EμMyc Nr4a1*-/- (n=12, white bars) mice were stained with antibodies against Cd19 and B220 (reactive B cells) and Tcrß (T cells). Each bar represents the mean values of expression levels ± standard error of the mean (SEM). p-values are depicted in the respective graphs.

To evaluate the possible contribution of immunoregulatory molecules, which may dampen the immune response against tumors exhibiting *Nr4a1* loss, we first investigated the expression levels of immune checkpoint inhibitors on B and T cells. Cd3 and Cd19 were used together with Pd1, Pdl1 and Tim3, respectively, to identify T (Cd45+Cd19-Cd3+Pd1+ or Cd45+Cd19-Cd3+Tim3+) and B cells (Cd19+Pdl1+) expressing these immunoregulatory molecules. As shown in Figure 33, we could detect higher mean fluorescence intensities (MFI) of all three marker molecules on tumors developed after transplantation of C57/Bl6 mice with *EμMyc Nr4a1*-/- tumors. Pd1 expression on Cd3 cells was 720.7 MFI vs 4034.5 MFI comparing transplanted tumor cells from *EμMyc Nr4a1*+/+ to *EμMyc Nr4a1*-/- mice (p=0.135). Likewise, we found elevated levels of Tim3 on Cd3 positive cells (44.2 MFI in *EμMyc Nr4a1*+/+ vs 227.5 MFI in *EμMyc Nr4a1*-/- derived tumors, p=0.161) and Pdl1 on Cd19 positive B cells (682.8 MFI in *EμMyc Nr4a1*+/+ vs 1234.5 MFI in *EμMyc Nr4a1*-/- derived tumors, p=0.273).

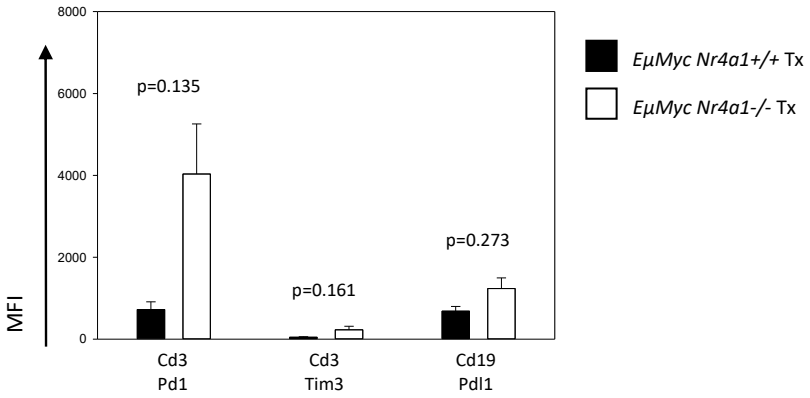

Figure 33: MFI of Pd1, Tim3 and Pdl1 expression on Cd3 and Cd19 positive cells in tumors after transplantation of C57/Bl6 mice with *EμMyc Nr4a1*+/+ or *EμMyc Nr4a1*-/- derived tumors.

Single cell suspensions of tumor cells derived from transplantation of wt mice with tumors from *EμMyc Nr4a1*+/+ (n=12, black bars) or *EμMyc Nr4a1*-/- (n=12, white bars) mice were stained with antibodies against Cd45, Cd19, Cd3 and Pd1or Tim3, respectively, and Cd45, Cd19 and Pdl1. Each bar represents the mean values of expression levels ± standard error of the mean (SEM). p-values are depicted in the respective graphs.

Thus, we looked more in detail into two major T cell subsets, the Cd4 and Cd8 T cells. Both types play a key role in adaptive immunity and while CD8 T cells exert cytotoxic functions (344), CD4 T cells – among other functions - provide help to stimulate immune responses (345). We could not detect a correlation of either more cytotoxic or helper T cells to the increased percentage of T cells in the tumor. In the Cd8 subset, (Cd45+Cd19-Cd3+Cd8+) the percentage of cells was comparable in both groups (1.0% in *EμMyc Nr4a1*+/+ vs 1.1% in *EμMyc Nr4a1*-/- derived tumors, p=0.538) while in the Cd4 subset (Cd45+Cd19-Cd3+Cd4+) we saw an increase in Cd4 T cells upon transplantation of *EμMyc Nr4a1*+/+ derived tumors (3% in *EμMyc Nr4a1*+/+ vs 1.9% in *EμMyc Nr4a1*-/- derived tumors, p=0.187) (Figure 34a). Importantly, results showed a higher expression of immunoregulatory marker molecules on cytototxic Cd8 T cells. We detected both, more Pd1 (Cd45+Cd19-Cd3+Cd8+Pd1+) (569.3 MFI for *EμMyc Nr4a1*+/+ vs 5061.7 MFI for *EμMyc Nr4a1*-/- derived tumors, p=0.063) and Tim3 (Cd45+Cd19-Cd3+Cd8+Tim3+) (10 MFI for *EμMyc Nr4a1*+/+ vs 73.02 MFI for *EμMyc Nr4a1*-/- derived tumors, p=0.053). In the Cd4 T cell subpopulation we could also show an increased expression of both immunomodulatory markers. We determined Pd1 (Cd45+Cd19-Cd3+Cd4+Pd1+) expression to be 838.4 MFI for *EμMyc Nr4a1*+/+ vs 5139 MFI for *EμMyc Nr4a1*-/- derived tumors (p=0.143), and Tim3 (Cd45+Cd19-Cd3+Cd4+Tim3+) expression to be 56.2 MFI for *EμMyc Nr4a1*+/+ vs 146.2 MFI for *EμMyc Nr4a1*-/- derived tumors (p=0.270) (Figure 34b).

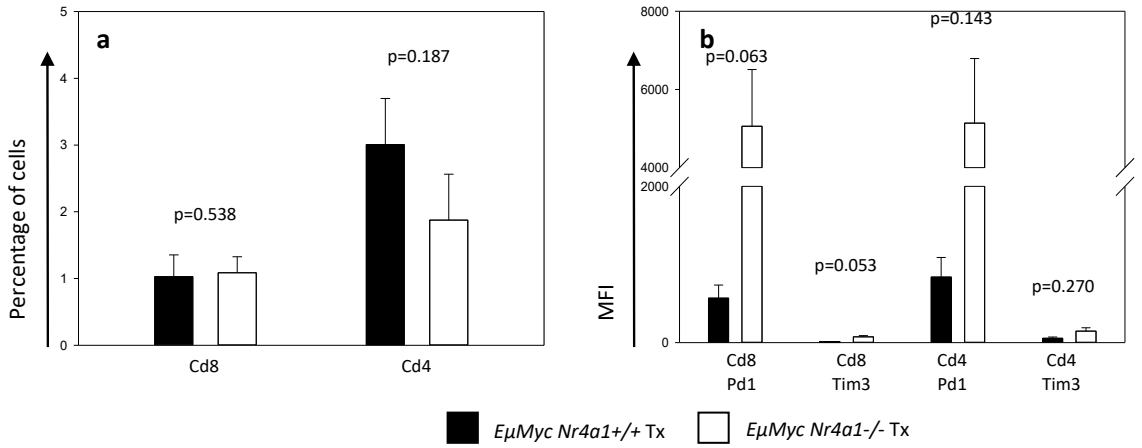

Figure 34: Percentages of Cd8+ and Cd4+ T cells and MFI of Pd1 and Tim3 expression on these cells in tumors after transplantation of C57/Bl6 mice with *EμMyc Nr4a1*+/+ or *EμMyc Nr4a1*-/- derived tumors.

(a) Single cell suspensions of tumor cells derived from transplantation of wt mice with tumors from *EμMyc Nr4a1*+/+ (n=12, black bars) or *EμMyc Nr4a1*-/- (n=12, white bars) mice were stained with antibodies against Cd45, Cd19, Cd3 and Cd8 or Cd4, respectively. (b) Single cell suspensions of tumor cells derived from transplantation of wt mice with tumors from *EμMyc Nr4a1*+/+ (n=12, black bars) or *EμMyc Nr4a1*-/- (n=12, white bars) mice were stained with antibodies against Cd45, Cd19, Cd3 and Cd8 or Cd4, respectively together with staining of either Pd1 or Tim3. Each bar represents the mean values of expression levels ± standard error of the mean (SEM). p-values are depicted in the respective graphs.

These results suggest that even though *Nr4a1* loss provokes higher immune cell infiltrates, these infiltrating cells might be blocked in their anti-tumoral activity as shown by higher MFI of Pd1 expression on T cells, leading to a faster outgrowth of tumors upon transplantation of *EμMyc Nr4a1*-/- derived tumor cells.

Another important characteristic of proper T cell function is the differentiation of naïve cells to more experienced memory and effector cells. Naïve, central memory, effector memory and effector cells can be characterized by combinations of different marker molecules and represent distinct features regarding extravasation from lymphoid tissue and cytokine secretion (346). Hence, we performed further evaluation of distinct T cell subpopulations using Cd62L and Cd44 expression. Analysis of T cell differentiation states using the pan T cell marker Cd3 - ranging from the naïve to more educated states with

prior antigen contact and cytotoxic populations – revealed no marked differences in Cd3 T cells. Naïve T cells (Cd45+Cd19-Cd3+Cd44-Cd62L+) were 3.6% vs 18.7% (p=0.121), central memory (CM, Cd45+Cd19-Cd3+Cd44+Cd62L+) were 9.5% vs 6.1% (p=0.083), effector memory (EM, Cd45+Cd19-Cd3+Cd44+Cd62L-) 32.2% vs 36.5% (p=0.770), and double negative (-/-, Cd45+Cd19-Cd3+Cd44-Cd62L-) were 62.6% vs 43.5% comparing tumors from wt mice transplated with *EμMyc Nr4a1*+/+ and *EμMyc Nr4a1*-/- tumors, respectively (Figure 35).

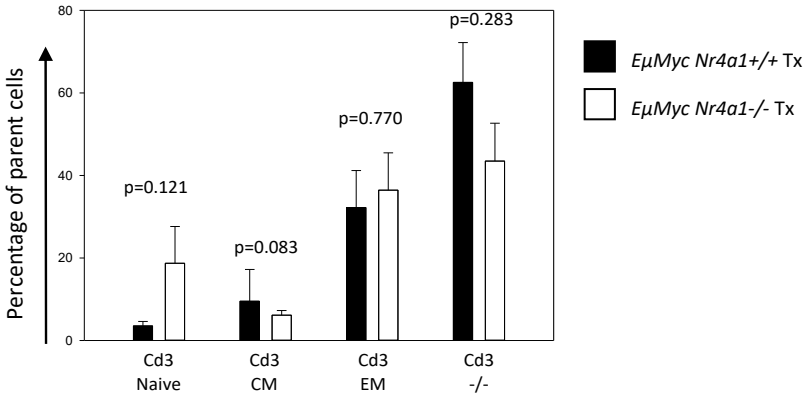

Figure 35: Percentages of T cell subpopulations of Cd3+ cells in tumors after transplantation of C57/Bl6 mice with *EμMyc Nr4a1*+/+ or *EμMyc Nr4a1*-/- derived tumors.

Single cell suspensions of tumor cells derived from transplantation of wt mice with tumors from *EμMyc Nr4a1*+/+ (n=12, black bars) or *EμMyc Nr4a1*-/- (n=12, white bars) mice were stained with antibodies against Cd45, Cd19, Cd3, Cd62L and Cd44, respectively. Each bar represents the mean values of expression levels ± standard error of the mean (SEM). p-values are depicted in the respective graphs.

Further characterization of Cd8 and Cd4 positive T cells demonstrated that subtypes where significantly changed in the Cd4 T cell population. In the Cd8 positive T cell population, naïve T cells (Cd45+Cd19-Cd3+Cd8+Cd44-Cd62L+) were 20.1% vs 30.3% (p=0.121), central memory (Cd45+Cd19-Cd3+Cd8+Cd44+Cd62L+) were 8.8% vs 12.0% (p=0.105), effector memory (Cd45+Cd19-Cd3+Cd8+CD44+Cd62L-) 14.7% vs 25.3% (p=0.196) comparing tumors from wt mice transplated with *EμMyc Nr4a1*+/+ or *EμMyc Nr4a1*-/- tumors (Figure 36a). In the Cd4 T cell compartment we detected 16.2% vs 30.2.7% naïve T cells (Cd45+Cd19-Cd3+Cd4+Cd44-Cd62L+, p=0.055), 1.2% vs 3.8% central memory Cd4 T cells (Cd45+Cd19-Cd3+Cd4+Cd44+Cd62L+, p=0.034), and 19.3% vs 37.9% (Cd45+Cd19-Cd3+Cd4+Cd44+Cd62L-, p=0.033) effector memory Cd4 T cells comparing

transplation of *EμMyc Nr4a1*+/+ or *EμMyc Nr4a1*-/- tumors (Figure 36b). Interestingly, in both subtypes we noted a decreased expression of double negative effector cells upon transplantation of tumors with *Nr4a1* loss (49.95% vs 39.8% in Cd8 T (Cd45+Cd19-Cd3+Cd8+Cd44-Cd62L-) cells and 63.3% vs 34.0% in Cd4 T (Cd45+Cd19-Cd3+Cd4+Cd44-Cd62L-) cells comparing *EμMyc Nr4a1*+/+ to *EμMyc Nr4a1*-/- tumors (Figure 36a and b).

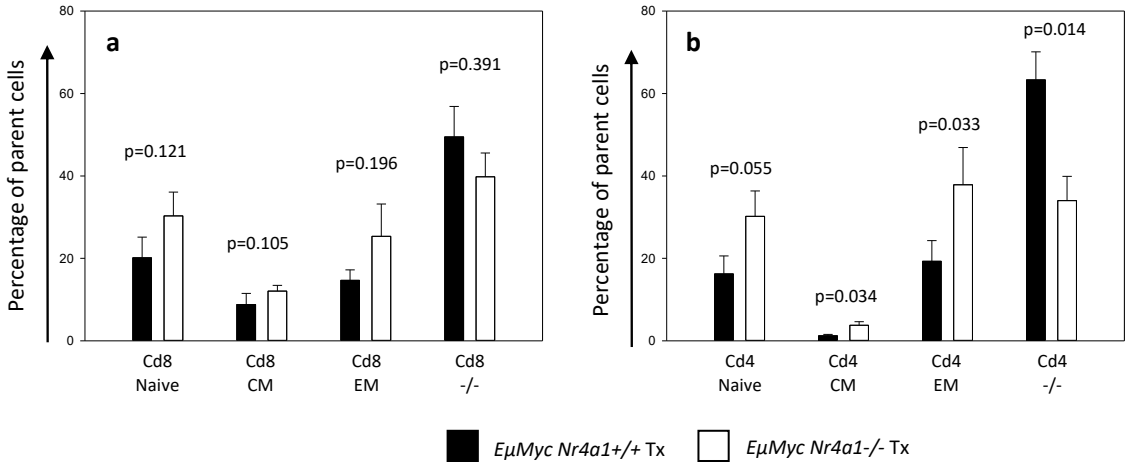

Figure 36: Percentages of T cell subpopulations in Cd8+ and Cd4+ T cells in tumors after transplantation of C57/Bl6 mice with *EμMyc Nr4a1*+/+ or *EμMyc Nr4a1*-/- derived tumors.

(a) Single cell suspensions of tumor cells derived from transplantation of wt mice with tumors from *EμMyc Nr4a1*+/+ (n=12, black bars) or *EμMyc Nr4a1*-/- (n=12, white bars) mice were stained with antibodies against Cd45, Cd19, Cd3, Cd8, Cd62L and Cd44, respectively. (b) Single cell suspensions of tumor cells derived from transplantation of wt mice with tumors from *EμMyc Nr4a1*+/+ (n=12, black bars) or *EμMyc Nr4a1*-/- (n=12, white bars) mice were stained with antibodies against Cd45, Cd19, Cd3, Cd4, Cd62L and Cd44, respectively. Each bar represents the mean values of expression levels ± standard error of the mean (SEM). p-values are depicted in the respective graphs.

Last, we investigated the contribution of two other T cell subtypes belonging to the Cd4 T cell subset and being characterized by Rorγt and Il17 (Cd45+Cd19-Cd3+Cd4+Rorγt+) or Cd25/Foxp3 (Treg cells, Cd45+Cd19-Cd3+Cd4+Foxp3+) expression. While T_H17 cells exert a proinflammatory function (347), regulatory T cells suppress other T cell populations (348). Therefore, cells were subjected to Cd3 and Cd4 staining together with intracellular staining of the transcription factors Rorγt or Foxp3, respectively. In the T_h17 subset we detected 14.1% vs 19.5% (p=0.644), and in the regulatory subset 13.2% vs 12.2% (p=0.510) in tumors derived from transplantation of *EμMyc Nr4a1*+/+ or *EμMyc Nr4a1*-/- derived tumor cells (Figure 37).

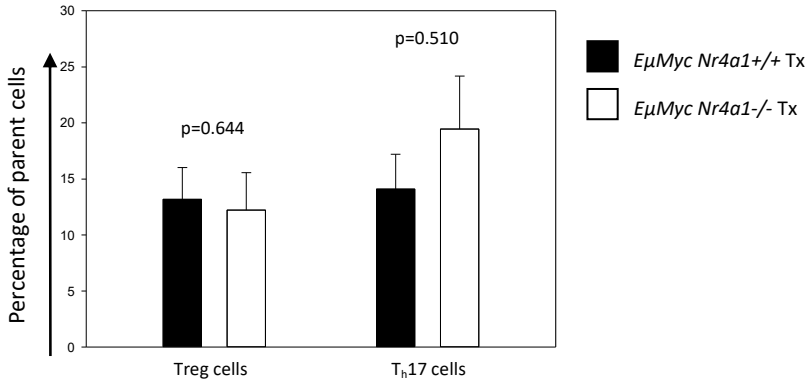

Figure 37: Percentages of Treg and T_h17 cells in tumors after transplantation of C57/Bl6 mice with *EμMyc Nr4a1*+/+ or *EμMyc Nr4a1*-/- derived tumors.

Single cell suspensions of tumor cells derived from transplantation of wt mice with tumors from *EμMyc Nr4a1*+/+ (n=12, black bars) or *EμMyc Nr4a1*-/- (n=12, white bars) derived tumors were stained with antibodies against Cd45, Cd19, Cd3, Cd4, Foxp3 and Rorγt, respectively. Each bar represents the mean values of expression levels ± standard error of the mean (SEM). p-values are depicted in the respective graphs.

These findings underpin the idea that higher expression of immunoregulatory molecules on T cells is rather responsible for reduced survival upon transplantation of *EμMyc Nr4a1*-/- tumors than regulatory T cells or an imbalance in other inflammatory T cell subsets. Moreover, distinct T cell subpopulations, especially in the Cd4 T cell subtype, might contribute to the observed effects.

Apart from looking at the adaptive immune system, we evaluated cells of the innate immune system and myeloid subpopulations. With respect to the innate cells, γδTcr, NKp46 and Cd3 were used to examine the expression levels of atypical T cells bearing the γδ T cell receptor as well as NK and NKT cells. As shown in Figure 38, all examined subpopulations were rarely found in the engrafted lymphomas. We detected 0.05% vs 0.18% γδ T cells (Cd45+Cd19-Cd3+Cd4-Cd8-γδTcr+), 0.06% vs 0.25% NKT cells (Cd45+Cd19-Cd3+Cd4-Cd8-NKp46+), and 0.21% vs 0.20% NK cells (Cd45+Cd19-Cd3-NKp46+) in tumors from transplantation of *EμMyc Nr4a1*+/+ or *EμMyc Nr4a1*-/- derived tumor cells, respectively.

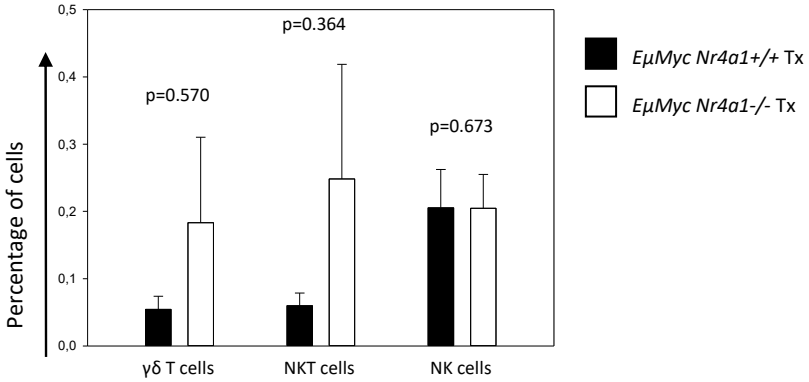

Figure 38: Percentages of γδ T cells, NKT cells and NK cells in tumors after transplantation of C57/Bl6 mice with *EμMyc Nr4a1*+/+ or *EμMyc Nr4a1*-/- derived tumors.

Single cell suspensions of tumor cells derived from transplantation of wt mice with tumors from *EμMyc Nr4a1*+/+ (n=12, black bars) or *EμMyc Nr4a1*-/- (n=12, white bars) mice were stained with antibodies against Cd45, Cd19, Cd3, Cd4, Cd8, γδTcr, and NKp46, respectively. Each bar represents the mean values of expression levels ± standard error of the mean (SEM). p-values are depicted in the respective graphs.

To check, whether differences were also present in cells of the myeloid lineage, we stained cells with markers against Cd11b, Ly6c, Ly6g, Cd11c and F4/80. Although infiltrates of myeloid cells in tumors were scarce, tumors derived from *EμMyc Nr4a1*-/- cells had 0.9% neutrophils (Cd45+Cd19-Ly6G+) and 0.4% monocytes (Cd45+Cd19-Ly6G-F4/80-Cd11c-Cd11b+Ly6C+) compared to tumors derived from transplantation of *EμMyc Nr4a1*+/+ cells (0.2%, p=0.007 and 0.2%, p=0.291, respectively). In contrast the percentage of macrophages (Cd45+Cd19-Ly6G-F4/80+Cd11c+) was lower in tumors derived from transplantation of *EμMyc Nr4a1*-/- cells (0.5%) than from *EμMyc Nr4a1*+/+ cells (0.6%,

p=0.210) (Figure 39a). Interestingly, we detected a significantly higher percentage of Pdl1 in all myeloid subpopulations examined (Figure 39b). Pdl1 expression was 420.8 MFI vs 825.6 MFI (p=0.030) on neutrophils (Cd45+Cd19-Ly6G+Pdl1+), 625.9 MFI vs 943.0 MFI (p=0.055) on monocytes (Cd45+Cd19-Ly6G-F4/80-Cd11c-Cd11b+Ly6C+Pdl1), and 1980.0 MFI vs 3420.6 MFI (p=0.017) on macrophages (Cd45+Cd19-Ly6G-F4/80+Cd11c+Pdl1) comparing tumors derived from *EμMyc Nr4a1*+/+ to *EμMyc Nr4a1*-/- cells (Figure 39b).

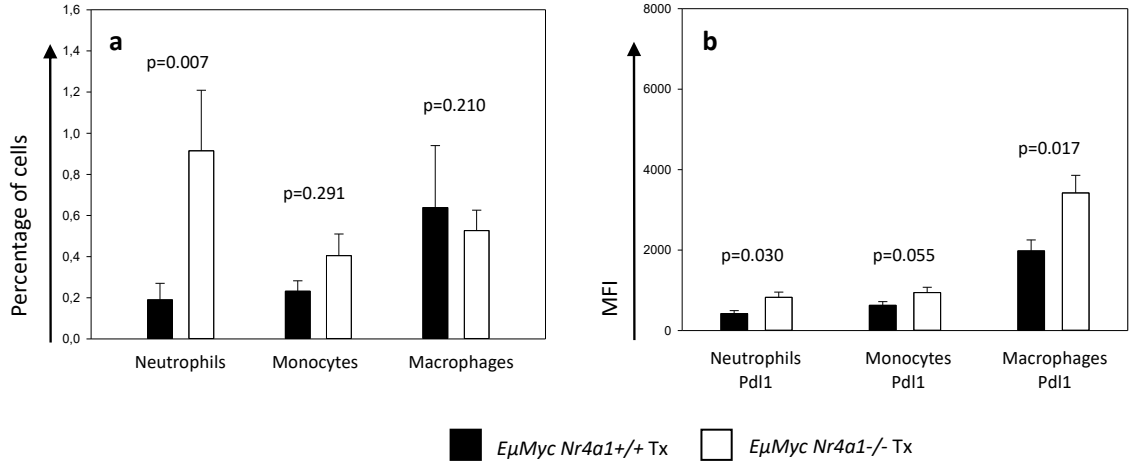

Figure 39: Percentages of neutrophils, monocytes, and macrophages and MFI of Pdl1 expression of these cells in tumors after transplantation of C57/Bl6 mice with *EμMyc Nr4a1*+/+ or *EμMyc Nr4a1*-/- derived tumors.

Single cell suspensions of tumor cells derived from transplantation of wt mice with tumors from *EμMyc Nr4a1*+/+ (n=12, black bars) or *EμMyc Nr4a1*-/- (n=12, white bars) mice were stained with antibodies against Cd11b, Ly6c, Ly6g, Cd11c, F4/80 and Pdl1, respectively. Each bar represents the mean values of expression levels ± standard error of the mean (SEM). p-values are depicted in the respective graphs.

This is in detail interesting as the immunosuppressive phenotype of myeloid cells, induced by changes in the tumor microenvironment (349), might contribute to or synergize with expression of immunoregulatory molecules on B and T cells, thereby presumably facilitating lymphoma development.

9 Discussion

The first part of this project (reproduced from Fechter K. *et al*. (286) with permission of Scientific Reports) was designed to investigate the subcellular expression pattern of NR4A1 in human aggressive lymphomas and so to elucidate the non-genomic - cytoplasmic - role of NR4A1 in induction of apoptosis in distinct lymphoma subtypes. Although there is growing evidence that NR4A1 plays an important role in human tumorigenesis and lymphomagenesis (258, 275, 284, 285) and that the apoptotic effects of a number of anti-tumoral agents are mediated by the cytoplasmic function of NR4A1 (258, 275), data on the clinico-pathological relevance of intracellular localization (cytoplasmic and nuclear) of NR4A1 in tumors and especially on lymphoma are scarce. To the best of our knowledge, only one study has dealt with protein levels in cytoplasm of another member of the Nur77 family of nuclear orphan receptors, namely NR4A2. In that study, high levels of cytoplasmic NR4A2 were associated with adverse outcome in bladder cancer patients (350). Contrary to that, our survival analysis clearly demonstrated that high cytoplasmic NR4A1 levels were associated with a favorable clinical course in DLBCLs by performing uni- and multivariate survival analyses. Survival analysis using cytoplasmic NR4A1 levels exhibited a lower p-value than using *NR4A1* expression levels, suggesting cytoplasmic NR4A1 as a better predictive marker in aggressive lymphomas. Nevertheless, it is noteworthy that cytoplasmic NR4A1 is highly associated with distinct DLBCL subtypes. Moreover, it is when compared to the univariate analysis, only borderline significant in the multivariate analysis, which itself is limited by the relatively small cohort size. Therefore, a more detailed investigation is needed to show if high cytoplasmic NR4A1 is indeed an independent factor for disease outcome or a characteristic of the GCB subtype. Together with the fact that rituximab and doxorubicin - two components of the R-CHOP regimen - induce *NR4A1* expression and that NR4A1 is mandatory for viral and BCR-mediated B cell apoptosis (351-355), it could be speculated that NR4A1, especially cytoplasmic NR4A1, influences the therapeutic effect of the cytostatic therapeutic strategies. We also observed that high cytoplasmic NR4A1 levels occurred with a higher incidence in GCB-DLBCL than in NGCB-DLBCL.

Several studies have demonstrated that NR4A1 targets the mitochondria in the cytoplasm, where it binds the hydrophobic groove of the BCL-2 protein, leading to a change in the BCL-2 conformation which changes its function from a cytoprotective to a cytodestructive

molecule triggering cytochrome C release and apoptosis (263, 267). In our lymphoma cohort, we showed that the level of cytoplasmic NR4A1 was associated with the number of lymphoma cells exhibiting a cleaved caspase 3, suggesting that NR4A1 might target the mitochondria in aggressive lymphomas and thereby induces apoptosis. In addition, we observed that the number of lymphoma cells expressing cleaved caspase 3 was significantly higher in GCB-DLBCL. Two other comprehensive studies also demonstrated cleavage of caspase 3 in nodal DLBCL, but they did not show any association with the GCB subtype (356, 357). GO and pathway analysis also determined an enrichment of genes involved in apoptosis. This aligns with our results of the cleaved caspase 3 assay and provides further support for the hypothesis that cytoplasmic NR4A1 is possibly an important factor in the better survival of aggressive lymphomas.

We determined that *XPO1* – encoding a protein known to transport NR4A1 from nucleus to cytoplasm (310) – was overexpressed in the GCB-DLBCL and NGCB-DLBCL subtype compared to GC-B control cells. Overexpression of *XPO1* was shown in primary mediastinal B cell lymphomas and classic Hodgkin lymphomas, mantle cell lymphomas (358, 359), as well as in indolent lymphomas and myeloid neoplasms (360, 361). However, to the best of our knowledge, *XPO1* overexpression has not been described in DLBCL so far. A significant number of NGCB- and GCB-DBCL specimens have been reported to exhibit a copy number gain in 2p15, the chromosomal locus of *XPO1* (362), suggesting this as an important mechanism for *XPO1* overexpression in DLBCL. XPO1 is a new target in cancer therapy based on the development of several XPO1 inhibitors only targeting tumor cells but not normal hematopoietic cells. Inhibitors like KPT-251 and KPT-330 (Selinexor) displayed anti-proliferative and pro-apoptotic activities in various hematological malignancies in both *in vivo* and *in vitro* settings (363-365). Importantly, Selinexor, an orally available irreversible XPO1 inhibitor, showed promising results with a response rate of 31% in patients with advanced NHL participating in a clinical phase I trial (366). However, a correlation between *XPO1* overexpression and levels of cytoplasmic NR4A1 could not be observed, suggesting that other factors/mechanisms might trigger NR4A1 translocation to the cytoplasm.

To identify other mechanisms that could lead to NR4A1 translocation to the cytoplasm and therefore to elevated apoptosis, we used functional profiling of GCB- and NGCB-DLBCL microarray samples, as the GCB subtype is highly associated with high cytoplasmic

NR4A1 levels. GO and pathway analysis revealed an enrichment of changes in AKT and ERK1/2 signaling. As a number of kinases have already been shown to phosphorylate NR4A1, causing translocation to the cytoplasm such as JNK, AKT, RSK, and ERK1/2 (269, 274, 321-323, 367, 368), activated AKT and/or ERK1/2 signaling might cause impaired NR4A1 translocation to the cytoplasm. As a consequence, NR4A1 would not be able to exert its pro-apoptotic function in the cytoplasm, which ultimately would lead to diminished apoptosis and thereby to decreased survival. Our explorative gene expression analysis of AKT-, ERK1-2-, JNK, and mTOR-targets genes demonstrated that five of eight ERK1/2 target genes investigated showed higher expression in DLBCLs with high cytoplasmic NR4A1 levels. The obtained data point to an association between activated ERK1/2 and cytoplasmic localization of NR4A1 and indicate that ERK1/2 signaling may play a role in cytoplasmic localization of NR4A1 in aggressive lymphomas.

In the second part of the project we examined *in vivo* the role of *Nr4a1* in lymphoma development. In order to first evaluate whether *Nr4a1* plays a role in lymphomagenesis we used two well described mouse models. Previous work from our group as well as other reports underlined the role of *Nr4a1* and *Nr4a3* in the development of lymphoid and myeloid malignancies. While *NR4A1* and *NR4A3* were found to be downregulated in aggressive lymphoid malignancies, which was associated with reduced survival and apoptosis (284, 285), the loss of *Nr4a1* and *Nr4a3* in double knockout mice led to the rapid development of AML (279). Moreover, gene dosage seems to be important as hypoallelic *Nr4a1*+/- *Nr4a3*-/- or *Nr4a1*-/- *Nr4a3*+/- mice developed a mixed myelodysplastic/ myeloproliferative disease (280). Likewise, crossing of the *Myc*-driven lymphoma mouse model with *Nr4a1*-/- mice clearly demonstrated that *Nr4a1* exerts a tumor suppressive function. Homozygous loss of *Nr4a1* led to reduced survival and accelerated lymphoma formation compared to heterozygous and control mice without *Nr4a1* loss, respectively.
A more detailed analysis of the role of *Nr4a1* in our lymphoma mouse model revealed that loss of the nuclear receptor suppressed the pro-survival effect of the *Myc* protooncogene causing the survival of several B cell populations in bone marrow and secondary lymphoid organs even ahead of tumor formation at pre-malignant stage. Our previous studies demonstrating that ectopic overexpression of *NR4A1* in aggressive lymphoma cells results in induction of apoptosis (284, 285) confirms our observation. In addition, the increased

number of transitional T3 B cells – known to be involved to some extent in unresponsiveness to B cell receptor stimuli and thereby possessing lower apoptosis rates (369) – confirmed the pro-apoptotic function of *Nr4a1* and its implication in B cell apoptosis of pre-malignant and malignant lymphoma cells. These observations suggest an important pro-apoptotic role of *Nr4a1* in lymphomagenesis even before lymphoma development.

Gene expression profiling revealed that *Nr4a1* loss resulted in a significant upregulation of 57 and downregulation of 18 genes, indicating that this nuclear receptor may act as transcriptional repressor. A more detailed bioinformatical analysis of the differentially expressed genes, showed that GO-terms associated with immunological processes were associated with deregulated genes sets. Validation of these genes participating in B- and T cell immunology, immune regulation, the Nf-kB pathway and cell cycle control by RQ-PCR, respectively, further indicated an immunological component in lymphomagenesis upon loss of *Nr4a1*. In particular, we found a significant upregulation of genes involved in T- and B cell responses and differentiation, the Nf-kB pathway, and immunoregulatory mechanisms in *EμMyc* mice with *Nr4a1* loss. Interestingly, the effect of overexpression of the majority of genes seemed to be more pronounced in IgM- tumors than in IgM+ tumors. Here, genes involved in B cell immunology as well as Nf-kB target genes and immunomodulatory molecules were higher expressed in IgM negative tumor specimens of *EμMyc Nr4a1*-/- mice as opposed to *EμMyc Nr4a1*+/+ mice. Therefore, it might be hypothesized that loss of *Nr4a1* also impacts immunological pathways in *Myc*-driven lymphomagenesis.

Several reports described immunological defects in *Nr4a1*-/- mice affecting myeloid and T cell subpopulations (339-341). Transplantation of tumor cells into immunocompetent and immunocompromised mice were performed to demonstrate that the accelerated lymphomagenesis is a lymphoma cell intrinsic effect and not mediated by the immunological phenotype of *Nr4a1*-/- mice. Transplantation of tumors cells derived from *EμMyc Nr4a1*-/- and *EμMyc Nr4a1*+/+ mice, respectively, into C57/Bl6 wt recipients showed that loss of *Nr4a1* resulted in a significantly reduced survival compared to transplanted tumors from *EμMyc Nr4a1*+/+ mice. In stark contrast, transplantation of the same tumor cells into immunodeficient Fox Chase SCID Beige mice resulted in no differences in survival. The median survival was similar to that of C57/Bl6 mice

transplanted with *EμMyc Nr4a1*-/- lymphoma cells. This proves the importance of the tumor microenvironment in *Nr4a1*-mediated lymphomagenesis and that loss of *Nr4a1* results in a suppression of anti-lymphoma immunity. In accordance with these results, we detected higher percentages of B220+Cd19+ lymphoma cells in the bone marrow of *EμMyc Nr4a1*-/- mice and C57/Bl6 wt mice transplanted with *EμMyc Nr4a1*-/- tumors. Contrary to that, there were no differences in B cells in bone marrow isolated from immunocompromised mice transplanted with *EμMyc Nr4a1*-/- tumors, suggesting the involvement of the immune system in lymphoma dissemination.

Gene expression analysis of immunomodulatory genes and cytokines in primary and transplanted lymphoma cells revealed that the majority of genes tested was overexpressed in tumors harboring a *Nr4a1* loss and those derived from transplantation of *EμMyc Nr4a1*-/- tumor cells. The higher expression levels of immunoinhibitory molecules and cytokines in primary tumors upon loss of *Nr4a1* indicates that *Nr4a1* regulates the expression of molecules important for proper immune response towards tumors. Expression levels of immunoinhibitory markers like *Pd1*, *Pdl1*, *Pdl2*, *Tim3* and *Gal9* were all higher in tumors derived from *EμMyc Nr4a1*-/- mice. While the immunoinhibitory molecules Pdl1 and Pdl2 bind to its receptor Pd1, Gal9 represents the ligand for Tim3. Compared to co-stimulatory and inhibitory receptors regulating immune cell activation, immunoinhibitory receptors and ligands are often overexpressed in the tumor microenvironment (197). *TIM3* has been shown to be expressed in various solid and blood-born malignancies, where it is involved in exhausted of T cells and inhibition of dendritic cells (202-204). With respect to GAL9, its function is more diverse, as it not solely binds to TIM3 but furthermore influences other cellular mechanisms like apoptosis, cell cycle control, migration and metastases (205). Likewise, the main function of constitutive or adaptive expression of PD1 and its ligands in cancer, is to limit the activation of T cells (197). Importantly, the immunoinhibitory role of the PD1 pathway is becoming more and more clear and several inhibitory antibodies have been shown promising results in clinics (244, 249, 370). Additionally, other immunoinhibitory molecules being widely expressed on lymphoid cells were found to be overexpressed in *EμMyc Nr4a1*-/- lymphomas (183). We detected a higher expression of the inhibitory molecules *Lag3 (207)* and *Cd96* and also of the immunostimulatory molecule *Cd226*. Furthermore, the same trend was observed for *Cd112* and *Cd155* – the ligands for Cd96, Cd226 and Tigit - in *EμMyc Nr4a1*-/- derived tumors. Likewise, the

expression levels of *Hvem* and its receptors *Btla* and *Cd160*, having all immunoinhibitory effects on most hematopoietic cells (194, 196), were higher in *EμMyc Nr4a1*-/- tumors. In contrast, we found similar expression levels of the immunoinhibitory markers *Ctla* - impeding prolonged T cell activation (172) - and *Tigit* - binding to Cd155 and Cd112 (185, 186) - in both tumor groups. With respect to the immunostimulatory molecules tested, we could see an increased expression of members of the Cd28 superfamily, *Cd28*, *Cd80*, *Cd86* (172), Icos as well as its ligand *IcosL* (174, 175), the *interleukin 2 receptor α chain* (*Cd25*) (180) and *Irak4* (182) in *EμMyc Nr4a1*-/- tumors. Moreover, analysis of cytokines and transcription factors revealed a slightly higher expression of the immunosuppressive cytokine *Il10* – inhibiting innate and adaptive immune responses (209, 210)- and *Ifnγ* - enhancing immunity (216) – in *EμMyc Nr4a1*+/+ lymphomas. In contrast, *Il2* – stimulating immune responses of various cells like T- and NK cells (179) – and *Foxp3* – inducing tolerance (211) – showed a higher expression in the same tumors. Last, members of the proinflammatory interleukin 12 family of cytokines (*Il12, Il23, Il27*) (371) were like the chemoattractant *Il16* (233) and the B cell differentiation cytokine *Il21* (229), but unlike *Il17a* - important for host defense but also contributing to autoimmune diseases (223) - found to be higher expressed in primary tumors from *EμMyc Nr4a1*-/- mice. Comparison of the results of primary to transplanted tumors showed that most of the genes examined in primary tumors followed the same trend, namely a higher expression in tumors derived from transplantation of *EμMyc Nr4a1*-/- lymphoma cells. Interestingly, we detected a slightly higher expression of *Tigit* and a massively higher expression of *Ctla4* in transplanted tumors from *EμMyc Nr4a1*-/- mice. Furthermore, while *Cd25*, *Cd80* and *Irak4*, respectively, showed a higher expression in primary tumors of *EμMyc Nr4a1*-/- mice, we could not see these effects in transplanted tumors. Rather, here the expression levels were comparable in both transplanted tumor types. The same trend was found when measuring the relative expression of *Foxp3* and *Il16*. Finally, expression of *Il17a* was higher in transplanted tumors from *EμMyc Nr4a1*-/- mice as opposed to primary tumors, and *Il10* expression was extremely increased in the same specimens. This suggests that *Nr4a1* results in immune evasion by upregulation of immunoregulatory genes like *Pd1*, *Ctla4*, *Il10* and many others. Noteworthy, further *in vivo* experiments using blocking antibodies targeting selected immune checkpoints together with transplantation of tumors cells, will lead to a more detailed picture of this influence on immune evasion.

Targeting the tumor microenvironment to circumvent immunosurveillance mechanisms is becoming more and more important in clinics (372). In this sense, we investigated immune cell infiltrates and the protein expression of Pd1, Tim3 and Pdl1 on T- and B cells of transplanted tumors. Importantly, we could confirm the results obtained on RNA level also on protein level. Staining of tumor cells of transplanted tumors showed more T cell infiltrates in tumors derived from *EμMyc Nr4a1*-/- mice. Furthermore, we found a higher expression of Pd1 and Tim3 on T cells and Pdl1 on B cells in tumors derived from *EμMyc Nr4a1*-/- mice. This trend was also visible when looking at Cd8 and Cd4 T cells separately, even though percentages of Cd8 and Cd4 T cells were similar and even higher in transplanted tumors of *EμMyc Nr4a1*+/+ mice, respectively. With respect to different T cell subpopulations, we detected higher percentages of naïve-, central- and effector memory cells on Cd3+, Cd4+ or Cd8+ T cells in transplanted tumors from *EμMyc Nr4a1*+/+ mice compared to double negative cells, which were higher in tumors from *EμMyc Nr4a1*-/- mice. While we could not detect any differences in other T cell subsets, we interestingly found a significantly higher percentage of infiltrating neutrophils and also monocytes in tumors derived from *EμMyc Nr4a1*-/- mice and additionally higher expression levels of Pdl1 on all myeloid populations tested. Collectively, these results underpin the immunological component of *Nr4a1* in *Myc*-driven lymphoma development. Hence, further studies are needed to obtain more information about the tumor suppressive role of *Nr4a1* in lymphomagenesis. Therefore, in future experiments, we aim to validate our observations in B cell-specific knockouts using the Cre-LoxP system, look in more detail into protein expression of immunoregulatory molecules in control mice at the premalignant and more advanced stages of lymphoma formation and last investigate more in detail distinct putative pathways involved in immunoregulation.

These two studies provide the first evidence that NR4A1 plays distinct roles in lymphomagenesis. The subcellular localization of NR4A1 can be clearly and robustly correlated to different lymphoma subtypes and cancer-specific survival of aggressive lymphoma patients. Likewise, the cytoplasmic NR4A1 expression pattern provides independent prognostic information, thereby representing a potentially useful marker for risk stratification and therapeutic intervention. Furthermore, in our mouse model of *Myc* – driven lymphomagenesis, *Nr4a1* supposedly functions as a tumor suppressor by

influencing the apoptotic potential and expression of immunomodulatory molecules and cytokines. Loss of *Nr4a1* is associated with reduced survival and increased tumor formation as well as increased expression of immunoregulatory molecules on tumor cells. Thus, more studies are needed to better explore the role and underlying mechanisms of *Nr4a1* in lymphoma development.

10 Bibliography

1. Pieper K, Grimbacher B, Eibel H. B-cell biology and development. J Allergy Clin Immunol. 2013;131(4):959-71.
2. Chung JB, Silverman M, Monroe JG. Transitional B cells: step by step towards immune competence. Trends Immunol. 2003;24(6):343-9.
3. Cariappa A, Tang M, Parng C, Nebelitskiy E, Carroll M, Georgopoulos K, et al. The follicular versus marginal zone B lymphocyte cell fate decision is regulated by Aiolos, Btk, and CD21. Immunity. 2001;14(5):603-15.
4. Basu S, Ray A, Dittel BN. Cannabinoid receptor 2 is critical for the homing and retention of marginal zone B lineage cells and for efficient T-independent immune responses. Journal of immunology. 2011;187(11):5720-32.
5. Hagman J, Lukin K. Transcription factors drive B cell development. Curr Opin Immunol. 2006;18(2):127-34.
6. Iwasaki H, Somoza C, Shigematsu H, Duprez EA, Iwasaki-Arai J, Mizuno S, et al. Distinctive and indispensable roles of PU.1 in maintenance of hematopoietic stem cells and their differentiation. Blood. 2005;106(5):1590-600.
7. Marecki S, McCarthy KM, Nikolajczyk BS. PU.1 as a chromatin accessibility factor for immunoglobulin genes. Mol Immunol. 2004;40(10):723-31.
8. Medina KL, Pongubala JM, Reddy KL, Lancki DW, Dekoter R, Kieslinger M, et al. Assembling a gene regulatory network for specification of the B cell fate. Dev Cell. 2004;7(4):607-17.
9. Bain G, Maandag EC, Izon DJ, Amsen D, Kruisbeek AM, Weintraub BC, et al. E2A proteins are required for proper B cell development and initiation of immunoglobulin gene rearrangements. Cell. 1994;79(5):885-92.
10. Lin H, Grosschedl R. Failure of B-cell differentiation in mice lacking the transcription factor EBF. Nature. 1995;376(6537):263-7.
11. Sigvardsson M, Clark DR, Fitzsimmons D, Doyle M, Akerblad P, Breslin T, et al. Early B-cell factor, E2A, and Pax-5 cooperate to activate the early B cell-specific mb-1 promoter. Molecular and cellular biology. 2002;22(24):8539-51.
12. Nikolajczyk BS, Sanchez JA, Sen R. ETS protein-dependent accessibility changes at the immunoglobulin mu heavy chain enhancer. Immunity. 1999;11(1):11-20.
13. Eastman QM, Leu TM, Schatz DG. Initiation of V(D)J recombination in vitro obeying the 12/23 rule. Nature. 1996;380(6569):85-8.
14. Max EE, Seidman JG, Leder P. Sequences of five potential recombination sites encoded close to an immunoglobulin kappa constant region gene. Proc Natl Acad Sci U S A. 1979;76(7):3450-4.
15. Early P, Huang H, Davis M, Calame K, Hood L. An immunoglobulin heavy chain variable region gene is generated from three segments of DNA: VH, D and JH. Cell. 1980;19(4):981-92.
16. Oettinger MA, Schatz DG, Gorka C, Baltimore D. RAG-1 and RAG-2, adjacent genes that synergistically activate V(D)J recombination. Science. 1990;248(4962):1517-23.
17. Mombaerts P, Iacomini J, Johnson RS, Herrup K, Tonegawa S, Papaioannou VE. RAG-1-deficient mice have no mature B and T lymphocytes. Cell. 1992;68(5):869-77.
18. Taccioli GE, Rathbun G, Oltz E, Stamato T, Jeggo PA, Alt FW. Impairment of V(D)J recombination in double-strand break repair mutants. Science. 1993;260(5105):207-10.

19. Dudley DD, Chaudhuri J, Bassing CH, Alt FW. Mechanism and control of V(D)J recombination versus class switch recombination: similarities and differences. Adv Immunol. 2005;86:43-112.
20. Ritchie KA, Brinster RL, Storb U. Allelic exclusion and control of endogenous immunoglobulin gene rearrangement in kappa transgenic mice. Nature. 1984;312(5994):517-20.
21. Alt FW, Enea V, Bothwell AL, Baltimore D. Activity of multiple light chain genes in murine myeloma cells producing a single, functional light chain. Cell. 1980;21(1):1-12.
22. Alt FW, Yancopoulos GD, Blackwell TK, Wood C, Thomas E, Boss M, et al. Ordered rearrangement of immunoglobulin heavy chain variable region segments. EMBO J. 1984;3(6):1209-19.
23. Nieuwenhuis P, Opstelten D. Functional anatomy of germinal centers. Am J Anat. 1984;170(3):421-35.
24. De Silva NS, Klein U. Dynamics of B cells in germinal centres. Nat Rev Immunol. 2015;15(3):137-48.
25. MacLennan IC. Germinal centers. Annu Rev Immunol. 1994;12:117-39.
26. Kerfoot SM, Yaari G, Patel JR, Johnson KL, Gonzalez DG, Kleinstein SH, et al. Germinal center B cell and T follicular helper cell development initiates in the interfollicular zone. Immunity. 2011;34(6):947-60.
27. Kitano M, Moriyama S, Ando Y, Hikida M, Mori Y, Kurosaki T, et al. Bcl6 protein expression shapes pre-germinal center B cell dynamics and follicular helper T cell heterogeneity. Immunity. 2011;34(6):961-72.
28. Szakal AK, Holmes KL, Tew JG. Transport of immune complexes from the subcapsular sinus to lymph node follicles on the surface of nonphagocytic cells, including cells with dendritic morphology. Journal of immunology. 1983;131(4):1714-27.
29. Mandel TE, Phipps RP, Abbot AP, Tew JG. Long-term antigen retention by dendritic cells in the popliteal lymph node of immunized mice. Immunology. 1981;43(2):353-62.
30. Suzuki K, Grigorova I, Phan TG, Kelly LM, Cyster JG. Visualizing B cell capture of cognate antigen from follicular dendritic cells. The Journal of experimental medicine. 2009;206(7):1485-93.
31. Garside P, Ingulli E, Merica RR, Johnson JG, Noelle RJ, Jenkins MK. Visualization of specific B and T lymphocyte interactions in the lymph node. Science. 1998;281(5373):96-9.
32. Okada T, Miller MJ, Parker I, Krummel MF, Neighbors M, Hartley SB, et al. Antigen-engaged B cells undergo chemotaxis toward the T zone and form motile conjugates with helper T cells. PLoS Biol. 2005;3(6):e150.
33. Allen CD, Okada T, Tang HL, Cyster JG. Imaging of germinal center selection events during affinity maturation. Science. 2007;315(5811):528-31.
34. Hauser AE, Junt T, Mempel TR, Sneddon MW, Kleinstein SH, Henrickson SE, et al. Definition of germinal-center B cell migration in vivo reveals predominant intrazonal circulation patterns. Immunity. 2007;26(5):655-67.
35. Zhang J, MacLennan IC, Liu YJ, Lane PJ. Is rapid proliferation in B centroblasts linked to somatic mutation in memory B cell clones? Immunol Lett. 1988;18(4):297-9.
36. Yoshino T, Kondo E, Cao L, Takahashi K, Hayashi K, Nomura S, et al. Inverse expression of bcl-2 protein and Fas antigen in lymphoblasts in peripheral lymph nodes and activated peripheral blood T and B lymphocytes. Blood. 1994;83(7):1856-61.
37. Cervenak L, Magyar A, Boja R, Laszlo G. Differential expression of GL7 activation antigen on bone marrow B cell subpopulations and peripheral B cells. Immunol

Lett. 2001;78(2):89-96.
38. Oliver AM, Martin F, Kearney JF. Mouse CD38 is down-regulated on germinal center B cells and mature plasma cells. Journal of immunology. 1997;158(3):1108-15.
39. Gatto D, Paus D, Basten A, Mackay CR, Brink R. Guidance of B cells by the orphan G protein-coupled receptor EBI2 shapes humoral immune responses. Immunity. 2009;31(2):259-69.
40. Basso K, Dalla-Favera R. BCL6: master regulator of the germinal center reaction and key oncogene in B cell lymphomagenesis. Adv Immunol. 2010;105:193-210.
41. Szakal AK, Taylor JK, Smith JP, Kosco MH, Burton GF, Tew JJ. Kinetics of germinal center development in lymph nodes of young and aging immune mice. Anat Rec. 1990;227(4):475-85.
42. Victora GD, Schwickert TA, Fooksman DR, Kamphorst AO, Meyer-Hermann M, Dustin ML, et al. Germinal center dynamics revealed by multiphoton microscopy with a photoactivatable fluorescent reporter. Cell. 2010;143(4):592-605.
43. Kepler TB, Perelson AS. Cyclic re-entry of germinal center B cells and the efficiency of affinity maturation. Immunol Today. 1993;14(8):412-5.
44. Oprea M, Perelson AS. Somatic mutation leads to efficient affinity maturation when centrocytes recycle back to centroblasts. Journal of immunology. 1997;158(11):5155-62.
45. Bannard O, Horton RM, Allen CD, An J, Nagasawa T, Cyster JG. Germinal center centroblasts transition to a centrocyte phenotype according to a timed program and depend on the dark zone for effective selection. Immunity. 2013;39(5):912-24.
46. Soulas-Sprauel P, Rivera-Munoz P, Malivert L, Le Guyader G, Abramowski V, Revy P, et al. V(D)J and immunoglobulin class switch recombinations: a paradigm to study the regulation of DNA end-joining. Oncogene. 2007;26(56):7780-91.
47. Xu Z, Fulop Z, Zhong Y, Evinger AJ, 3rd, Zan H, Casali P. DNA lesions and repair in immunoglobulin class switch recombination and somatic hypermutation. Ann N Y Acad Sci. 2005;1050:146-62.
48. Allen CD, Ansel KM, Low C, Lesley R, Tamamura H, Fujii N, et al. Germinal center dark and light zone organization is mediated by CXCR4 and CXCR5. Nat Immunol. 2004;5(9):943-52.
49. Victora GD, Nussenzweig MC. Germinal centers. Annu Rev Immunol. 2012;30:429-57.
50. Goidl EA, Paul WE, Siskind GW, Benacerraf B. The effect of antigen dose and time after immunization on the amount and affinity of anti-hapten antibody. Journal of immunology. 1968;100(2):371-5.
51. Han S, Hathcock K, Zheng B, Kepler TB, Hodes R, Kelsoe G. Cellular interaction in germinal centers. Roles of CD40 ligand and B7-2 in established germinal centers. Journal of immunology. 1995;155(2):556-67.
52. Meyer-Hermann ME, Maini PK, Iber D. An analysis of B cell selection mechanisms in germinal centers. Math Med Biol. 2006;23(3):255-77.
53. Shen HM, Peters A, Baron B, Zhu X, Storb U. Mutation of BCL-6 gene in normal B cells by the process of somatic hypermutation of Ig genes. Science. 1998;280(5370):1750-2.
54. Ying CY, Dominguez-Sola D, Fabi M, Lorenz IC, Hussein S, Bansal M, et al. MEF2B mutations lead to deregulated expression of the oncogene BCL6 in diffuse large B cell lymphoma. Nat Immunol. 2013;14(10):1084-92.
55. Wilker PR, Kohyama M, Sandau MM, Albring JC, Nakagawa O, Schwarz JJ, et al. Transcription factor Mef2c is required for B cell proliferation and survival after antigen

receptor stimulation. Nat Immunol. 2008;9(6):603-12.
56. Bollig N, Brustle A, Kellner K, Ackermann W, Abass E, Raifer H, et al. Transcription factor IRF4 determines germinal center formation through follicular T-helper cell differentiation. Proc Natl Acad Sci U S A. 2012;109(22):8664-9.
57. Saito M, Gao J, Basso K, Kitagawa Y, Smith PM, Bhagat G, et al. A signaling pathway mediating downregulation of BCL6 in germinal center B cells is blocked by BCL6 gene alterations in B cell lymphoma. Cancer Cell. 2007;12(3):280-92.
58. Klein U, Casola S, Cattoretti G, Shen Q, Lia M, Mo T, et al. Transcription factor IRF4 controls plasma cell differentiation and class-switch recombination. Nat Immunol. 2006;7(7):773-82.
59. Ochiai K, Maienschein-Cline M, Simonetti G, Chen J, Rosenthal R, Brink R, et al. Transcriptional regulation of germinal center B and plasma cell fates by dynamical control of IRF4. Immunity. 2013;38(5):918-29.
60. Dominguez-Sola D, Victora GD, Ying CY, Phan RT, Saito M, Nussenzweig MC, et al. The proto-oncogene MYC is required for selection in the germinal center and cyclic reentry. Nat Immunol. 2012;13(11):1083-91.
61. Calado DP, Sasaki Y, Godinho SA, Pellerin A, Kochert K, Sleckman BP, et al. The cell-cycle regulator c-Myc is essential for the formation and maintenance of germinal centers. Nat Immunol. 2012;13(11):1092-100.
62. Vikstrom I, Carotta S, Luthje K, Peperzak V, Jost PJ, Glaser S, et al. Mcl-1 is essential for germinal center formation and B cell memory. Science. 2010;330(6007):1095-9.
63. Smith KG, Light A, Nossal GJ, Tarlinton DM. The extent of affinity maturation differs between the memory and antibody-forming cell compartments in the primary immune response. EMBO J. 1997;16(11):2996-3006.
64. Toyama H, Okada S, Hatano M, Takahashi Y, Takeda N, Ichii H, et al. Memory B cells without somatic hypermutation are generated from Bcl6-deficient B cells. Immunity. 2002;17(3):329-39.
65. Obukhanych TV, Nussenzweig MC. T-independent type II immune responses generate memory B cells. The Journal of experimental medicine. 2006;203(2):305-10.
66. Zotos D, Coquet JM, Zhang Y, Light A, D'Costa K, Kallies A, et al. IL-21 regulates germinal center B cell differentiation and proliferation through a B cell-intrinsic mechanism. The Journal of experimental medicine. 2010;207(2):365-78.
67. Campo E, Swerdlow SH, Harris NL, Pileri S, Stein H, Jaffe ES. The 2008 WHO classification of lymphoid neoplasms and beyond: evolving concepts and practical applications. Blood. 2011;117(19):5019-32.
68. Scott DW, Gascoyne RD. The tumour microenvironment in B cell lymphomas. Nat Rev Cancer. 2014;14(8):517-34.
69. Jaffe ES, Harris NL, Stein H, Vardiman JW. World Health Organisation classification of tumors, Pathology and genetics of tumors of Haematopoietic and Lymphoid tissues. Lyon, France: IARC Press; 2001.
70. Swerdlow SH, Campo E, Pileri SA, Harris NL, Stein H, Siebert R, et al. The 2016 revision of the World Health Organization classification of lymphoid neoplasms. Blood. 2016;127(20):2375-90.
71. Anderson JR, Armitage JO, Weisenburger DD. Epidemiology of the non-Hodgkin's lymphomas: distributions of the major subtypes differ by geographic locations. Non-Hodgkin's Lymphoma Classification Project. Annals of oncology : official journal of the European Society for Medical Oncology / ESMO. 1998;9(7):717-20.
72. Howlader N NA, Krapcho M, Miller D, Bishop K, Altekruse SF, Kosary CL, Yu

M, Ruhl J, Tatalovich Z, Mariotto A, Lewis DR, Chen HS, Feuer EJ, Cronin KA (eds). . SEER Cancer Statistics Review, 1975-2013, National Cancer Institute. Bethesda, MD, http://seer.cancer.gov/csr/1975_2013/.
73. Gascoyne RD. Hematopathology approaches to diagnosis and prognosis of indolent B-cell lymphomas. Hematology Am Soc Hematol Educ Program. 2005:299-306.
74. Jaglowski SM, Linden E, Termuhlen AM, Flynn JM. Lymphoma in adolescents and young adults. Seminars in oncology. 2009;36(5):381-418.
75. Schwaenen C, Viardot A, Berger H, Barth TF, Bentink S, Dohner H, et al. Microarray-based genomic profiling reveals novel genomic aberrations in follicular lymphoma which associate with patient survival and gene expression status. Genes, chromosomes & cancer. 2009;48(1):39-54.
76. Johnson NA, Al-Tourah A, Brown CJ, Connors JM, Gascoyne RD, Horsman DE. Prognostic significance of secondary cytogenetic alterations in follicular lymphomas. Genes, chromosomes & cancer. 2008;47(12):1038-48.
77. Morin RD, Johnson NA, Severson TM, Mungall AJ, An J, Goya R, et al. Somatic mutations altering EZH2 (Tyr641) in follicular and diffuse large B-cell lymphomas of germinal-center origin. Nature genetics. 2010;42(2):181-5.
78. O'Riain C, O'Shea DM, Yang Y, Le Dieu R, Gribben JG, Summers K, et al. Array-based DNA methylation profiling in follicular lymphoma. Leukemia. 2009;23(10):1858-66.
79. Gribben JG. Implications of the tumor microenvironment on survival and disease response in follicular lymphoma. Current opinion in oncology. 2010;22(5):424-30.
80. de Jong D, Koster A, Hagenbeek A, Raemaekers J, Veldhuizen D, Heisterkamp S, et al. Impact of the tumor microenvironment on prognosis in follicular lymphoma is dependent on specific treatment protocols. Haematologica. 2009;94(1):70-7.
81. Isaacson P, Wright DH. Extranodal malignant lymphoma arising from mucosa-associated lymphoid tissue. Cancer. 1984;53(11):2515-24.
82. Thieblemont C, Berger F, Dumontet C, Moullet I, Bouafia F, Felman P, et al. Mucosa-associated lymphoid tissue lymphoma is a disseminated disease in one third of 158 patients analyzed. Blood. 2000;95(3):802-6.
83. Troppan K, Wenzl K, Neumeister P, Deutsch A. Molecular Pathogenesis of MALT Lymphoma. Gastroenterology research and practice. 2015;2015:102656.
84. Hallek M, Cheson BD, Catovsky D, Caligaris-Cappio F, Dighiero G, Dohner H, et al. Guidelines for the diagnosis and treatment of chronic lymphocytic leukemia: a report from the International Workshop on Chronic Lymphocytic Leukemia updating the National Cancer Institute-Working Group 1996 guidelines. Blood. 2008;111(12):5446-56.
85. Hallek M, German CLLSG. Prognostic factors in chronic lymphocytic leukemia. Annals of oncology : official journal of the European Society for Medical Oncology / ESMO. 2008;19 Suppl 4:iv51-3.
86. Yang SM, Li JY, Gale RP, Huang XJ. The mystery of chronic lymphocytic leukemia (CLL): Why is it absent in Asians and what does this tell us about etiology, pathogenesis and biology? Blood reviews. 2015;29(3):205-13.
87. Dighiero G, Hamblin TJ. Chronic lymphocytic leukaemia. Lancet. 2008;371(9617):1017-29.
88. Foa R, Del Giudice I, Guarini A, Rossi D, Gaidano G. Clinical implications of the molecular genetics of chronic lymphocytic leukemia. Haematologica. 2013;98(5):675-85.
89. Zenz T, Mertens D, Stilgenbauer S. Biological diversity and risk-adapted treatment of chronic lymphocytic leukemia. Haematologica. 2010;95(9):1441-3.
90. Inamdar KV, Bueso-Ramos CE. Pathology of chronic lymphocytic leukemia: an

update. Annals of diagnostic pathology. 2007;11(5):363-89.
91. Kapoor P, Ansell SM, Braggio E. Waldenstrom Macroglobulinemia: Genomic Aberrations and Treatment. Cancer Treat Res. 2016;169:321-61.
92. Treon SP, Xu L, Yang G, Zhou Y, Liu X, Cao Y, et al. MYD88 L265P somatic mutation in Waldenstrom's macroglobulinemia. The New England journal of medicine. 2012;367(9):826-33.
93. Sambade C, Sällström JF, Sundström C. Molecular pathology in the diagnosis of hematologic neoplasia. Review article. APMIS. 1997;105(12):895-903.
94. Kuppers R. Mechanisms of B-cell lymphoma pathogenesis. Nat Rev Cancer. 2005;5(4):251-62.
95. Fowler NH, Cheah CY, Gascoyne RD, Gribben J, Neelapu SS, Ghia P, et al. Role of the tumor microenvironment in mature B-cell lymphoid malignancies. Haematologica. 2016;101(5):531-40.
96. Said JW. Aggressive B-cell lymphomas: how many categories do we need? Mod Pathol. 2013;26 Suppl 1:S42-56.
97. Montoto S, Fitzgibbon J. Transformation of indolent B-cell lymphomas. J Clin Oncol. 2011;29(14):1827-34.
98. Alizadeh AA, Eisen MB, Davis RE, Ma C, Lossos IS, Rosenwald A, et al. Distinct types of diffuse large B-cell lymphoma identified by gene expression profiling. Nature. 2000;403(6769):503-11.
99. Pasqualucci L, Dalla-Favera R. The genetic landscape of diffuse large B-cell lymphoma. Semin Hematol. 2015;52(2):67-76.
100. Lossos IS, Alizadeh AA, Eisen MB, Chan WC, Brown PO, Botstein D, et al. Ongoing immunoglobulin somatic mutation in germinal center B cell-like but not in activated B cell-like diffuse large cell lymphomas. Proc Natl Acad Sci U S A. 2000;97(18):10209-13.
101. Goodman RH, Smolik S. CBP/p300 in cell growth, transformation, and development. Genes Dev. 2000;14(13):1553-77.
102. Pasqualucci L, Dominguez-Sola D, Chiarenza A, Fabbri G, Grunn A, Trifonov V, et al. Inactivating mutations of acetyltransferase genes in B-cell lymphoma. Nature. 2011;471(7337):189-95.
103. Pasqualucci L, Trifonov V, Fabbri G, Ma J, Rossi D, Chiarenza A, et al. Analysis of the coding genome of diffuse large B-cell lymphoma. Nat Genet. 2011;43(9):830-7.
104. Pasqualucci L, Khiabanian H, Fangazio M, Vasishtha M, Messina M, Holmes AB, et al. Genetics of follicular lymphoma transformation. Cell Rep. 2014;6(1):130-40.
105. Iqbal J, Greiner TC, Patel K, Dave BJ, Smith L, Ji J, et al. Distinctive patterns of BCL6 molecular alterations and their functional consequences in different subgroups of diffuse large B-cell lymphoma. Leukemia. 2007;21(11):2332-43.
106. Pasqualucci L, Migliazza A, Basso K, Houldsworth J, Chaganti RS, Dalla-Favera R. Mutations of the BCL6 proto-oncogene disrupt its negative autoregulation in diffuse large B-cell lymphoma. Blood. 2003;101(8):2914-23.
107. Trinh DL, Scott DW, Morin RD, Mendez-Lago M, An J, Jones SJ, et al. Analysis of FOXO1 mutations in diffuse large B-cell lymphoma. Blood. 2013;121(18):3666-74.
108. Challa-Malladi M, Lieu YK, Califano O, Holmes AB, Bhagat G, Murty VV, et al. Combined genetic inactivation of beta2-Microglobulin and CD58 reveals frequent escape from immune recognition in diffuse large B cell lymphoma. Cancer Cell. 2011;20(6):728-40.
109. Aukema SM, Siebert R, Schuuring E, van Imhoff GW, Kluin-Nelemans HC, Boerma EJ, et al. Double-hit B-cell lymphomas. Blood. 2011;117(8):2319-31.

110. Staiger AM, Ziepert M, Horn H, Scott DW, Barth TFE, Bernd HW, et al. Clinical Impact of the Cell-of-Origin Classification and the MYC/ BCL2 Dual Expresser Status in Diffuse Large B-Cell Lymphoma Treated Within Prospective Clinical Trials of the German High-Grade Non-Hodgkin's Lymphoma Study Group. J Clin Oncol. 2017;35(22):2515-26.
111. Caganova M, Carrisi C, Varano G, Mainoldi F, Zanardi F, Germain PL, et al. Germinal center dysregulation by histone methyltransferase EZH2 promotes lymphomagenesis. J Clin Invest. 2013;123(12):5009-22.
112. Muppidi JR, Schmitz R, Green JA, Xiao W, Larsen AB, Braun SE, et al. Loss of signalling via Galpha13 in germinal centre B-cell-derived lymphoma. Nature. 2014;516(7530):254-8.
113. Davis RE, Ngo VN, Lenz G, Tolar P, Young RM, Romesser PB, et al. Chronic active B-cell-receptor signalling in diffuse large B-cell lymphoma. Nature. 2010;463(7277):88-92.
114. Ngo VN, Young RM, Schmitz R, Jhavar S, Xiao W, Lim KH, et al. Oncogenically active MYD88 mutations in human lymphoma. Nature. 2011;470(7332):115-9.
115. Compagno M, Lim WK, Grunn A, Nandula SV, Brahmachary M, Shen Q, et al. Mutations of multiple genes cause deregulation of NF-kappaB in diffuse large B-cell lymphoma. Nature. 2009;459(7247):717-21.
116. Pasqualucci L, Compagno M, Houldsworth J, Monti S, Grunn A, Nandula SV, et al. Inactivation of the PRDM1/BLIMP1 gene in diffuse large B cell lymphoma. The Journal of experimental medicine. 2006;203(2):311-7.
117. Tam W, Gomez M, Chadburn A, Lee JW, Chan WC, Knowles DM. Mutational analysis of PRDM1 indicates a tumor-suppressor role in diffuse large B-cell lymphomas. Blood. 2006;107(10):4090-100.
118. Rosenwald A, Wright G, Chan WC, Connors JM, Campo E, Fisher RI, et al. The use of molecular profiling to predict survival after chemotherapy for diffuse large-B-cell lymphoma. The New England journal of medicine. 2002;346(25):1937-47.
119. Lenz G, Wright G, Dave SS, Xiao W, Powell J, Zhao H, et al. Stromal gene signatures in large-B-cell lymphomas. The New England journal of medicine. 2008;359(22):2313-23.
120. Molyneux EM, Rochford R, Griffin B, Newton R, Jackson G, Menon G, et al. Burkitt's lymphoma. Lancet. 2012;379(9822):1234-44.
121. Schmitz R, Ceribelli M, Pittaluga S, Wright G, Staudt LM. Oncogenic mechanisms in Burkitt lymphoma. Cold Spring Harb Perspect Med. 2014;4(2).
122. Dalla-Favera R, Bregni M, Erikson J, Patterson D, Gallo RC, Croce CM. Human c-myc onc gene is located on the region of chromosome 8 that is translocated in Burkitt lymphoma cells. Proc Natl Acad Sci U S A. 1982;79(24):7824-7.
123. Dave SS, Fu K, Wright GW, Lam LT, Kluin P, Boerma EJ, et al. Molecular diagnosis of Burkitt's lymphoma. The New England journal of medicine. 2006;354(23):2431-42.
124. Sander S, Calado DP, Srinivasan L, Kochert K, Zhang B, Rosolowski M, et al. Synergy between PI3K signaling and MYC in Burkitt lymphomagenesis. Cancer Cell. 2012;22(2):167-79.
125. Cory S. Activation of cellular oncogenes in hemopoietic cells by chromosome translocation. Adv Cancer Res. 1986;47:189-234.
126. Harris AW, Pinkert CA, Crawford M, Langdon WY, Brinster RL, Adams JM. The E mu-myc transgenic mouse. A model for high-incidence spontaneous lymphoma and leukemia of early B cells. The Journal of experimental medicine. 1988;167(2):353-71.

127. Adams JM, Harris AW, Pinkert CA, Corcoran LM, Alexander WS, Cory S, et al. The c-myc oncogene driven by immunoglobulin enhancers induces lymphoid malignancy in transgenic mice. Nature. 1985;318(6046):533-8.
128. Langdon WY, Harris AW, Cory S, Adams JM. The c-myc oncogene perturbs B lymphocyte development in E-mu-myc transgenic mice. Cell. 1986;47(1):11-8.
129. Eischen CM, Weber JD, Roussel MF, Sherr CJ, Cleveland JL. Disruption of the ARF-Mdm2-p53 tumor suppressor pathway in Myc-induced lymphomagenesis. Genes Dev. 1999;13(20):2658-69.
130. Eischen CM, Woo D, Roussel MF, Cleveland JL. Apoptosis triggered by Myc-induced suppression of Bcl-X(L) or Bcl-2 is bypassed during lymphomagenesis. Molecular and cellular biology. 2001;21(15):5063-70.
131. Strasser A, Harris AW, Bath ML, Cory S. Novel primitive lymphoid tumours induced in transgenic mice by cooperation between myc and bcl-2. Nature. 1990;348(6299):331-3.
132. Valente LJ, Grabow S, Vandenberg CJ, Strasser A, Janic A. Combined loss of PUMA and p21 accelerates c-MYC-driven lymphoma development considerably less than loss of one allele of p53. Oncogene. 2016;35(29):3866-71.
133. Abbas AK, Lichtman AH. Basic immunology : functions and disorders of the immune system. 2nd ed., updated ed. 2006-2007. ed. Philadelphia, Pa. ; Edinburgh: Elsevier Saunders; 2006.
134. Janeway CA. Immunobiology 5 : the immune system in health and disease. 5th ed. ed. New York: Garland ; Edinburgh : Churchill Livingstone; 2001.
135. Appelberg R. Neutrophils and intracellular pathogens: beyond phagocytosis and killing. Trends Microbiol. 2007;15(2):87-92.
136. Zychlinsky A, Weinrauch Y, Weiss J. Introduction: Forum in immunology on neutrophils. Microbes Infect. 2003;5(14):1289-91.
137. Witko-Sarsat V, Rieu P, Descamps-Latscha B, Lesavre P, Halbwachs-Mecarelli L. Neutrophils: molecules, functions and pathophysiological aspects. Lab Invest. 2000;80(5):617-53.
138. Geissmann F, Manz MG, Jung S, Sieweke MH, Merad M, Ley K. Development of monocytes, macrophages, and dendritic cells. Science. 2010;327(5966):656-61.
139. Shi C, Pamer EG. Monocyte recruitment during infection and inflammation. Nat Rev Immunol. 2011;11(11):762-74.
140. Geissmann F, Auffray C, Palframan R, Wirrig C, Ciocca A, Campisi L, et al. Blood monocytes: distinct subsets, how they relate to dendritic cells, and their possible roles in the regulation of T-cell responses. Immunol Cell Biol. 2008;86(5):398-408.
141. van Furth R, Cohn ZA. The origin and kinetics of mononuclear phagocytes. J Exp Med. 1968;128(3):415-35.
142. Gonzalez-Mejia ME, Doseff AI. Regulation of monocytes and macrophages cell fate. Front Biosci (Landmark Ed). 2009;14:2413-31.
143. Moretta L, Moretta A. Unravelling natural killer cell function: triggering and inhibitory human NK receptors. EMBO J. 2004;23(2):255-9.
144. Yokoyama WM, Riley JK. NK cells and their receptors. Reprod Biomed Online. 2008;16(2):173-91.
145. Altincicek B, Moll J, Campos N, Foerster G, Beck E, Hoeffler JF, et al. Cutting edge: human gamma delta T cells are activated by intermediates of the 2-C-methyl-D-erythritol 4-phosphate pathway of isoprenoid biosynthesis. J Immunol. 2001;166(6):3655-8.
146. Tanaka Y, Morita CT, Nieves E, Brenner MB, Bloom BR. Natural and synthetic

non-peptide antigens recognized by human gamma delta T cells. Nature. 1995;375(6527):155-8.
147. Constant P, Davodeau F, Peyrat MA, Poquet Y, Puzo G, Bonneville M, et al. Stimulation of human gamma delta T cells by nonpeptidic mycobacterial ligands. Science. 1994;264(5156):267-70.
148. Bukowski JF, Morita CT, Brenner MB. Human gamma delta T cells recognize alkylamines derived from microbes, edible plants, and tea: implications for innate immunity. Immunity. 1999;11(1):57-65.
149. Fisch P, Malkovsky M, Kovats S, Sturm E, Braakman E, Klein BS, et al. Recognition by human V gamma 9/V delta 2 T cells of a GroEL homolog on Daudi Burkitt's lymphoma cells. Science. 1990;250(4985):1269-73.
150. Wilhelm M, Kunzmann V, Eckstein S, Reimer P, Weissinger F, Ruediger T, et al. Gammadelta T cells for immune therapy of patients with lymphoid malignancies. Blood. 2003;102(1):200-6.
151. Dieli F, Vermijlen D, Fulfaro F, Caccamo N, Meraviglia S, Cicero G, et al. Targeting human {gamma}delta} T cells with zoledronate and interleukin-2 for immunotherapy of hormone-refractory prostate cancer. Cancer Res. 2007;67(15):7450-7.
152. Wucherpfennig KW, Gagnon E, Call MJ, Huseby ES, Call ME. Structural biology of the T-cell receptor: insights into receptor assembly, ligand recognition, and initiation of signaling. Cold Spring Harb Perspect Biol. 2010;2(4):a005140.
153. Chambers CA, Allison JP. Costimulatory regulation of T cell function. Curr Opin Cell Biol. 1999;11(2):203-10.
154. Peto J. Cancer epidemiology in the last century and the next decade. Nature. 2001;411(6835):390-5.
155. Marshall BJ, Warren JR. Unidentified curved bacilli in the stomach of patients with gastritis and peptic ulceration. Lancet. 1984;1(8390):1311-5.
156. Ehrlich P. Über den jetzigen stand der karzinomforschung. Ned. Tijdschr. Geneeskd.1909. p. 273-90.
157. BURNET M. Cancer: a biological approach. III. Viruses associated with neoplastic conditions. IV. Practical applications. Br Med J. 1957;1(5023):841-7.
158. Thomas L. Discussion. In Cellular and Humoral Aspects of the Hypersensitive States, H. S. Lawrence (ed.), Hoeber-Harper, New York,; 1959. p. 529–33.
159. Stutman O. Tumor development after 3-methylcholanthrene in immunologically deficient athymic-nude mice. Science. 1974;183(4124):534-6.
160. Outzen HC, Custer RP, Eaton GJ, Prehn RT. Spontaneous and induced tumor incidence in germfree "nude" mice. J Reticuloendothel Soc. 1975;17(1):1-9.
161. Rygaard J, Povlsen CO. The mouse mutant nude does not develop spontaneous tumours. An argument against immunological surveillance. Acta Pathol Microbiol Scand B Microbiol Immunol. 1974;82(1):99-106.
162. Shinkai Y, Rathbun G, Lam KP, Oltz EM, Stewart V, Mendelsohn M, et al. RAG-2-deficient mice lack mature lymphocytes owing to inability to initiate V(D)J rearrangement. Cell. 1992;68(5):855-67.
163. Shankaran V, Ikeda H, Bruce AT, White JM, Swanson PE, Old LJ, et al. IFNgamma and lymphocytes prevent primary tumour development and shape tumour immunogenicity. Nature. 2001;410(6832):1107-11.
164. Girardi M, Oppenheim DE, Steele CR, Lewis JM, Glusac E, Filler R, et al. Regulation of cutaneous malignancy by gammadelta T cells. Science. 2001;294(5542):605-9.
165. Marigo I, Dolcetti L, Serafini P, Zanovello P, Bronte V. Tumor-induced tolerance

and immune suppression by myeloid derived suppressor cells. Immunol Rev. 2008;222:162-79.
166. Mantovani A, Sica A, Allavena P, Garlanda C, Locati M. Tumor-associated macrophages and the related myeloid-derived suppressor cells as a paradigm of the diversity of macrophage activation. Hum Immunol. 2009;70(5):325-30.
167. Curiel TJ. Tregs and rethinking cancer immunotherapy. J Clin Invest. 2007;117(5):1167-74.
168. Penn I. Posttransplant malignancies. Transplant Proc. 1999;31(1-2):1260-2.
169. Penn I. Malignant melanoma in organ allograft recipients. Transplantation. 1996;61(2):274-8.
170. Sheil AG. Cancer after transplantation. World J Surg. 1986;10(3):389-96.
171. Esensten JH, Helou YA, Chopra G, Weiss A, Bluestone JA. CD28 Costimulation: From Mechanism to Therapy. Immunity. 2016;44(5):973-88.
172. Sansom DM. CD28, CTLA-4 and their ligands: who does what and to whom? Immunology. 2000;101(2):169-77.
173. Yoshinaga SK, Whoriskey JS, Khare SD, Sarmiento U, Guo J, Horan T, et al. T-cell co-stimulation through B7RP-1 and ICOS. Nature. 1999;402(6763):827-32.
174. Hutloff A, Dittrich AM, Beier KC, Eljaschewitsch B, Kraft R, Anagnostopoulos I, et al. ICOS is an inducible T-cell co-stimulator structurally and functionally related to CD28. Nature. 1999;397(6716):263-6.
175. Coyle AJ, Lehar S, Lloyd C, Tian J, Delaney T, Manning S, et al. The CD28-related molecule ICOS is required for effective T cell-dependent immune responses. Immunity. 2000;13(1):95-105.
176. Kopf M, Coyle AJ, Schmitz N, Barner M, Oxenius A, Gallimore A, et al. Inducible costimulator protein (ICOS) controls T helper cell subset polarization after virus and parasite infection. The Journal of experimental medicine. 2000;192(1):53-61.
177. McAdam AJ, Greenwald RJ, Levin MA, Chernova T, Malenkovich N, Ling V, et al. ICOS is critical for CD40-mediated antibody class switching. Nature. 2001;409(6816):102-5.
178. Waldmann TA. The interleukin-2 receptor. The Journal of biological chemistry. 1991;266(5):2681-4.
179. Liao W, Lin JX, Leonard WJ. IL-2 family cytokines: new insights into the complex roles of IL-2 as a broad regulator of T helper cell differentiation. Curr Opin Immunol. 2011;23(5):598-604.
180. Malek TR, Castro I. Interleukin-2 receptor signaling: at the interface between tolerance and immunity. Immunity. 2010;33(2):153-65.
181. Ansell SM, Hurvitz SA, Koenig PA, LaPlant BR, Kabat BF, Fernando D, et al. Phase I study of ipilimumab, an anti-CTLA-4 monoclonal antibody, in patients with relapsed and refractory B-cell non-Hodgkin lymphoma. Clin Cancer Res. 2009;15(20):6446-53.
182. Rhyasen GW, Starczynowski DT. IRAK signalling in cancer. British journal of cancer. 2015;112(2):232-7.
183. Dougall WC, Kurtulus S, Smyth MJ, Anderson AC. TIGIT and CD96: new checkpoint receptor targets for cancer immunotherapy. Immunol Rev. 2017;276(1):112-20.
184. Levin SD, Taft DW, Brandt CS, Bucher C, Howard ED, Chadwick EM, et al. Vstm3 is a member of the CD28 family and an important modulator of T-cell function. European journal of immunology. 2011;41(4):902-15.
185. Joller N, Hafler JP, Brynedal B, Kassam N, Spoerl S, Levin SD, et al. Cutting edge: TIGIT has T cell-intrinsic inhibitory functions. Journal of immunology. 2011;186(3):1338-

186. Stanietsky N, Simic H, Arapovic J, Toporik A, Levy O, Novik A, et al. The interaction of TIGIT with PVR and PVRL2 inhibits human NK cell cytotoxicity. Proc Natl Acad Sci U S A. 2009;106(42):17858-63.
187. Wang PL, O'Farrell S, Clayberger C, Krensky AM. Identification and molecular cloning of tactile. A novel human T cell activation antigen that is a member of the Ig gene superfamily. Journal of immunology. 1992;148(8):2600-8.
188. Burns GF, Triglia T, Werkmeister JA, Begley CG, Boyd AW. TLiSA1, a human T lineage-specific activation antigen involved in the differentiation of cytotoxic T lymphocytes and anomalous killer cells from their precursors. The Journal of experimental medicine. 1985;161(5):1063-78.
189. Chan CJ, Andrews DM, Smyth MJ. Receptors that interact with nectin and nectin-like proteins in the immunosurveillance and immunotherapy of cancer. Curr Opin Immunol. 2012;24(2):246-51.
190. Montgomery RI, Warner MS, Lum BJ, Spear PG. Herpes simplex virus-1 entry into cells mediated by a novel member of the TNF/NGF receptor family. Cell. 1996;87(3):427-36.
191. Sedy JR, Gavrieli M, Potter KG, Hurchla MA, Lindsley RC, Hildner K, et al. B and T lymphocyte attenuator regulates T cell activation through interaction with herpesvirus entry mediator. Nat Immunol. 2005;6(1):90-8.
192. Gonzalez LC, Loyet KM, Calemine-Fenaux J, Chauhan V, Wranik B, Ouyang W, et al. A coreceptor interaction between the CD28 and TNF receptor family members B and T lymphocyte attenuator and herpesvirus entry mediator. Proc Natl Acad Sci U S A. 2005;102(4):1116-21.
193. Han P, Goularte OD, Rufner K, Wilkinson B, Kaye J. An inhibitory Ig superfamily protein expressed by lymphocytes and APCs is also an early marker of thymocyte positive selection. Journal of immunology. 2004;172(10):5931-9.
194. Watanabe N, Gavrieli M, Sedy JR, Yang J, Fallarino F, Loftin SK, et al. BTLA is a lymphocyte inhibitory receptor with similarities to CTLA-4 and PD-1. Nat Immunol. 2003;4(7):670-9.
195. Anumanthan A, Bensussan A, Boumsell L, Christ AD, Blumberg RS, Voss SD, et al. Cloning of BY55, a novel Ig superfamily member expressed on NK cells, CTL, and intestinal intraepithelial lymphocytes. Journal of immunology. 1998;161(6):2780-90.
196. Cai G, Anumanthan A, Brown JA, Greenfield EA, Zhu B, Freeman GJ. CD160 inhibits activation of human CD4+ T cells through interaction with herpesvirus entry mediator. Nat Immunol. 2008;9(2):176-85.
197. Pardoll DM. The blockade of immune checkpoints in cancer immunotherapy. Nat Rev Cancer. 2012;12(4):252-64.
198. Xu-Monette ZY, Zhou J, Young KH. PD-1 expression and clinical PD-1 blockade in B-cell lymphomas. Blood. 2018;131(1):68-83.
199. Sakuishi K, Apetoh L, Sullivan JM, Blazar BR, Kuchroo VK, Anderson AC. Targeting Tim-3 and PD-1 pathways to reverse T cell exhaustion and restore anti-tumor immunity. The Journal of experimental medicine. 2010;207(10):2187-94.
200. Nayak L, Iwamoto FM, LaCasce A, Mukundan S, Roemer MGM, Chapuy B, et al. PD-1 blockade with nivolumab in relapsed/refractory primary central nervous system and testicular lymphoma. Blood. 2017;129(23):3071-3.
201. Monney L, Sabatos CA, Gaglia JL, Ryu A, Waldner H, Chernova T, et al. Th1-specific cell surface protein Tim-3 regulates macrophage activation and severity of an autoimmune disease. Nature. 2002;415(6871):536-41.
202. Zhou Q, Munger ME, Veenstra RG, Weigel BJ, Hirashima M, Munn DH, et al.

Coexpression of Tim-3 and PD-1 identifies a CD8+ T-cell exhaustion phenotype in mice with disseminated acute myelogenous leukemia. Blood. 2011;117(17):4501-10.
203. Yang ZZ, Grote DM, Ziesmer SC, Niki T, Hirashima M, Novak AJ, et al. IL-12 upregulates TIM-3 expression and induces T cell exhaustion in patients with follicular B cell non-Hodgkin lymphoma. J Clin Invest. 2012;122(4):1271-82.
204. Chiba S, Baghdadi M, Akiba H, Yoshiyama H, Kinoshita I, Dosaka-Akita H, et al. Tumor-infiltrating DCs suppress nucleic acid-mediated innate immune responses through interactions between the receptor TIM-3 and the alarmin HMGB1. Nat Immunol. 2012;13(9):832-42.
205. Heusschen R, Griffioen AW, Thijssen VL. Galectin-9 in tumor biology: a jack of multiple trades. Biochim Biophys Acta. 2013;1836(1):177-85.
206. Huard B, Gaulard P, Faure F, Hercend T, Triebel F. Cellular expression and tissue distribution of the human LAG-3-encoded protein, an MHC class II ligand. Immunogenetics. 1994;39(3):213-7.
207. Workman CJ, Dugger KJ, Vignali DA. Cutting edge: molecular analysis of the negative regulatory function of lymphocyte activation gene-3. Journal of immunology. 2002;169(10):5392-5.
208. Workman CJ, Wang Y, El Kasmi KC, Pardoll DM, Murray PJ, Drake CG, et al. LAG-3 regulates plasmacytoid dendritic cell homeostasis. Journal of immunology. 2009;182(4):1885-91.
209. Blackburn SD, Wherry EJ. IL-10, T cell exhaustion and viral persistence. Trends Microbiol. 2007;15(4):143-6.
210. Couper KN, Blount DG, Riley EM. IL-10: the master regulator of immunity to infection. Journal of immunology. 2008;180(9):5771-7.
211. Campbell DJ, Koch MA. Phenotypical and functional specialization of FOXP3+ regulatory T cells. Nat Rev Immunol. 2011;11(2):119-30.
212. Thornton AM, Shevach EM. CD4+CD25+ immunoregulatory T cells suppress polyclonal T cell activation in vitro by inhibiting interleukin 2 production. The Journal of experimental medicine. 1998;188(2):287-96.
213. Green EA, Gorelik L, McGregor CM, Tran EH, Flavell RA. CD4+CD25+ T regulatory cells control anti-islet CD8+ T cells through TGF-beta-TGF-beta receptor interactions in type 1 diabetes. Proc Natl Acad Sci U S A. 2003;100(19):10878-83.
214. Asseman C, Mauze S, Leach MW, Coffman RL, Powrie F. An essential role for interleukin 10 in the function of regulatory T cells that inhibit intestinal inflammation. The Journal of experimental medicine. 1999;190(7):995-1004.
215. Liang B, Workman C, Lee J, Chew C, Dale BM, Colonna L, et al. Regulatory T cells inhibit dendritic cells by lymphocyte activation gene-3 engagement of MHC class II. Journal of immunology. 2008;180(9):5916-26.
216. Schroder K, Hertzog PJ, Ravasi T, Hume DA. Interferon-gamma: an overview of signals, mechanisms and functions. Journal of leukocyte biology. 2004;75(2):163-89.
217. Gately MK, Renzetti LM, Magram J, Stern AS, Adorini L, Gubler U, et al. The interleukin-12/interleukin-12-receptor system: role in normal and pathologic immune responses. Annu Rev Immunol. 1998;16:495-521.
218. Trinchieri G, Rengaraju M, D'Andrea A, Valiante NM, Kubin M, Aste M, et al. Producer cells of interleukin 12. Parasitol Today. 1993;9(3):97.
219. Du C, Sriram S. Mechanism of inhibition of LPS-induced IL-12p40 production by IL-10 and TGF-beta in ANA-1 cells. Journal of leukocyte biology. 1998;64(1):92-7.
220. Oppmann B, Lesley R, Blom B, Timans JC, Xu Y, Hunte B, et al. Novel p19 protein engages IL-12p40 to form a cytokine, IL-23, with biological activities similar as

well as distinct from IL-12. Immunity. 2000;13(5):715-25.
221. Belladonna ML, Renauld JC, Bianchi R, Vacca C, Fallarino F, Orabona C, et al. IL-23 and IL-12 have overlapping, but distinct, effects on murine dendritic cells. Journal of immunology. 2002;168(11):5448-54.
222. Aggarwal S, Ghilardi N, Xie MH, de Sauvage FJ, Gurney AL. Interleukin-23 promotes a distinct CD4 T cell activation state characterized by the production of interleukin-17. The Journal of biological chemistry. 2003;278(3):1910-4.
223. Iwakura Y, Nakae S, Saijo S, Ishigame H. The roles of IL-17A in inflammatory immune responses and host defense against pathogens. Immunol Rev. 2008;226:57-79.
224. Devergne O, Birkenbach M, Kieff E. Epstein-Barr virus-induced gene 3 and the p35 subunit of interleukin 12 form a novel heterodimeric hematopoietin. Proc Natl Acad Sci U S A. 1997;94(22):12041-6.
225. Collison LW, Workman CJ, Kuo TT, Boyd K, Wang Y, Vignali KM, et al. The inhibitory cytokine IL-35 contributes to regulatory T-cell function. Nature. 2007;450(7169):566-9.
226. Pflanz S, Hibbert L, Mattson J, Rosales R, Vaisberg E, Bazan JF, et al. WSX-1 and glycoprotein 130 constitute a signal-transducing receptor for IL-27. Journal of immunology. 2004;172(4):2225-31.
227. Lucas S, Ghilardi N, Li J, de Sauvage FJ. IL-27 regulates IL-12 responsiveness of naive CD4+ T cells through Stat1-dependent and -independent mechanisms. Proc Natl Acad Sci U S A. 2003;100(25):15047-52.
228. Molle C, Nguyen M, Flamand V, Renneson J, Trottein F, De Wit D, et al. IL-27 synthesis induced by TLR ligation critically depends on IFN regulatory factor 3. Journal of immunology. 2007;178(12):7607-15.
229. Mehta DS, Wurster AL, Grusby MJ. Biology of IL-21 and the IL-21 receptor. Immunol Rev. 2004;202:84-95.
230. Leonard WJ, Wan CK. IL-21 Signaling in Immunity. F1000Res. 2016;5.
231. Center DM, Cruikshank W. Modulation of lymphocyte migration by human lymphokines. I. Identification and characterization of chemoattractant activity for lymphocytes from mitogen-stimulated mononuclear cells. Journal of immunology. 1982;128(6):2563-8.
232. Zhang Y, Center DM, Wu DM, Cruikshank WW, Yuan J, Andrews DW, et al. Processing and activation of pro-interleukin-16 by caspase-3. The Journal of biological chemistry. 1998;273(2):1144-9.
233. Richmond J, Tuzova M, Cruikshank W, Center D. Regulation of cellular processes by interleukin-16 in homeostasis and cancer. J Cell Physiol. 2014;229(2):139-47.
234. Cogdill AP, Andrews MC, Wargo JA. Hallmarks of response to immune checkpoint blockade. British journal of cancer. 2017;117(1):1-7.
235. Topalian SL, Hodi FS, Brahmer JR, Gettinger SN, Smith DC, McDermott DF, et al. Safety, activity, and immune correlates of anti-PD-1 antibody in cancer. The New England journal of medicine. 2012;366(26):2443-54.
236. Topalian SL, Sznol M, McDermott DF, Kluger HM, Carvajal RD, Sharfman WH, et al. Survival, durable tumor remission, and long-term safety in patients with advanced melanoma receiving nivolumab. Journal of clinical oncology : official journal of the American Society of Clinical Oncology. 2014;32(10):1020-30.
237. Robert C, Ribas A, Wolchok JD, Hodi FS, Hamid O, Kefford R, et al. Anti-programmed-death-receptor-1 treatment with pembrolizumab in ipilimumab-refractory advanced melanoma: a randomised dose-comparison cohort of a phase 1 trial. Lancet. 2014;384(9948):1109-17.

238. Powles T, Eder JP, Fine GD, Braiteh FS, Loriot Y, Cruz C, et al. MPDL3280A (anti-PD-L1) treatment leads to clinical activity in metastatic bladder cancer. Nature. 2014;515(7528):558-62.
239. Dyck L, Mills KHG. Immune checkpoints and their inhibition in cancer and infectious diseases. Eur J Immunol. 2017;47(5):765-79.
240. Carreras J, Lopez-Guillermo A, Roncador G, Villamor N, Colomo L, Martinez A, et al. High numbers of tumor-infiltrating programmed cell death 1-positive regulatory lymphocytes are associated with improved overall survival in follicular lymphoma. J Clin Oncol. 2009;27(9):1470-6.
241. Farinha P, Al-Tourah A, Gill K, Klasa R, Connors JM, Gascoyne RD. The architectural pattern of FOXP3-positive T cells in follicular lymphoma is an independent predictor of survival and histologic transformation. Blood. 2010;115(2):289-95.
242. Farinha P, Masoudi H, Skinnider BF, Shumansky K, Spinelli JJ, Gill K, et al. Analysis of multiple biomarkers shows that lymphoma-associated macrophage (LAM) content is an independent predictor of survival in follicular lymphoma (FL). Blood. 2005;106(6):2169-74.
243. Armand P. Checkpoint blockade in lymphoma. Hematology Am Soc Hematol Educ Program. 2015;2015:69-73.
244. Georgiou K, Chen L, Berglund M, Ren W, de Miranda NF, Lisboa S, et al. Genetic basis of PD-L1 overexpression in diffuse large B-cell lymphomas. Blood. 2016;127(24):3026-34.
245. Andorsky DJ, Yamada RE, Said J, Pinkus GS, Betting DJ, Timmerman JM. Programmed death ligand 1 is expressed by non-hodgkin lymphomas and inhibits the activity of tumor-associated T cells. Clin Cancer Res. 2011;17(13):4232-44.
246. Green MR, Monti S, Rodig SJ, Juszczynski P, Currie T, O'Donnell E, et al. Integrative analysis reveals selective 9p24.1 amplification, increased PD-1 ligand expression, and further induction via JAK2 in nodular sclerosing Hodgkin lymphoma and primary mediastinal large B-cell lymphoma. Blood. 2010;116(17):3268-77.
247. Green MR, Rodig S, Juszczynski P, Ouyang J, Sinha P, O'Donnell E, et al. Constitutive AP-1 activity and EBV infection induce PD-L1 in Hodgkin lymphomas and posttransplant lymphoproliferative disorders: implications for targeted therapy. Clinical cancer research : an official journal of the American Association for Cancer Research. 2012;18(6):1611-8.
248. Kiyasu J, Miyoshi H, Hirata A, Arakawa F, Ichikawa A, Niino D, et al. Expression of programmed cell death ligand 1 is associated with poor overall survival in patients with diffuse large B-cell lymphoma. Blood. 2015;126(19):2193-201.
249. Ansell SM, Gutierrez ME, Shipp MA, Galdstone D, Moskowitz A, Borello I, et al., editors. A Phase 1 Study of Nivolumab in Combination with Ipilimumab for Relapsed or Refractory Hematologic Malignancies (CheckMate 039). Blood; 2016.
250. Lesokhin AM, Ansell SM, Armand P, Scott EC, Halwani A, Gutierrez M, et al. Nivolumab in Patients With Relapsed or Refractory Hematologic Malignancy: Preliminary Results of a Phase Ib Study. J Clin Oncol. 2016;34(23):2698-704.
251. Armand P, Nagler A, Weller EA, Devine SM, Avigan DE, Chen YB, et al. Disabling immune tolerance by programmed death-1 blockade with pidilizumab after autologous hematopoietic stem-cell transplantation for diffuse large B-cell lymphoma: results of an international phase II trial. J Clin Oncol. 2013;31(33):4199-206.
252. Ding W, LaPlant BR, Call TG, Parikh SA, Leis JF, He R, et al. Pembrolizumab in patients with CLL and Richter transformation or with relapsed CLL. Blood. 2017;129(26):3419-27.

253. Hsu HC, Zhou T, Mountz JD. Nur77 family of nuclear hormone receptors. Curr Drug Targets Inflamm Allergy. 2004;3(4):413-23.
254. Lee SO, Li X, Khan S, Safe S. Targeting NR4A1 (TR3) in cancer cells and tumors. Expert Opin Ther Targets. 2011;15(2):195-206.
255. Zhang XK. Targeting Nur77 translocation. Expert Opin Ther Targets. 2007;11(1):69-79.
256. Li QX, Ke N, Sundaram R, Wong-Staal F. NR4A1, 2, 3--an orphan nuclear hormone receptor family involved in cell apoptosis and carcinogenesis. Histol Histopathol. 2006;21(5):533-40.
257. Maxwell MA, Muscat GE. The NR4A subgroup: immediate early response genes with pleiotropic physiological roles. Nucl Recept Signal. 2006;4:e002.
258. Deutsch AJ, Angerer H, Fuchs TE, Neumeister P. The nuclear orphan receptors NR4A as therapeutic target in cancer therapy. Anticancer Agents Med Chem. 2012;12(9):1001-14.
259. de Leseleuc L, Denis F. Nur77 forms novel nuclear structures upon DNA damage that cause transcriptional arrest. Experimental cell research. 2006;312(9):1507-13.
260. Malewicz M, Kadkhodaei B, Kee N, Volakakis N, Hellman U, Viktorsson K, et al. Essential role for DNA-PK-mediated phosphorylation of NR4A nuclear orphan receptors in DNA double-strand break repair. Genes Dev. 2011;25(19):2031-40.
261. Suzuki S, Suzuki N, Mirtsos C, Horacek T, Lye E, Noh SK, et al. Nur77 as a survival factor in tumor necrosis factor signaling. Proc Natl Acad Sci U S A. 2003;100(14):8276-80.
262. Zhang J, DeYoung A, Kasler HG, Kabra NH, Kuang AA, Diehl G, et al. Receptor-mediated apoptosis in T lymphocytes. Cold Spring Harb Symp Quant Biol. 1999;64:363-71.
263. Li H, Kolluri SK, Gu J, Dawson MI, Cao X, Hobbs PD, et al. Cytochrome c release and apoptosis induced by mitochondrial targeting of nuclear orphan receptor TR3. Science. 2000;289(5482):1159-64.
264. Bras A, Albar JP, Leonardo E, de Buitrago GG, Martinez AC. Ceramide-induced cell death is independent of the Fas/Fas ligand pathway and is prevented by Nur77 overexpression in A20 B cells. Cell Death Differ. 2000;7(3):262-71.
265. Uemura H, Chang C. Antisense TR3 orphan receptor can increase prostate cancer cell viability with etoposide treatment. Endocrinology. 1998;139(5):2329-34.
266. Wu Q, Liu S, Ye XF, Huang ZW, Su WJ. Dual roles of Nur77 in selective regulation of apoptosis and cell cycle by TPA and ATRA in gastric cancer cells. Carcinogenesis. 2002;23(10):1583-92.
267. Lin B, Kolluri SK, Lin F, Liu W, Han YH, Cao X, et al. Conversion of Bcl-2 from protector to killer by interaction with nuclear orphan receptor Nur77/TR3. Cell. 2004;116(4):527-40.
268. Fahrner TJ, Carroll SL, Milbrandt J. The NGFI-B protein, an inducible member of the thyroid/steroid receptor family, is rapidly modified posttranslationally. Molecular and cellular biology. 1990;10(12):6454-9.
269. Han YH, Cao X, Lin B, Lin F, Kolluri SK, Stebbins J, et al. Regulation of Nur77 nuclear export by c-Jun N-terminal kinase and Akt. Oncogene. 2006;25(21):2974-86.
270. Katagiri Y, Takeda K, Yu ZX, Ferrans VJ, Ozato K, Guroff G. Modulation of retinoid signalling through NGF-induced nuclear export of NGFI-B. Nat Cell Biol. 2000;2(7):435-40.
271. Sohn SJ, Lewis GM, Winoto A. Non-redundant function of the MEK5-ERK5 pathway in thymocyte apoptosis. EMBO J. 2008;27(13):1896-906.

272. Masuyama N, Oishi K, Mori Y, Ueno T, Takahama Y, Gotoh Y. Akt inhibits the orphan nuclear receptor Nur77 and T-cell apoptosis. The Journal of biological chemistry. 2001;276(35):32799-805.
273. Jacobs CM, Boldingh KA, Slagsvold HH, Thoresen GH, Paulsen RE. ERK2 prohibits apoptosis-induced subcellular translocation of orphan nuclear receptor NGFI-B/TR3. The Journal of biological chemistry. 2004;279(48):50097-101.
274. Wingate AD, Arthur JS. Post-translational control of Nur77. Biochem Soc Trans. 2006;34(Pt 6):1107-9.
275. Wenzl K, Troppan K, Neumeister P, Deutsch AJ. The nuclear orphan receptor NR4A1 and NR4A3 as tumor suppressors in hematologic neoplasms. Current drug targets. 2015;16(1):38-46.
276. McEvoy AN, Murphy EA, Ponnio T, Conneely OM, Bresnihan B, FitzGerald O, et al. Activation of nuclear orphan receptor NURR1 transcription by NF-kappa B and cyclic adenosine 5'-monophosphate response element-binding protein in rheumatoid arthritis synovial tissue. Journal of immunology. 2002;168(6):2979-87.
277. Labelle Y, Zucman J, Stenman G, Kindblom LG, Knight J, Turc-Carel C, et al. Oncogenic conversion of a novel orphan nuclear receptor by chromosome translocation. Hum Mol Genet. 1995;4(12):2219-26.
278. Boylan MO, Athanassiou M, Houle B, Wang Y, Zarbl H. Activation of tumor suppressor genes in nontumorigenic revertants of the HeLa cervical carcinoma cell line. Cell Growth Differ. 1996;7(6):725-35.
279. Mullican SE, Zhang S, Konopleva M, Ruvolo V, Andreeff M, Milbrandt J, et al. Abrogation of nuclear receptors Nr4a3 and Nr4a1 leads to development of acute myeloid leukemia. Nature medicine. 2007;13(6):730-5.
280. Ramirez-Herrick AM, Mullican SE, Sheehan AM, Conneely OM. Reduced NR4A gene dosage leads to mixed myelodysplastic/myeloproliferative neoplasms in mice. Blood. 2011;117(9):2681-90.
281. Borup R, Rossing M, Henao R, Yamamoto Y, Krogdahl A, Godballe C, et al. Molecular signatures of thyroid follicular neoplasia. Endocr Relat Cancer. 2010;17(3):691-708.
282. Yu H, Kumar SM, Fang D, Acs G, Xu X. Nuclear orphan receptor TR3/Nur77 mediates melanoma cell apoptosis. Cancer Biol Ther. 2007;6(3):405-12.
283. Shipp MA, Ross KN, Tamayo P, Weng AP, Kutok JL, Aguiar RC, et al. Diffuse large B-cell lymphoma outcome prediction by gene-expression profiling and supervised machine learning. Nature medicine. 2002;8(1):68-74.
284. Deutsch AJ, Rinner B, Wenzl K, Pichler M, Troppan K, Steinbauer E, et al. NR4A1-mediated apoptosis suppresses lymphomagenesis and is associated with a favorable cancer-specific survival in patients with aggressive B-cell lymphomas. Blood. 2014;123(15):2367-77.
285. Deutsch AJA, Rinner B, Pichler M, Prochazka K, Pansy K, Bischof M, et al. NR4A3 Suppresses Lymphomagenesis through Induction of Proapoptotic Genes. Cancer research. 2017;77(9):2375-86.
286. Fechter K, Feichtinger J, Prochazka K, Unterluggauer JJ, Pansy K, Steinbauer E, et al. Cytoplasmic location of NR4A1 in aggressive lymphomas is associated with a favourable cancer specific survival. Sci Rep. 2018;8(1):14528.
287. Hans CP, Weisenburger DD, Greiner TC, Gascoyne RD, Delabie J, Ott G, et al. Confirmation of the molecular classification of diffuse large B-cell lymphoma by immunohistochemistry using a tissue microarray. Blood. 2004;103(1):275-82.
288. Davies AJ, Rosenwald A, Wright G, Lee A, Last KW, Weisenburger DD, et al.

Transformation of follicular lymphoma to diffuse large B-cell lymphoma proceeds by distinct oncogenic mechanisms. British journal of haematology. 2007;136(2):286-93.
289. R Development Core Team. R: A language and environment for statistical analysis Austria: R Foundation for statistical analysis; 2016
290. Therneau TM, Grambsch PM. Modeling survival data: Extending the Cox model. 1st ed. New York, USA: Springer-Verlag New York; 2000.
291. Kassambara A, Kosinski M. survminer: Drawing Survival Curves using 'ggplot2' R package version 0.3.1.; 2017
292. Gordon M, Seifert R. Regression Helper Functions. R package version 1.2.; 2016.
293. Lenz G, Staudt LM. Aggressive lymphomas. The New England journal of medicine. 2010;362(15):1417-29.
294. Gautier L, Cope L, Bolstad BM, Irizarry RA. affy--analysis of Affymetrix GeneChip data at the probe level. Bioinformatics. 2004;20(3):307-15.
295. Abell AN, Granger DA, Johnson NL, Vincent-Jordan N, Dibble CF, Johnson GL. Trophoblast stem cell maintenance by fibroblast growth factor 4 requires MEKK4 activation of Jun N-terminal kinase. Molecular and cellular biology. 2009;29(10):2748-61.
296. Ritchie ME, Phipson B, Wu D, Hu Y, Law CW, Shi W, et al. limma powers differential expression analyses for RNA-sequencing and microarray studies. Nucleic acids research. 2015;43(7):e47.
297. Benjamini Y, Hochberg Y. Controlling the False Discovery Rate: A Practical and Powerful Approach to Multiple Testing. Journal of the Royal Statistical Society Series B (Methodological). 1995;57:289-300.
298. Falcon S, Gentleman R. Using GOstats to test gene lists for GO term association. Bioinformatics. 2007;23(2):257-8.
299. Yu G, He QY. ReactomePA: an R/Bioconductor package for reactome pathway analysis and visualization. Mol Biosyst. 2016;12(2):477-9.
300. Croy BA, Chapeau C. Evaluation of the pregnancy immunotrophism hypothesis by assessment of the reproductive performance of young adult mice of genotype scid/scid.bg/bg. J Reprod Fertil. 1990;88(1):231-9.
301. Martin M. Cutadapt removes adapter sequences from high-throughput sequencing reads. EMBnetjournal 2011;17(10).
302. Bolger AM, Lohse M, Usadel B. Trimmomatic: a flexible trimmer for Illumina sequence data. Bioinformatics. 2014;30(15):2114-20.
303. Dobin A, Davis CA, Schlesinger F, Drenkow J, Zaleski C, Jha S, et al. STAR: ultrafast universal RNA-seq aligner. Bioinformatics. 2013;29(1):15-21.
304. Langmead B, Salzberg SL. Fast gapped-read alignment with Bowtie 2. Nat Methods. 2012;9(4):357-9.
305. Anders S, Pyl PT, Huber W. HTSeq--a Python framework to work with high-throughput sequencing data. Bioinformatics. 2015;31(2):166-9.
306. Love MI, Huber W, Anders S. Moderated estimation of fold change and dispersion for RNA-seq data with DESeq2. Genome Biol. 2014;15(12):550.
307. Maere S, Heymans K, Kuiper M. BiNGO: a Cytoscape plugin to assess overrepresentation of gene ontology categories in biological networks. Bioinformatics. 2005;21(16):3448-9.
308. Killcoyne S, Carter GW, Smith J, Boyle J. Cytoscape: a community-based framework for network modeling. Methods Mol Biol. 2009;563:219-39.
309. Bindea G, Mlecnik B, Hackl H, Charoentong P, Tosolini M, Kirilovsky A, et al. ClueGO: a Cytoscape plug-in to decipher functionally grouped gene ontology and pathway annotation networks. Bioinformatics. 2009;25(8):1091-3.

310. Thompson J, Burger ML, Whang H, Winoto A. Protein kinase C regulates mitochondrial targeting of Nur77 and its family member Nor-1 in thymocytes undergoing apoptosis. European journal of immunology. 2010;40(7):2041-9.
311. Manning BD, Cantley LC. AKT/PKB signaling: navigating downstream. Cell. 2007;129(7):1261-74.
312. Kumar N, Crocker T, Smith T, Pow-Sang J, Spiess PE, Connors S, et al. Prostate Cancer Chemoprevention Targeting High Risk Populations: Model for Trial Design and Outcome Measures. Journal of cancer science & therapy. 2012;2011(S3).
313. Birkenkamp KU, Coffer PJ. Regulation of cell survival and proliferation by the FOXO (Forkhead box, class O) subfamily of Forkhead transcription factors. Biochemical Society transactions. 2003;31(Pt 1):292-7.
314. Grill C, Gheyas F, Dayananth P, Jin W, Ding W, Qiu P, et al. Analysis of the ERK1,2 transcriptome in mammary epithelial cells. Biochem J. 2004;381(Pt 3):635-44.
315. Schmid CA, Robinson MD, Scheifinger NA, Muller S, Cogliatti S, Tzankov A, et al. DUSP4 deficiency caused by promoter hypermethylation drives JNK signaling and tumor cell survival in diffuse large B cell lymphoma. The Journal of experimental medicine. 2015;212(5):775-92.
316. Gururajan M, Chui R, Karuppannan AK, Ke J, Jennings CD, Bondada S. c-Jun N-terminal kinase (JNK) is required for survival and proliferation of B-lymphoma cells. Blood. 2005;106(4):1382-91.
317. Ezell SA, Wang S, Bihani T, Lai Z, Grosskurth SE, Tepsuporn S, et al. Differential regulation of mTOR signaling determines sensitivity to AKT inhibition in diffuse large B cell lymphoma. Oncotarget. 2016;7(8):9163-74.
318. Xu ZZ, Xia ZG, Wang AH, Wang WF, Liu ZY, Chen LY, et al. Activation of the PI3K/AKT/mTOR pathway in diffuse large B cell lymphoma: clinical significance and inhibitory effect of rituximab. Annals of hematology. 2013;92(10):1351-8.
319. Majchrzak A, Witkowska M, Smolewski P. Inhibition of the PI3K/Akt/mTOR signaling pathway in diffuse large B-cell lymphoma: current knowledge and clinical significance. Molecules. 2014;19(9):14304-15.
320. Alain T, Morita M, Fonseca BD, Yanagiya A, Siddiqui N, Bhat M, et al. eIF4E/4E-BP ratio predicts the efficacy of mTOR targeted therapies. Cancer research. 2012;72(24):6468-76.
321. Kolluri SK, Bruey-Sedano N, Cao X, Lin B, Lin F, Han YH, et al. Mitogenic effect of orphan receptor TR3 and its regulation by MEKK1 in lung cancer cells. Molecular and cellular biology. 2003;23(23):8651-67.
322. Slagsvold HH, Ostvold AC, Fallgren AB, Paulsen RE. Nuclear receptor and apoptosis initiator NGFI-B is a substrate for kinase ERK2. Biochem Biophys Res Commun. 2002;291(5):1146-50.
323. Wang A, Rud J, Olson CM, Jr., Anguita J, Osborne BA. Phosphorylation of Nur77 by the MEK-ERK-RSK cascade induces mitochondrial translocation and apoptosis in T cells. Journal of immunology. 2009;183(5):3268-77.
324. Schmitt CA, Fridman JS, Yang M, Baranov E, Hoffman RM, Lowe SW. Dissecting p53 tumor suppressor functions in vivo. Cancer Cell. 2002;1(3):289-98.
325. Schmitt CA, McCurrach ME, de Stanchina E, Wallace-Brodeur RR, Lowe SW. INK4a/ARF mutations accelerate lymphomagenesis and promote chemoresistance by disabling p53. Genes Dev. 1999;13(20):2670-7.
326. Romero-Camarero I, Jiang X, Natkunam Y, Lu X, Vicente-Duenas C, Gonzalez-Herrero I, et al. Germinal centre protein HGAL promotes lymphoid hyperplasia and amyloidosis via BCR-mediated Syk activation. Nat Commun. 2013;4:1338.

327. Lu X, Sicard R, Jiang X, Stockus JN, McNamara G, Abdulreda M, et al. HGAL localization to cell membrane regulates B-cell receptor signaling. Blood. 2015;125(4):649-57.
328. Yamazaki T, Yang XO, Chung Y, Fukunaga A, Nurieva R, Pappu B, et al. CCR6 regulates the migration of inflammatory and regulatory T cells. Journal of immunology. 2008;181(12):8391-401.
329. Kanhere A, Hertweck A, Bhatia U, Gokmen MR, Perucha E, Jackson I, et al. T-bet and GATA3 orchestrate Th1 and Th2 differentiation through lineage-specific targeting of distal regulatory elements. Nat Commun. 2012;3:1268.
330. Dong C, Juedes AE, Temann UA, Shresta S, Allison JP, Ruddle NH, et al. ICOS co-stimulatory receptor is essential for T-cell activation and function. Nature. 2001;409(6816):97-101.
331. Vogler M. BCL2A1: the underdog in the BCL2 family. Cell Death Differ. 2012;19(1):67-74.
332. Mori S, Rempel RE, Chang JT, Yao G, Lagoo AS, Potti A, et al. Utilization of pathway signatures to reveal distinct types of B lymphoma in the Emicro-myc model and human diffuse large B-cell lymphoma. Cancer research. 2008;68(20):8525-34.
333. Davids MS. Targeting BCL-2 in B-cell lymphomas. Blood. 2017;130(9):1081-8.
334. Safa AR. c-FLIP, a master anti-apoptotic regulator. Exp Oncol. 2012;34(3):176-84.
335. Al-Kawaaz M, Mathew S, Liu Y, Gomez ML, Chaviano F, Knowles DM, et al. Cyclin D1-positive diffuse large B-cell lymphoma with IGH-CCND1 translocation and BCL6 rearrangement: a report of two cases. Am J Clin Pathol. 2015;143(2):288-99.
336. Ehinger M, Linderoth J, Christensson B, Sander B, Cavallin-Stahl E. A subset of CD5- diffuse large B-cell lymphomas expresses nuclear cyclin D1 with aberrations at the CCND1 locus. Am J Clin Pathol. 2008;129(4):630-8.
337. Forster R, Schubel A, Breitfeld D, Kremmer E, Renner-Muller I, Wolf E, et al. CCR7 coordinates the primary immune response by establishing functional microenvironments in secondary lymphoid organs. Cell. 1999;99(1):23-33.
338. Kato M, Sanada M, Kato I, Sato Y, Takita J, Takeuchi K, et al. Frequent inactivation of A20 in B-cell lymphomas. Nature. 2009;459(7247):712-6.
339. Hanna RN, Carlin LM, Hubbeling HG, Nackiewicz D, Green AM, Punt JA, et al. The transcription factor NR4A1 (Nur77) controls bone marrow differentiation and the survival of Ly6C- monocytes. Nat Immunol. 2011;12(8):778-85.
340. Hamers AA, Argmann C, Moerland PD, Koenis DS, Marinkovic G, Sokolovic M, et al. Nur77-deficiency in bone marrow-derived macrophages modulates inflammatory responses, extracellular matrix homeostasis, phagocytosis and tolerance. BMC Genomics. 2016;17:162.
341. Fassett MS, Jiang W, D'Alise AM, Mathis D, Benoist C. Nuclear receptor Nr4a1 modulates both regulatory T-cell (Treg) differentiation and clonal deletion. Proc Natl Acad Sci U S A. 2012;109(10):3891-6.
342. Pals ST, de Gorter DJ, Spaargaren M. Lymphoma dissemination: the other face of lymphocyte homing. Blood. 2007;110(9):3102-11.
343. Janssen LME, Ramsay EE, Logsdon CD, Overwijk WW. The immune system in cancer metastasis: friend or foe? J Immunother Cancer. 2017;5(1):79.
344. Golstein P, Griffiths GM. An early history of T cell-mediated cytotoxicity. Nat Rev Immunol. 2018.
345. Zhu J, Paul WE. CD4 T cells: fates, functions, and faults. Blood. 2008;112(5):1557-69.
346. Broere F, Apasov SG, Sitkovsky MV, van Eden W. T cell subsets and T cell-

mediated immunity. In: Parnham FPNaMJ, editor. Principles of Immunopharmacology: 3rd revised and extended edition: Springer Basel AG 2011; 2011.
347. Miossec P, Kolls JK. Targeting IL-17 and TH17 cells in chronic inflammation. Nat Rev Drug Discov. 2012;11(10):763-76.
348. Fontenot JD, Rasmussen JP, Gavin MA, Rudensky AY. A function for interleukin 2 in Foxp3-expressing regulatory T cells. Nat Immunol. 2005;6(11):1142-51.
349. Gabrilovich DI, Ostrand-Rosenberg S, Bronte V. Coordinated regulation of myeloid cells by tumours. Nat Rev Immunol. 2012;12(4):253-68.
350. Inamoto T, Czerniak BA, Dinney CP, Kamat AM. Cytoplasmic mislocalization of the orphan nuclear receptor Nurr1 is a prognostic factor in bladder cancer. Cancer. 2010;116(2):340-6.
351. Lee JM, Lee KH, Weidner M, Osborne BA, Hayward SD. Epstein-Barr virus EBNA2 blocks Nur77- mediated apoptosis. Proc Natl Acad Sci U S A. 2002;99(18):11878-83.
352. Mapara MY, Weinmann P, Bommert K, Daniel PT, Bargou R, Dorken B. Involvement of NAK-1, the human nur77 homologue, in surface IgM-mediated apoptosis in Burkitt lymphoma cell line BL41. European journal of immunology. 1995;25(9):2506-10.
353. Villeneuve DJ, Hembruff SL, Veitch Z, Cecchetto M, Dew WA, Parissenti AM. cDNA microarray analysis of isogenic paclitaxel- and doxorubicin-resistant breast tumor cell lines reveals distinct drug-specific genetic signatures of resistance. Breast Cancer Res Treat. 2006;96(1):17-39.
354. Cittera E, Onofri C, D'Apolito M, Cartron G, Cazzaniga G, Zelante L, et al. Rituximab induces different but overlapping sets of genes in human B-lymphoma cell lines. Cancer immunology, immunotherapy : CII. 2005;54(3):273-86.
355. Franke A, Niederfellner GJ, Klein C, Burtscher H. Antibodies against CD20 or B-cell receptor induce similar transcription patterns in human lymphoma cell lines. PloS one. 2011;6(2):e16596.
356. Arai M, Sasaki A, Saito N, Nakazato Y. Immunohistochemical analysis of cleaved caspase-3 detects high level of apoptosis frequently in diffuse large B-cell lymphomas of the central nervous system. Pathology international. 2005;55(3):122-9.
357. Muris JJ, Cillessen SA, Vos W, van Houdt IS, Kummer JA, van Krieken JH, et al. Immunohistochemical profiling of caspase signaling pathways predicts clinical response to chemotherapy in primary nodal diffuse large B-cell lymphomas. Blood. 2005;105(7):2916-23.
358. Jardin F, Pujals A, Pelletier L, Bohers E, Camus V, Mareschal S, et al. Recurrent mutations of the exportin 1 gene (XPO1) and their impact on selective inhibitor of nuclear export compounds sensitivity in primary mediastinal B-cell lymphoma. American journal of hematology. 2016;91(9):923-30.
359. Yoshimura M, Ishizawa J, Ruvolo V, Dilip A, Quintas-Cardama A, McDonnell TJ, et al. Induction of p53-mediated transcription and apoptosis by exportin-1 (XPO1) inhibition in mantle cell lymphoma. Cancer science. 2014;105(7):795-801.
360. Falini B, Mecucci C, Tiacci E, Alcalay M, Rosati R, Pasqualucci L, et al. Cytoplasmic nucleophosmin in acute myelogenous leukemia with a normal karyotype. The New England journal of medicine. 2005;352(3):254-66.
361. Puente XS, Pinyol M, Quesada V, Conde L, Ordonez GR, Villamor N, et al. Whole-genome sequencing identifies recurrent mutations in chronic lymphocytic leukaemia. Nature. 2011;475(7354):101-5.
362. Lenz G, Wright GW, Emre NC, Kohlhammer H, Dave SS, Davis RE, et al.

Molecular subtypes of diffuse large B-cell lymphoma arise by distinct genetic pathways. Proceedings of the National Academy of Sciences of the United States of America. 2008;105(36):13520-5.
363. Etchin J, Sun Q, Kentsis A, Farmer A, Zhang ZC, Sanda T, et al. Antileukemic activity of nuclear export inhibitors that spare normal hematopoietic cells. Leukemia. 2013;27(1):66-74.
364. Lapalombella R, Sun Q, Williams K, Tangeman L, Jha S, Zhong Y, et al. Selective inhibitors of nuclear export show that CRM1/XPO1 is a target in chronic lymphocytic leukemia. Blood. 2012;120(23):4621-34.
365. Das A, Wei G, Parikh K, Liu D. Selective inhibitors of nuclear export (SINE) in hematological malignancies. Experimental hematology & oncology. 2015;4:7.
366. Kuruvilla J, Savona M, Baz R, Mau-Sorensen PM, Gabrail N, Garzon R, et al. Selective inhibition of nuclear export with selinexor in patients with non-Hodgkin lymphoma. Blood. 2017;129(24):3175-83.
367. Swanson KD, Taylor LK, Haung L, Burlingame AL, Landreth GE. Transcription factor phosphorylation by pp90(rsk2). Identification of Fos kinase and NGFI-B kinase I as pp90(rsk2). The Journal of biological chemistry. 1999;274(6):3385-95.
368. Wingate AD, Campbell DG, Peggie M, Arthur JS. Nur77 is phosphorylated in cells by RSK in response to mitogenic stimulation. Biochem J. 2006;393(Pt 3):715-24.
369. Liubchenko GA, Appleberry HC, Holers VM, Banda NK, Willis VC, Lyubchenko T. Potentially autoreactive naturally occurring transitional T3 B lymphocytes exhibit a unique signaling profile. J Autoimmun. 2012;38(4):293-303.
370. Brahmer JR, Drake CG, Wollner I, Powderly JD, Picus J, Sharfman WH, et al. Phase I study of single-agent anti-programmed death-1 (MDX-1106) in refractory solid tumors: safety, clinical activity, pharmacodynamics, and immunologic correlates. J Clin Oncol. 2010;28(19):3167-75.
371. Gee K, Guzzo C, Che Mat NF, Ma W, Kumar A. The IL-12 family of cytokines in infection, inflammation and autoimmune disorders. Inflamm Allergy Drug Targets. 2009;8(1):40-52.
372. Ramsay AG. Immune checkpoint blockade immunotherapy to activate anti-tumour T-cell immunity. Br J Haematol. 2013;162(3):313-25.

11 Appendix

Publication resulting from the dissertation and representing part I of this thesis:

Fechter K, Feichtinger J, Prochazka K, Unterluggauer JJ, Pansy K, Steinbauer E, Pichler M, Haybaeck J, Prokesch A, Greinix HT, Beham-Schmid C, Neumeister P, Thallinger GG, Deutsch AJA. Cytoplasmic location of NR4A1 in aggressive lymphomas is associated with a favourable cancer specific survival. Sci Rep. 2018 Sep 28;8(1):14528. doi: 10.1038/s41598-018-32972-4

Original Article

https://www.nature.com/articles/s41598-018-32972-4#Sec15

Supplementary Figure S1-S7, Supplementary Table S1 S6

https://static-content.springer.com/esm/art%3A10.1038%2Fs41598-018-32972-4/MediaObjects/41598_2018_32972_MOESM1_ESM.pdf

Supplementary Table 2-5

https://static-content.springer.com/esm/art%3A10.1038%2Fs41598-018-32972-4/MediaObjects/41598_2018_32972_MOESM2_ESM.xlsx